DISSERTATION APPROVAL SHEET

Title of Dissertation: Modeling and PDE Theory for The Large Deflections of Elastic Cantilevers

Name of Candidate: Maria Deliyianni

Doctor of Philosophy, 2022

Graduate Program: Applied Mathematics

Dissertation and Abstract Approved:

Justin Webster

Justin Webster

Assistant Professor

Mathematics and Statistics

4/24/2022 | 12:20:03 PM EDT

NOTE: *The Approval Sheet with the original signature must accompany the thesis or dissertation. No terminal punctuation is to be used.

ABSTRACT

Title of dissertation: Modeling and PDE Theory for The Large Deflections of Elastic Cantilevers

Maria Deliyianni, Doctor of Philosophy, 2022

Dissertation directed by: Dr. Justin T. Webster
Department of Mathematics & Statistics

Flutter is defined as a self-excitation of a thin structure where a surrounding flow destabilizes its natural elastic modes. Cantilevers are particularly prone to flutter, and it has been shown that this instability can induce large displacements from which mechanical energy can be captured via piezoelectric laminates. To effectively harvest energy in this manner, one must have viable models that describe the behavior of the cantilever's large deflections after the onset of flutter. The aim of this dissertation is to introduce the modeling and the mathematical analysis that correspond to such systems.

The first part of this dissertation focuses on a recent PDE model that derives the equations of motion for an inextensible cantilevered beam via Hamilton's principle. The theoretical results are centered around the existence, uniqueness, and decay of strong solutions. In addition, numerical results are available where a modal approach is used to provide insight into the features and limitations of this model.

The next part of this dissertation is centered around two-dimensional cantilevered plates. Firstly, the modeling of large deflections for a cantilevered plate

is addressed. Various modeling hypotheses are explored and Hamilton's principle is employed to derive the corresponding equations of motion. Following this, the linear (Kirchhoff–Love) cantilevered plate is used to develop a semigroup argument that addresses the well-posedness of this configuration.

In the last part, a system that considers the coupling between the structure of a linear cantilevered beam with a full potential flow is introduced. This flow is given by a perturbed wave equation but taken with mixed boundary conditions of *Kutta–Joukowsky* type.

Modeling and PDE Theory for The Large Deflections of Elastic Cantilevers

by

Maria Deliyianni

Dissertation submitted to the Faculty of the Graduate School of the
University of Maryland, Baltimore County in partial fulfillment
of the requirements for the degree of
Doctor of Philosophy
2022

Advisory Committee:
Dr. Justin Webster, Chair/Advisor
Dr. Animikh Biswas
Dr. Sebastian Deffner
Dr. Muruhan Rathinam
Dr. Rouben Rostamian

Dedication

To all the people who believed in me...

Acknowledgments

Looking through the pages of this dissertation I revisit all the ups, the downs, the failures, and the victories I have experienced in my lengthy journey of my doctorate years. Even though these experiences are different in nature, they all share a common component: I always had people next to me who supported me in each and every step.

First and foremost, my biggest gratitude goes to my advisor, Dr. Justin Webster, for his continuous support, his time, and devotion he has shown me. I will forever cherish the memories of conversations we shared and how these have sculpted me into the mathematician I am today. But most importantly, I will always remember how he set an example for us, his students, on how a good professor is not only in paper but also in heart. Dr. Webster thank you for everything.

A gigantic thank you goes to my parents who always believed in me. Both of them sacrificed a lot to bring me here. Dad and mom I tried my best to make sure that your hard work is fruitful and I hope you are proud of your accomplishments through me.

To all my friends, here and there, a big thank you from the bottom of my heart, for all their love. We made memories together, we shared the good and the bad, and they were always there for me. I thank each and every one of you.

Lastly, I would like to thank my department and UMBC in general. My special thank you goes to my dissertation committee and the readers of my work, Dr. Rostamian and Dr. Rathinam, for their helpful comments.

Table of Contents

List of Figures

Chapter 1: Introduction

1.1 Motivation and Overview

A cantilever is a beam (1D) or a plate (2D) that is clamped on one end/edge and free at the other(s). Cantilevers, as a class of elastic objects, have received less attention in the voluminous literature on beams and plates. In particular, there is a dearth of work analyzing the *large deflections* of cantilevers, as this requires models that are *nonlinear* in displacement variables. The linear theory of elasticity is well established in both engineering and mathematics for beams and plates (e.g., [1,12,18, 37, 49, 62]). Often, standard models—such as that of Euler–Bernoulli, Rayleigh, or Timoshenko for beams, and Kirchhoff–Love or von Karman for plates—are utilized because they are sufficiently accurate, while being analytically and computationally tractable. Having said that, the main focus of this dissertation is to produce a theory which *generalizes* the traditional linear theory of cantilevers in the realm of (nonlinear) large deflections.

The large deflections of elastic beams and plates have broad applicability in engineering and other physical sciences (see, e.g., [16, 18, 29]). Specifically, with respect to fluid-structure interaction models, the large deflections of panel, airfoil, and flap structures are of particular interest [15,25] (and references therein). In these circumstances, the presence of a fluid flow can act as a destabilizing mechanism, giving rise to a self-excitation instability known as aeroelastic *flutter* [15, 61]. This manifests as a limit cycle oscillation (LCO).

Flutter can occur in many applications such as paneling [23], suspension bridges [13], pipes conveying fluid [63], and energy harvesting devices [28]. Also, flutter is the main mechanism for producing sound in reeded musical instruments such as the oboe, clarinet, accordion, and harmonica [77]. In the majority of these applications one seeks to suppress or minimize flutter, due to the catastrophic implications it can have on a structure. Nevertheless, in energy harvesting, dynamic instability is actually *encouraged* since it has been recently shown that it is possible to capture mechanical energy via large, flow-induced cantilever deflections.

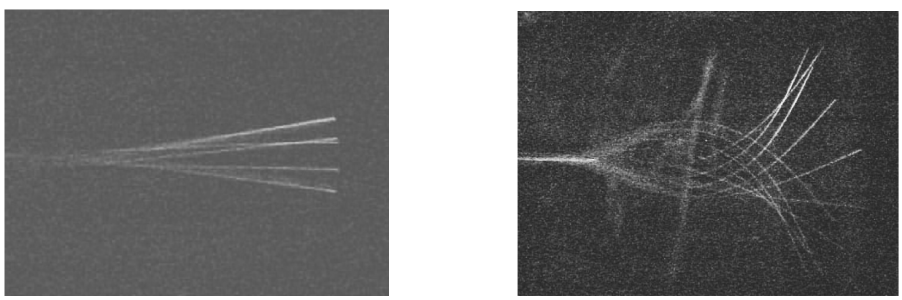

Figure 1.1: Temporal snapshots of post onset, small amplitude LCO (left) and large amplitude LCO (right) for a cantilever in axial flow captured from wind-tunnel simulations [73, 75]. In these experiments, the airflow runs from left to right.

More particularly, it was observed that a cantilever in axial flow, i.e. when an airflow runs along its principal axis, is particularly prone to flutter. This aeroelastic instability leads to sustained LCOs; a fact that is useful in the development of vibration-based energy harvesting devices [28, 31]. In such applications, dynamic

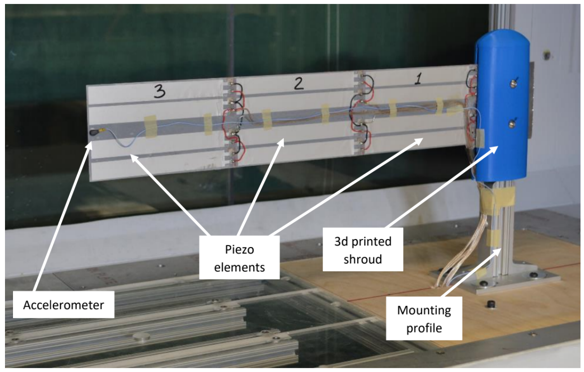

Figure 1.2: Experimental setup from [56]. The flow here will run from right to left.

instability is encouraged to extract energy from LCOs of the elastic cantilever, after the onset of flutter. The main idea for large displacement harvesters is to capture mechanical energy via piezoelectric laminates or patches (for which oscillating strains induce current [31]). The feasibility of such a system has been recently demonstrated with affixed piezo (SMART) materials [28, 31, 33, 71]. (See Figure 1.2.)

To effectively and efficiently harvest energy in this manner, one must be able capture and predict the post-onset behaviors of a cantilever, and thus, one must have a viable model for its large deflections. In such applications, relevant models require nonlinear restoring forces that take into account higher order effects, typically appearing via a potential energy expression above the "quadratic" level. In addition, unlike traditional nonlinear theories of beams and plates where the boundaries are fully restricted, we should not assume that nonlinear forces result from local stretching (extensibility), as would be the case for fully clamped or hinged structures. Rather, we will assume certain *inextensibility* conditions—that the beam or plate in fact does not stretch in specified ways throughout deflection.

1.2 The Need For Inextensibility

Cantilever flutter is associated with large deflections in the order of the beam's length [73, 75]. For such deflections, structural nonlinearity arises in modeling as a byproduct of the inclusion of higher order terms in strain and energy expressions. From a mathematical point of view, the presence of non-conservative (energy building) flow-effects gives rise to a bifurcation in beam dynamics (this is flutter [21, 39, 40]), which would yield exponential growth in time for a purely linear model, according to destabilized eigenvalues. To ensure that flow-destabilized trajectories remain bounded, one must consider a nonlinear elastic restoring force, active for large displacements, slopes, or curvatures. The typical way to achieve this in the theory of elasticity is through the inclusion of cubic-type forces that arise from the effect of local stretching on bending [40, 49].

In the case of extensible structures, models and theory are well-established, especially in scenarios where the boundary is fully restricted (e.g., paneling [12, 16, 23]); such nonlinear restoring forces are based on the effect of local stretching on bending. In the case of beams, a prominent example is the Woinowsky–Krieger beam [78] which appends a semilinear extensible force to any of the standard linear beams such as those of Euler–Bernoulli, Rayleigh, shear, or Timoshenko [37]. Examples of classical mathematical references for the analysis of such extensible beams include [6, 30], as well as the more recent [39, 40]. Alternatively, [49] provides a modeling account (with subsequent analysis of solutions and their stability) for an extensible beam that is intimately related to the so-called *full von Karman* model for plates.

Indeed, for plates, the linear theory of Kirchhoff–Love is well-established, and the prominent nonlinear generalization for large deflections is the theory of von Karman [18] (and references therein). One can consult [9,12,62] for classical discussions, and the rigorous mathematical justifications of these models in [18, 51]. The more modern references of [16, 50] provide detailed discussion of solutions, stability, and dynamical systems aspects of von Karman dynamics (among others). Finally, [47] deals with the analysis of the *full von Karman* plate, which is an extensible plate system that accounts for both in-plane and transverse inertial terms (in contrast to the scalar von Karman equations [16]).

Since extensibility is *not* physically dominant for cantilevers, engineers have posited that the prevailing nonlinear forces may result from inextensibility [26,69,75]. It should be noted that the theory of von Karman may not be viable (the operative hypotheses invoke the effect of stretching on bending) in most cantilevers. As such, a theory based on inextensibility must be developed from first prinsciples. The earlier work of Païdoussis derives and discusses 1D inextensible pipes conveying fluid, along with associated numerical stability analysis [63,69]. Subsequently, the thesis [57] focuses on inextensible beams and plates, but primarily focuses on finite dimensional descriptions through Rayleigh–Ritz considerations, not providing the explicit equations of motion in the standard Euclidean frame. The work of Dowell et al. further elaborates on inextensible beams and plates, developing several related approaches and investigating an inextensible theory experimentally and numerically in the sequence of papers [73–75]. Finally, the work of McHugh et al. [26,58,60] provided the first explicit calculus of variations derivation of the PDE equations of motion of an inextensible beam (in both the free-free and cantilever configurations). Apart from these papers, other aforementioned analyses primarily employ the Rayleigh–Ritz procedure to obtain finite dimensional equations of motion directly from specified energies, circumventing the PDE equations of motion. The discussion of boundary conditions for the 2D system (from first principles) is typically omitted, and *the rigorous analysis of solutions, as well as the well-posedness thereof, are not made.*

1.3 A Brief Discussion of the Work of this Dissertation

Apart from the obvious challenges that nonlinear models possess for analysis, enforcing inextensibility—as a nonlinear constraint—can be quite difficult. Thus, *the main focus of this dissertation is to explore inextensibility in cantilevers, derive corresponding models that take into account the large deflections of such inextensible elastics structures, and eventually develop rigorous well-posedness theory for the aforementioned models.*

The foundation of our work is based on a modeling work [26, 75] for an inextensible beam that utilizes a simplified approach which accounts for both nonlinear stiffness and nonlinear inertia effects. There, using tools from calculus of variations and employing Hamilton's principle, the authors derive the equations of motion for an inextensible cantilevered beam that is both quasilinear and nonlocal in space. Considering that model, the first part of this dissertation focuses on analyzing and developing a rigorous mathematical theory that addresses well-posedness. To achieve this, we proceed with constructing approximate solutions via Galerkin procedure and then obtaining the regularity that is necessary to prove that these solutions are indeed strong. Existence of weak solutions is still an open problem.

Upon addressing the well-posedness for the beam, and as an analogue and a natural continuation of our work, we are interested in deriving a model that will capture the dynamics of large deflections of a 2D inextensible plate. To the best of our knowledge such models were not present in literature. For this reason, we proceed with centering the following part of the dissertation around the derivation of equations of motion that describe an inextensible cantilevered plate and the exploration of the notion of inextensibility in two dimensions. That being said, there is no single, clear plate extension of our beam model; certain modeling and order choices yield a different system for the equations of motion. Our work produces three distinct models with associated nonlinear boundary conditions.

After obtaining the equations of motion for the nonlinear cantilevered plates, we have an eye on establishing results for the existence and uniqueness of associated solutions. Owing to the challenging nature of these models, it became apparent that it is important to understand the machinery employed for linear cantilevered plates. Even in this case, we observe some difficulties in the analysis: the mixed and higher order boundary conditions for the free plate, and the corners of the domain, cause a significant challenge to the *elliptic regularity* associated with the system. In addition, interpreting the higher order boundary conditions is a subtle issue. Our aim to show a semigroup well-posedness using a semigroup argument. This entails the definition of an operator that describes the dynamics and the domain of this system, and the application of Lumer–Phillips theorem (showing that the defined operator is dissipative and maximal) to prove the generation.

Lastly, as formerly mentioned, the motivation for this work is focused on energy harvesting, which dictates the coupling of the structure with a fluid flow. Thus, the last part of this dissertation is related to the coupling of inextensible cantilevered beams, for which we have already established well-posedness results, with a full potential flow ϕ. This flow is given by a perturbed wave equation in the variable ϕ on $\mathbb{R}^2_+$, but taken with mixed boundary conditions of *Kutta–Joukowsky* ("KJ") type. These conditions are homogeneous Neumann on the domain of the beam, and $(\partial_t + U\partial_x)\phi = 0$ off the domain [5]. This is a challenging mixed boundary condition hyperbolic problem. For this, we aim to use the constructed semigroup (which admits smooth solutions in the domain of the dissipative operator) to run a fixed point argument for the 2D flow-beam system. If we can show that trajectories are bounded, we expect to be able to expand our analysis to attractors and other post-flutter dynamical systems analyses.

1.4 Outline of the Remainder of the Dissertation

In *Chapter 2* of this dissertation, we present rigorously the derivation of the equations of motion for an *inextensible cantilevered beam.* We then proceed with the mathematical analysis of this model which consists of the discussion and the details about the existence and uniqueness of solutions and their dependence on the initial data. For the full system, we will see how the inclusion of a strong damping (which will be defined later) is necessary for tackling the well-posedness of our model.

Lastly, we show the exponential decay of solutions that correspond to small initial data.

Chapter 3 is devoted to numerical simulations of the inextensible cantilever dynamics that utilize a modal approach.

In *Chapter 4* we go over the derivation of the equations of motion of an inextensible cantilevered rectangular plate that undergoes large deflections. There, we walk through our choices for the potential energies, as well as the interpretation and enforcement of "inextensibility" in the plate. Ultimately, we present three distinct models; each one of them is presented as a system of partial differential equations in the elastic deflection variables, as well as constraint variables.

Chapter 5 deals with the setup and application of the Lumer–Phillips theorem to prove semigroup well-posedness of a linear cantilevered plate defined on a rectangular domain.

Lastly, in *Chapter 6*, we present the model that corresponds to the coupling of a cantilevered beam with a potential flow that has mixed boundary conditions of the Kutta–Joukowsky type.

Chapter 2: Large Deflections of Inextensible Cantilevered Beams

2.1 Summary of the Chapter

In this chapter we analyze recent equations of motion for the large deflections of an inextensible cantilevered elastic beam. For this model, smooth solutions are constructed via a spectral Galerkin approach. Additional compactness is needed to pass to the limit and identify weak limits, and this is obtained through a procession of higher energy estimates. Uniqueness is obtained through a non-trivial polynomial decomposition of the nonlinearity. The confounding effects of nonlinear inertia are overcome via the addition of some structural (Kelvin–Voigt) damping to the equations of motion. Local well-posedness of smooth solutions is shown first in the absence of nonlinear inertial effects, and then shown with these inertial effects present, taking into account structural damping. With damping in force, global-in-time, strong well-posedness result is obtained by achieving exponential decay for small data and zero forcing.

2.2 Introduction

This chapter is dedicated to the modeling of an inextensible elastic beam and the development of a rigorous well-posedness theory for smooth solutions. We begin our discussion with a brief outline of the results that will be presented herein.

Firstly, we introduce the reader to the equations that will govern the work in this chapter and include a short discussion about the novel mathematical contributions and technical challenges of this model. Section 2.3 presents a derivation of the equations of motion, as well as a brief discussion of structural damping central to this analysis. Section 2.4 presents the functional setup for the analysis and technical definitions of solutions used in subsequent well-posedness and stability proofs.

Each of the remaining sections corresponds to a main result. In those latter sections, we will: (i) state a main result technically, using the terminology and concepts established in Section 2.4; (ii) outline the proof briefly; and (iii) execute the proof in detail. Below, we give a short, nontechnical description of each of these main sections.

Section 2.5 provides a *local*[1] *well-posedness for strong solutions* for (2.2.1) *in the absence of nonlinear inertia with no imposed damping.* The resulting system is a conservative, quasilinear beam system. The result—Theorem 2.5.1—is built upon higher order energy estimates used to obtain additional compactness needed in executing a Galerkin procedure with cantilever eigenfunctions..

Section 2.6 provides a *local well-posedness result—in the presence of nonlinear*

[1]local, in the sense that the time of existence depends on the size of the initial data in the associated solution topology.

inertia—for strong solutions in Theorem 2.6.1; in this case, *some damping is required* to obtain estimates in the construction of solutions. The damping addresses the nonlocal and implicit nature of the inertial terms.

Section 2.7 provides our final main result: *global existence of strong solutions for small data* (in the presence of both inertia and damping). This result is typical for quasilinear hyperbolic dynamics, whereby the presence of damping and small data allow for stabilization estimates that ensure exponential decay, yielding an arbitrary time of existence.

Lastly, Section 2.8 gives a brief discussion of open problems related to this particular model.

2.2.1 The Equations of Motion of Interest

Let $(u, w) \in \mathbb{R}^2$ denote the Lagrangian displacement of a beam whose centerline equilibrium position is $x \in [0, L]$. This is to say that $u(x, t)$ is the axial (longitudinal) displacement from equilibrium and $w(x, t)$ is the transverse beam deflection.

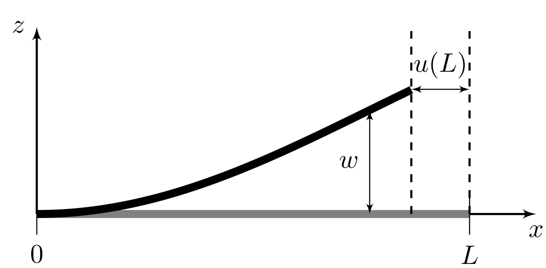

Then, the **inextensible equations of motion** of interest—derived later in

Section 2.3—are:

$$\begin{cases} w_{tt} + D\partial_x^4 w + k_2 \partial_x^4 w_t + \mathbf{A}[w, u_{tt}] = p(x,t) & \text{in } (0,L)\times(0,T); \\ w(0,t) = w_x(0,t) = 0; \quad w_{xx}(L,t) = w_{xxx}(L,t) = 0 & \text{in } (0,T); \\ w(x,0) = w_0, \quad w_t(x,0) = w_1, \end{cases} \tag{2.2.1}$$

with
$$\mathbf{A}[w, u_{tt}] = -D\partial_x\Big[w_{xx}^2 w_x\Big] + D\partial_{xx}\Big[w_{xx}w_x^2\Big] + \partial_x\left[w_x \int_x^L u_{tt}d\xi\right] \tag{2.2.2}$$

$$u_{tt}(x) = -\int_0^x [w_{xt}^2 + w_x w_{xtt}]d\xi. \tag{2.2.3}$$

We denote by D the standard (mass-normalized) beam stiffness coefficient [26], L is the beam's length, and $k_2 \geq 0$ corresponds to structural damping of Kelvin–Voigt type (discussed further in Section 2.3). The RHS $p(x,t)$ constitutes a given transverse pressure differential across the deflected beam.

2.2.2 Novel Contributions and Technical Challenges

The model we focus on here only appeared for the first time in the context of elastic cantilevers in the recent papers [26, 75]. These (and other earlier works focusing on inextensible pipes conveying fluid such as [63,69]) are largely engineering-oriented, making use of finite dimensional analyses via modal truncation or the Rayleigh–Ritz method at the energetic level. Thus, to the knowledge of the authors, *this is the first treatment to rigorously address the theory of solutions for inextensible elasticity.*

Although the central problem here is a 1-D beam, the following issues render the analysis quite challenging. Some of these issues are common for quasilinear dynamics, but many are not (e.g., those associated with nonlinear inertia), and we also point to the non-trivial *interaction* between (high order) free boundary conditions, nonlinear stiffness, and nonlocal inertial terms.

The **technical challenges faced in the analysis** are:

- Despite a good, conservative structure for the baseline equations of motion, quasilinear and semilinear terms do not straightforwardly admit (semigroup or fixed point) perturbation methods.
- The term $\partial_x[w_{xx}^2 w_x]$ precludes weak limit point identification at the baseline energy level.
- Nonlinear terms and free boundary conditions (i) do not readily permit differentiation of the equations to obtain higher energy estimates, and (ii) convolute the standard technique of *going back through the equations* to trade time and space regularity.
- Nonlinear inertial terms (i) present themselves at a level above finite energy, (ii) are also nonlocal, and (iii) are implicit terms in w_{tt}, and hence do not constitute a traditional evolution. The truncated version of the dynamics is in fact *quasilinear in time* (2.6.3).

In addressing the issues above, we note the following specific **novelties of this analysis**:

- The sequence of multipliers used to close estimates in obtaining compactness are non-standard, including the use of stabilization-type multipliers.
- A novel decomposition of nonlinear differences exploits polynomial symmetry for a non-obvious uniqueness proof, relying critically on smooth trajectory estimates obtained earlier.
- The inclusion of damping to permit appropriate estimates for well-posedness of the full model is a peculiarity, one that, at present, we cannot avoid. On the other hand, including damping in the full model (2.2.1)–(2.2.2) successfully obtains global solutions for small data.

2.3 PDE Model Derivation

Recall that $w(x,t)$ is the transverse deflection and $u(x,t)$ is the in-axis displacement from equilibrium of a beam at $t \in [0,T]$ and a spatial point $x \in [0,L]$. Let $\varepsilon(x,t)$ describe the *axial strain* along the centerline of the beam. In this section we derive the in-vacuo equations of motion via Hamilton's principle. The inextensibility condition is simplified to an *effective inextensibility constraint*, which is enforced via a Lagrange multiplier. Our derivation tracks the one first appearing in [26], and we point to the earlier references [63, 69] for inextensibility treated in the context of pipes conveying fluid.

2.3.1 Inextensibility

According to classical work (e.g. [69,72]) we have the Lagrangian strain relation [69]

$$\left[1+\varepsilon\right]^2 = (1+u_x)^2 + w_x^2.$$

When the beam is *inextensible*, we take $\varepsilon(x,t) = 0$, which immediately yields the condition

$$1 = (1+u_x)^2 + w_x^2. \tag{2.3.1}$$

From [18, 26, 69], large deflections dictate that higher order nonlinear terms should be retained, namely, *up to cubic order*. (For variational purposes, then, energetic expressions will be accurate up to quartic order.) By expanding the inextensibility condition (2.3.1), we see that if $w_x \sim \epsilon$, we will have $u_x \sim \epsilon^2$:

$$2u_x + u_x^2 + w_x^2 = 0.$$

As in [26], we drop $u_x^2 \sim \epsilon^4$, owing to its relative order being above cubic. Approximating, then

$$0 = 2u_x + w_x^2 \quad \Longrightarrow \quad u_x = -\frac{1}{2}w_x^2.$$

This yields what we henceforth refer to as the *effective inextensibility constraint*, providing a direct relationship between u and w:

$$u(x,t) = -\frac{1}{2}\int_0^x [w_x(\xi,t)]^2 d\xi. \tag{2.3.2}$$

2.3.2 Nonlinear Elasticity

Define the elastic potential energy (E_P) via beam curvature κ and constant stiffness D (flexural rigidity) [69] in the standard way

$$E_P \equiv \frac{D}{2}\int_0^L \kappa^2 dx.$$

Let's take the beam's displaced state, $\{(x+u(x), w(x)) : x \in [0, L]\}$, as a parametrized curve. The standard expression for curvature in this scenario is:

$$\kappa = \frac{(1+u_x)w_{xx} - u_{xx}w_x}{[(w_x)^2 + (1+u_x)^2]^{3/2}}.$$

From inextensibility (2.3.1) (without approximation), we see that the denominator is one. From (2.3.1), we can also write $u_x = \sqrt{1-w_x^2} - 1$ which leads to $u_{xx} = -w_x w_{xx}(1-w_x^2)^{-1/2}$. Substituting in κ, we obtain:

$$\kappa = (1+u_x)w_{xx} - w_x u_{xx} = (1-w_x^2)^{1/2}w_{xx} + w_x(w_x w_{xx}(1-w_x^2)^{-1/2}) = \frac{w_{xx}}{(1-w_x^2)^{1/2}}.$$

To be consistent with the approximation that yields (2.3.2), we must retain terms at the level of w_x^2 in approximating E_P [26, 69]. Via a Taylor expansion, we take $\kappa \approx w_{xx}(1+\frac{1}{2}w_x^2)$.

Remark 2.3.1. This point distinguishes the derivation from linear elasticity in w, where $\kappa \approx w_{xx}$.

Finally, the effective potential energy for the problem at hand, after order considerations becomes

$$E_P = \frac{D}{2} \int_0^L w_{xx}^2 \left(1 + w_x^2\right) dx. \tag{2.3.3}$$

The kinetic energy (E_K) for the dynamics taken in the standard way for a mass-normalized beam:

$$E_K = \frac{1}{2} \int_0^L \left(u_t^2 + w_t^2\right) dx. \tag{2.3.4}$$

2.3.3 Hamilton's Principle

To derive the equations of motion and the associated boundary conditions, we utilize Hamilton's Principle [26, 49]. We consider displacements u and w (and hence virtual displacements δu and δw) which are smooth and respect the essential boundary conditions at $x = 0$, namely:

$$w,\ w_x,\ \delta w,\ \delta w_x :\ 0 \ \text{ at } \ x = 0; \qquad\qquad u,\ \delta u :\ 0 \ \text{ at } \ x = 0.$$

The effective inextensibility constraint, $f \equiv u_x + (1/2)w_x^2 = 0$, will be appended to the system via a *Lagrange multiplier* λ. Thus, we express the Lagrangian in the usual way:

$$\mathcal{L} = E_K - E_P + \int_0^L \lambda f dx. \tag{2.3.5}$$

Taking the variation of (2.3.5) and performing the necessary integration by parts with respect to both time and space, Hamilton's principle provides the Euler–Lagrange equations of motion and the associated boundary conditions. Virtual changes are considered for both displacements, u and w.[2]

To minimize the Lagrangian, we set $\delta \int_{t_1}^{t_2} \mathcal{L} dt \equiv 0$ and utilize the arbitrariness of the virtual changes δu and δw. For interior terms, we gather virtual changes and set the totals equal. The relevant calculation pertains to the E_P:

$$\delta E_P = D \int_0^L \Big[(1 + w_x^2) w_{xx}\Big] \delta w_{xx} + \Big[(w_x w_{xx}^2)\Big] \delta w_x dx. \tag{2.3.6}$$

Integrating by parts until only δw appears, and utilizing the arbitrariness of the virtual changes, we obtain the unforced equations of motion:

$$\text{from} \quad \delta u : \quad u_{tt} + \lambda_x = 0 \tag{2.3.7}$$

$$\text{from} \quad \delta w : \quad w_{tt} - D\partial_x \left(w_{xx}^2 w_x \right) + D\partial_{xx} \left(w_{xx} \left[1 + w_x^2 \right] \right) + \partial_x \left(\lambda w_x \right) = 0. \tag{2.3.8}$$

For the (natural) boundary conditions at $x = L$, the relevant calculations pertain to w (the u and λ conditions can then be inferred). In the integration by parts proceeding from (2.3.6), we obtain by the arbitrariness of δw, δw_x and δu:

$$\lambda(L) = 0; \quad (1 + w_x^2(L)) w_{xx}(L) = 0; \quad (1 + w_x^2(L)) w_{xxx}(L) + w_x(L) w_{xx}^2(L) = 0. \tag{2.3.9}$$

From (2.3.9), we infer that $w_{xx}(L) = w_{xxx}(L) = 0$—the standard free boundary conditions.

Remark 2.3.2. This fact is both critical and somewhat surprising, as the nonlinear

[2]Note that virtual change in λ simply produces the effective inextensibility constraint.

effects (and their previously discussed simplifications) do not alter the standard *linear* boundary conditions for a cantilever. Note that in extensible elasticity, this is not always the case [16, 40].

Now, using the equation (2.3.7) we can formally write

$$\lambda(x) = -\int_0^x u_{tt}(\xi)d\xi + \lambda(0).$$

We then utilize the fact that $\lambda(L) = 0$ to conclude $\lambda(0) = \int_0^L u_{tt}(\xi)d\xi$. From this we deduce:

$$\lambda(x) = \int_x^L u_{tt}(\xi)d\xi.$$

With the preceding calculations and substituting the above expression in (2.3.8) we *finally obtain the equations of motion* (2.2.1)–(2.2.2), and the corresponding boundary conditions for w, as well as for u and λ at $x = L$.

Remark 2.3.3. It is possible to obtain a a higher order model by retaining terms up to fourth order (ϵ^4). Repeating the steps mentioned above, we can keep terms up to ϵ^4 in the effective inextensibility condition and the curvature expression κ^2. Following these steps one can obtain the ϵ^4 *inextensible beam* system (omitting initial conditions):

$$
\begin{aligned}
& u_{tt} + \lambda_x = 0 \\
& w_{tt} - D\partial_x \left([w_x + 2w_x^3]w_{xx}^2\right) + D\partial_x^2 \left(w_{xx}\left[1 + w_x^2 + w_x^4\right]\right) + \partial_x\left(\lambda w_x\right) = 0 \\
& u_x = \; -\frac{1}{2}w_x^2 - \frac{1}{8}w_x^4 \\
& w(0) = w_x(0) = 0;\; w_{xx}(L) = w_{xxx}(L) = 0; \\
& u(0) = 0;\; u_x(L) = -\frac{1}{2}w_x^2(L) - \frac{1}{8}w_x^4(L) \\
& \lambda(0) = \int_0^L u_{tt}(\xi)d\xi; \quad \lambda(L) = 0.
\end{aligned}
$$

2.3.4 Damping

Discussion of damping in beams goes far back in both the engineering literature [12,69] as well as the mathematical literature [14,66]. In the treatment at hand, some additional velocity regularization is needed to address the nonlinear inertial terms; namely w_t must be “better” than $C([0,T];L^2(0,L))$. We obtain this by imposing Kelvin–Voigt type structural damping. Note, this type of damping is in fact invoked in the engineering-oriented references [63, 69] for improving numerical simulations. The recent article [68] addresses local damping and stiffness in a cantilever from a modeling and experimental point of view.

Let us here refer to the damped, linear Euler–Bernoulli beam equation

$$w_{tt} + D\partial_x^4 w + [k_0 - k_1\partial_x^2 + k_2\partial_x^4]w_t = p.$$

Weak (viscous) damping has the form $k_0 w_t$, providing no velocity regularization. In the elasticity context, Kelvin–Voigt damping $k_2\partial_x^4 w_t$ is strain-rate type, and mirrors the principal (linear) operator, providing a strong dissipative effect. In fact, this damping transforms the underlying dynamics to parabolic type [14,53]. Square root-like damping, $-k_1\partial_x^2 w_t$ [33] (which is comparable to the square root of dx^4) interpolates between the previous two damping types. (See [21,40] for more discuss of damping in the context of nonlinear cantilevers.)

Remark 2.3.4. Square root-type damping corresponds to modal damping models [25], as one finds frequently in the engineering literature [12, 60, 61]. However, the boundary conditions for a given problem affect the physical interpretation of square-root type damping; in [66] it is noted that square-root type damping has a questionable physical interpretation for a cantilevered configuration. See also [39] for more recent discussion. In the analysis here, we utilize the (strong) Kelvin–Voigt damping.

Remark 2.3.5. In this treatment the damping is primarily included to mitigate the effects of nonlinear inertia. We discuss this further in Section 2.8.

2.4 Functional Setup and Key Notions

2.4.1 Equations of Motion

With the derivation above, we recall the equations of motion, allowing for Kelvin–Voigt damping $k_2 \geq 0$:

$$\begin{cases} w_{tt} + D\partial_x^4 w + k_2\partial_x^4 w_t + \mathbf{A}_{\iota,\sigma}(w, u_{tt}) = p(x,t) & \text{in } (0,L)\times(0,T) \\ w(x,0) = w_0(x), w_t(x,0) = w_1(x) \\ w(0,t) = w_x(0,t) = 0;\; w_{xx}(L,t) = w_{xxx}(L,t) = 0, \end{cases} \tag{2.4.1}$$

$$\mathbf{A}_{\iota,\sigma}(w, u_{tt}) = -\sigma D\partial_x\Big[w_{xx}^2 w_x\Big] + \sigma D\partial_{xx}\Big[w_{xx}w_x^2\Big] + \iota\partial_x\left[w_x\int_x^L u_{tt}(\xi)d\xi\right] \tag{2.4.2}$$

$$u(x) = -\frac{1}{2}\int_0^x [w_x(\xi)]^2\, d\xi. \tag{2.4.3}$$

To simplify terminology, we use the following language from here on:

$$[\textbf{NL Stiffness}] = -D\partial_x\Big[w_{xx}^2 w_x\Big] + D\partial_{xx}\Big[w_x^2 w_{xx}\Big]$$
$$[\textbf{NL Inertia}] = \partial_x\left[w_x\int_x^L u_{tt}(\xi)d\xi\right],$$

the latter of which is nonlocal, when written in w through (2.4.3). The constants $\iota, \sigma = 0$ or 1 in (2.4.2) serve as flags to easily isolate particular nonlinear effects. This is to say, when $\iota = 0$, we say that [**NL Inertia**] is turned off.

Remark 2.4.1. For convenience, we note two expansions. First

$$[\textbf{NL}\quad \textbf{Stiffness}] = D[w_{xxx}^3 + 4w_x w_{xx} w_{xxx} + w_x^2 \partial_x^4 w],$$

which highlights the quasilinear nature of the PDE (with high order semilinearity). Secondly,

$$[\textbf{NL Inertia}] = -w_x u_{tt} + w_{xx} \int_x^L u_{tt} d\xi, \text{ with } \quad u_{tt} = -\int_0^x [w_{xt}^2 + w_x w_{xtt}] d\xi, \tag{2.4.4}$$

which highlights that, when closed in w, (i) there is high temporal regularity required to interpret the strong form of the PDE, and (ii) the equation is implicit in the acceleration w_{tt}.

2.4.2 Notation and Conventions

For a given spatial domain D, its associated $L^2(D)$ norm will be denoted as $||\cdot||_D$ (or simply $||\cdot||$ when the context is clear). Inner products in a Hilbert space are written $(\cdot,\cdot)_H$ (or simply $(\cdot,\cdot)$ when $H = L^2(D)$ and the context is clear). We will also denote pertinent duality pairings as $\langle\cdot,\cdot\rangle_{X\times X'}$, for a given Banach space X, as well as the general notation for a norm, $||\cdot||_X$. The open ball of radius R in X will be denoted $B_R(X)$. The space $H^s(D)$ will indicate the standard Sobolev space of order s, defined on domain D, and $H_0^s(D)$ will be the closure of $C_0^\infty(D)$ in the $H^s(D)$-norm $\|\cdot\|_{H^s(D)}$, also written as $\|\cdot\|_s$. For $\Gamma \subset \partial D$, boundary restrictions $u\Big|_\Gamma$ are taken in the sense of the trace theorem for $u \in H^{1/2^+}(D)$.

The constant C we take to mean a generic constant that may change from line to line. In estimates where dependencies are critical, we will write $C(q_i)$, where q_i are relevant quantities. Additionally, in our involved estimates below, for situations where $||q_1||_X \le C||q_2||_Y$ for some quantities q_1, q_2 in spaces X and Y, with C having no critical dependencies, *we will simply write* $||q_1||_X \lesssim ||q_2||_Y$.

Finally, we will frequently make use of standard Sobolev embeddings (in particular, that of

$H^{1/2^+}(0,L) \hookrightarrow L^\infty(0,L)$) as well as the Sobolev interpolation inequalities [32].

2.4.3 Energies

With reference to Section 2.3, we employ the following energies:

$$E(t) \equiv E_K(t) + E_P(t) \equiv \frac{1}{2}\left[||w_t||^2 + \iota||u_t||^2\right] + \frac{D}{2}\left[||w_{xx}||^2 + \sigma||w_x w_{xx}||^2\right]. \quad (2.4.5)$$

The energies now include the nonlinear flags. This can be written in w explicitly using $u_t = -\int_0^x w_x w_{xt} d\xi$.

In the unforced situation, with $p(x,t) \equiv 0$, the formal energy identity is obtained by the velocity multiplier w_t on (2.4.1) taken with the relation (2.4.3), yielding

$$E(t) + k_2 \int_s^t ||w_{xxt}||^2_{L^2(0,L)} d\tau = E(s), \quad 0 \le s \le t.$$

Higher order energies corresponding to smooth solutions will be defined in later sections.

2.4.4 Spaces and Operators

The principal state space for cantilevered beam displacement takes into account the clamped conditions:

$$H^2_* = \{v \in H^2(0,L) : v(0) = 0, \quad v_x(0) = 0\}.$$

This space is equipped with an $H^2(0,L)$ equivalent inner product:

$$(v,w)_{H^2_*} = D(v_{xx}, w_{xx}). \tag{2.4.6}$$

Denoting R as the Riesz isomorphism $H^2_* \to [H^2_*]'$, we see it is given by:

$$R(v)(w) \equiv (v,w)_{H^2_*}. \tag{2.4.7}$$

This framework is conveniently induced by the generator of the linear cantilever dynamics:

$$\mathcal{A} : \mathcal{D}(\mathcal{A}) \subset L^2(0,L) \to L^2(0,L), \;\; \mathcal{A}f \equiv D\partial_x^4 f,$$

$$\mathcal{D}(\mathcal{A}) = \{w \in H^4(0,L) : w(0) = w_x(0) = 0;\; w_{xx}(L) = w_{xxx}(L) = 0\}. \tag{2.4.8}$$

From this we have in a standard fashion [53]:

$$\mathcal{D}(\mathcal{A}^{1/2}) = H^2_*, \quad \mathcal{D}(\mathcal{A}^{-1/2}) = [H^2_*]' \;\text{ and }\; \mathcal{A}^{1/2} = R \quad \text{in (2.4.7)}.$$

Then $(u,\cdot)_{H^2_*}$ is the extension of $(\mathcal{A}u,\cdot)$ from $\mathcal{D}(\mathcal{A})$ to H^2_* which gives (2.4.6).

Using the above spaces we can define the appropriate state space(s) for our dynamics. The finite energy space will be denoted as:

$$\mathscr{H} \equiv \mathscr{D}(\mathcal{A}^{1/2}) \times L^2(0,L) = H^2_* \times L^2(0,L),$$

with the inner product $y=(y_1,y_2),\ \tilde{y}=(\tilde{y}_1,\tilde{y}_2)\in\mathscr{H}$

$$(y,\tilde{y})_{\mathscr{H}} = (y_1,\tilde{y}_1)_{H^2_*} + (y_2,\tilde{y}_2)_{L^2(0,L)}. \tag{2.4.9}$$

In our discussions, we will also require stronger state spaces (corresponding to *strong* solutions):

$$\mathscr{H}_s \equiv \mathcal{D}(\mathcal{A}) \times \mathcal{D}(\mathcal{A}^{1/2}), \quad \text{for } \iota = k_2 = 0, \tag{2.4.10}$$

$$\mathscr{H}_s^I \equiv \mathcal{D}(\mathcal{A}) \times \mathcal{D}(\mathcal{A}), \quad \text{for } \ \iota = 1, k_2 > 0. \tag{2.4.11}$$

The norm in $\mathscr{H}_s$ is taken (equivalent[3] to the natural operator-induced norm) to be:

$$||y||^2_{\mathscr{H}_s} = ||\partial_x^4 y_1||^2 + ||\partial_x^2 y_2||^2, \quad \text{for } \iota = k_2 = 0,$$

$$||y||^2_{\mathscr{H}_s^I} = ||\partial_x^4 y_1||^2 + ||\partial_x^4 y_2||^2, \quad \text{for } \ \iota = 1, k_2 > 0.$$

[3]The topological equivalences on $\mathscr{D}(\mathcal{A})$ follow from repeated applications of the Poincaré inequality.

2.4.5 Mode Functions

We will utilize the so called *in vacuo modes* (eigenfunctions) associated to the operator $\mathcal{A}$. Specifically, we work with the Euler–Bernoulli cantilever eigenfunctions as our approximants in H^2_*; namely, the eigenvalues and eigenfunctions $\{\lambda_n, s_n(x)\}_{n=1}^{\infty}$ of $\mathcal{A}$ on $L^2(0,L)$. These modes and associated eigenvalues are computed in an elementary way. The $C^{\infty}([0,L])$ mode shapes take the form

$$s_n(x) \equiv c_n[\cos(\kappa_n x) - \cosh(\kappa_n x)] + C_n[\sin(\kappa_n x) - \sinh(\kappa_n x)], \;\; \kappa_n^4 = \lambda_n, \quad (2.4.12)$$

where the κ_n are obtained (numerically) by solving the associated characteristic equation

$$\cos(\kappa_n L)\cosh(\kappa_n L) = -1.$$

The C_n are obtained by invoking the boundary conditions:

$$C_n = \frac{-c_n\Big(\cos(\kappa_n L) + \cosh(\kappa_n L)\Big)}{\sin(\kappa_n L) + \sinh(\kappa_n L)},$$

and the c_n values are chosen to normalize the functions in $L^2(0,L)$.

Via the spectral theorem, these functions are *complete* and *orthonormal* in $L^2(0,L)$, as well as complete and orthogonal in H^2_* (with respect to $(\cdot,\cdot)_{H^2_*}$). These eigenvalues have the property that $0 < \lambda_1 < \lambda_2 < ... \to \infty$.

2.4.6 Definition of Solutions

We provide the natural setting for the weak formulation of the problem; this will yield the appropriate starting point for our Galerkin procedure to construct solutions. Ultimately, we will construct weak solutions that possess additional regularity; these, in turn, will be strong solutions.

We begin with the *weak form* of (2.4.1) which we define for functions that are smooth in time:

$$
\begin{aligned}
(w_{tt},\phi)+D(w_{xx},\phi_{xx})+k_2(w_{xxt},\phi_{xx})+\sigma D\Big(w_{xx}w_x,w_x\phi_{xx}\Big)+\sigma D(w_{xx}w_x,w_{xx}\phi_x)\\
-\iota\left(w_x\int_x^L u_{tt}dx,\phi_x\right)=(p,\phi),\ \forall\ \phi\in H^2_*.
\end{aligned}
\tag{2.4.13}
$$

When $\sigma>0$, the [**NL Stiffness**] is in force; similarly, when $\iota>0$, [**NL Inertia**] is in force. When $k_2>0$, Kelvin–Voigt damping is imposed.

We now give precise definitions of solutions making reference to the weak form (2.4.13) above:

Definition 1. *We say a* weak *solution to* (2.4.1)*, with $k_2=\iota=0$ and $\sigma=1$ is a function w, with*

$$
w\in L^2\left(0,T;H^2_*\right);\ w_t\in L^2\left(0,T;L^2(0,L)\right);\ w_{tt}\in L^2\left(0,T;[H^2_*]'\right)
$$

that satisfies (2.4.13)*, replacing $L^2(0,L)$ inner products with $(H^2_*,[H^2_*]')$ duality pair-*

ings where necessary.

Moreover, for any $\chi \in H^2_*$, $\psi \in L^2(0,L)$, we require

$$(w,\chi)_{H^2_*}\Big|_{t\to 0^+} = (w_0,\chi)_{H^2_*}, \quad (w_t,\psi)\Big|_{t\to 0^+} = (w_1,\psi). \tag{2.4.14}$$

Definition 2. *A* weak *solution to* (2.4.1) *with $k_2 > 0$ and $\iota = \sigma = 1$ is a function w, with*

$$w \in L^2\left(0,T;H^2_*\right);\ w_t \in L^2\left(0,T;H^2_*\right);\ w_{tt} \in L^2\left(0,T;[H^2_*]'\right),$$

such that (2.4.13) *holds, replacing $L^2(0,L)$ inner products with $(H^2_*,[H^2_*]')$ duality pairings where necessary.*

Moreover, for any $\chi \in H^2_*$, $\psi \in L^2(0,L)$, we require

$$(w,\chi)_{H^2_*}\Big|_{t\to 0^+} = (w_0,\chi)_{H^2_*}, \quad (w_t,\psi)\Big|_{t\to 0^+} = (w_1,\psi). \tag{2.4.15}$$

Remark 2.4.2. For $k_2 > 0$ and $\iota > 0$, the definition of weak solution is self-consistent; this is to say, for such a function w, all terms in (2.4.13) are well-defined. We note that for $k_2 = 0$, there are complications with the a priori regularity of $w_t \in L^2(0,T;L^2(0,L))$ and the interpretation of the [**NL Inertia**] terms.

Now, we define strong solutions as weak solutions with additional regularity.

Definition 3. *A* strong *solution to* (2.4.1) *with $k_2 = \iota = 0$ and $\sigma = 1$ is a weak* *solution (as in Definition 1) with the additional regularity*

$$w \in L^2\left(0, T; \mathcal{D}(\mathcal{A})\right); \;\; w_t \in L^2(0, T; H^2_*); \;\; w_{tt} \in L^2\left(0, T; L^2(0, L)\right).$$

Definition 4. *A* strong *solution to* (2.4.1) *with* $k_2 > 0$, $\iota = \sigma = 1$ *is a weak solution (as in Definition 2) with the additional regularity*

$$w \in L^2\left(0, T; \mathcal{D}(\mathcal{A})\right); \;\; w_t \in L^2\left(0, T; \mathcal{D}(\mathcal{A})\right); \;\; w_{tt} \in L^2\left(0, T; H^2_*\right).$$

As we will show below in Corollaries 2.5.2 and 2.6.2, strong solutions will satisfy the pointwise form of the PDE in (2.4.1) as well as the higher order boundary conditions at $x = L$.

2.5 The Case of Only Stiffness Effects: $\sigma = 1$, $\iota = k_2 = 0$

2.5.1 Precise Statement of the Theorem

Theorem 2.5.1. *Take* $\sigma = 1$ *with* $\iota = k_2 = 0$, *and consider* $p \in H^2_{loc}(0, \infty; L^2(0, L))$. *For smooth data* $(w_0, w_1) \in \mathscr{H}_s = \mathcal{D}(\mathcal{A}) \times H^2_*$, *strong solutions exist up to some time* $T^*(w_0, w_1, p)$. *For all* $t \in [0, T^*)$, *the solution* w *is unique and obeys the energy identity*

$$E(t) = E(0) + \int_0^t (p, w_t)_{L^2(0,L)} d\tau.$$

Restricting to $B_R(\mathscr{H}_s)$, *for any* $T < T^*(R, p)$ *solutions depend continuously on the data in the sense of* $C([0, T]; \mathscr{H})$ *with an estimate on the difference of two* *trajectories, $z = w^1 - w^2$:*

$$\sup_{t\in[0,T]} \Big|\Big|(z(t), z_t(t))\Big|\Big|_{\mathscr{H}} \leq C(R,T)\Big|\Big|\Big(z(0), z_t(0)\Big)\Big|\Big|_{\mathscr{H}}, \quad \forall\ t \in [0,T].$$

Remark 2.5.1. The time of existence T^* depends on the data in the sense of

$$T^* = T^*\left(||(w_0, w_1)||_{\mathscr{H}_s}, ||p||_{H^2(0,T;L^2(0,L))}\right),$$

namely, the size of the data in the appropriate space, rather than the individual data itself.

2.5.2 Proof Outline

We will commence with a Galerkin procedure, using the mode functions $\{s_j\}_{j=1}^{\infty}$ described above. This will yield approximate solutions, with the baseline energy identity providing associated weak limit points. Identifying the nonlinear weak limits is non-trivial, hence, two higher-order multipliers will be used to provide more regular a priori bounds; one is an energy estimate corresponding to the time-differentiated version of the equation, and the other is a stability type estimate resulting from the multiplier $\partial_x^4 w$. Additional compactness is obtained through these estimates with appropriately smooth initial data. With a weak solution in hand corresponding to smooth data, we will show that this strong solution satisfies the PDE pointwise, along with all four cantilever boundary conditions. Lastly, we will tackle the uniqueness and continuous dependence in this case through a particular decomposition of the polynomial structure of the nonlinear stiffness.

2.5.3 Proof of Theorem 2.5.1

2.5.3.1 Existence

Consider the positive eigenfunctions of $\mathcal{A}$ described in Section 2.4.5, with $\lambda_n \to \infty$; these constitute an *orthonormal* basis for $L^2(0,L)$ and *orthogonal* basis for any $\mathcal{D}(\mathcal{A}^s)$, $s \in \mathbb{R}$. Now, for each $n = 1, 2, \ldots$, we denote

$$S_n \equiv \text{span}\{s_1, s_2, \ldots, s_n\}. \tag{2.5.1}$$

Step 1 - Approximants: For fixed smooth data, $w_0 \in \mathcal{D}(\mathcal{A})$ and $w_1 \in H^2_*$, we can construct two approximating sequences $\{w_0^n\}_{n=1}^\infty$ and $\{w_1^n\}_{n=1}^\infty$ such that

$$w_0^n := \sum_{j=1}^{n} (w_0, s_j)\, s_j \;\in S_n \quad \text{and} \quad w_1^n := \sum_{j=1}^{n} (w_1, s_j)\, s_j \;\in S_n. \tag{2.5.2}$$

By construction:
$$w_0^n \to w_0 \;\text{ in } \mathcal{D}(\mathcal{A}), \qquad w_1^n \to w_1 \;\text{ in } H^2_*. \tag{2.5.3}$$

and we can proceed to define smooth finite-dimensional approximations,

$$w^n(x,t) := \sum_{j=1}^{n} q_j(t) s_j(x),$$

where each $q_j(t)$ is a smooth function of time.

From the weak form, (2.4.13), we construct a corresponding matrix system by taking $\phi = s_j$ and then define the following for ease of writing:

$$\mathcal{S}_{ijkl} = \ (\phi_{i,xx}\phi_{j,xx}, \phi_{k,x}\phi_{l,x}). \tag{2.5.4}$$

Summing the expression below over j, we have the separated form of the equations:

$$[q_i''(s_i, s_j)] + Dq_i\left[\kappa_i^4(s_i, s_j)\right] + Dq_i^3\left[\mathcal{S}_{iiij} + \mathcal{S}_{jiii}\right] = (p, s_j), \tag{2.5.5}$$

where primes represent ∂_t. Initialization is given by

$$q_j(0) = (w_0, s_j)\,, \quad q_j'(0) = (w_1, s_j)\,, \quad j = 1, 2, \ldots\ .$$

We may then invoke standard ODE existence and uniqueness for this finite dimensional system. Noting the hypotheses on p_t, p_{tt}, we obtain a solution $\{q_j\}_{j=1}^n \in C^3(0, t^*)$, for some small $t^*(n)$.

Step 2 - Energy Level 0: The estimate below for (2.5.5) on the approximant w^n follows immediately using w_t as the multiplier in the equations (2.4.1)–(2.4.3), taken with $\iota = k_2 = 0$:

$$E_0^n(t) = E_0^n(0) + \int_0^t (p, w_t^n)\, d\tau \ \text{ for all } \ t > 0,$$

where

$$E_0^n(t) = \frac{1}{2}\left[||w_t^n||^2 + D||w_{xx}^n||^2 + D||w_x^n w_{xx}^n||^2\right]. \tag{2.5.6}$$

Now, via Young's and Grönwall's inequalities applied to (2.5.6), and noting that by (2.5.3) that $\{E_0^n(0)\}_{n=1}^{\infty}$ is uniformly bounded in terms of the initial data $||(w_0, w_1)||^2_{\mathscr{H}}$, we obtain:

$$E_0^n(t) \leq f_0\left(||p||_{L^2(0,t;L^2(0,L))}, ||w_0||_{\mathcal{D}(\mathcal{A})}, ||w_1||_{H_*^2}\right) e^{t/2} \quad \text{for all} \quad t > 0. \tag{2.5.7}$$

The function f_0 is increasing in its arguments. The estimate in (2.5.7) ensures that the time of existence for the approximants, t^*, is independent of n.

Step 3 - Boundedness of $w_{tt}^n(0)$: We will consider $E_1(t)$ as the natural "energy" corresponding to the *time*-differentiated version of the stiffness-only equation ($\iota = k_2 = 0$). For this calculation it is pivotal to establish boundedness of the sequence $\{w_{tt}^n(0)\}_{n=1}^{\infty}$ in $L^2(0, L)$. To that end, it is true that the following holds for all $\phi \in S_n$, $n = 1, 2, \ldots$:

$$\left(w_{tt}^n + D\partial_x^4 w^n - D\partial_x\left[(w_{xx}^n)^2 w_x^n\right] + D\partial_{xx}\left[w_{xx}^n (w_x^n)^2\right] - p, \phi\right) = 0. \tag{2.5.8}$$

We consider $\phi = s_j(x)$, $j = 1, 2, \ldots, n$. Then, multiplying (2.5.8) by $q_j''(t)$, summing over the $j's$, and rearranging the terms we obtain:

$$||w_{tt}^n||^2 = (p, w_{tt}^n) - D(\partial_x^4 w^n, w_{tt}^n) + D(\partial_x([w_{xx}^n]^2 w_x^n), w_{tt}^n) - D(\partial_{xx}([w_x^n]^2 w_{xx}^n), w_{tt}^n). \tag{2.5.9}$$

Owing to the C^3 temporal regularity of w^n, we can take $t = 0$ in the above expression. Therefore, using (i) the expanded version of [**NL Stiffness**] shown in *Remark* 2.4.1, (ii) the Sobolev embedding into $H^1 \hookrightarrow L^\infty$, (iii) and Poincaré inequality for various derivatives, we have:

$$
\begin{aligned}
||w^n_{tt}(0)|| \lesssim ||p(0)|| + ||w^n_{xxx}(0)||\ ||\partial_x^4 w^n(0)||^2 + ||w^n_{xx}(0)||\ ||w^n_{xxx}(0)||^2 \\
+ \left(1 + ||w^n_{xx}(0)||^2\right) ||\partial_x^4 w^n(0)||.
\end{aligned}
$$

The expression on the right-hand side is bounded. Indeed, by (2.5.3), $||\partial_x^4 w^n(0)|| \lesssim ||w_0||_{\mathcal{D}(\mathcal{A})}$. Moreover, by hypothesis, since $p, p_t \in L^2(0,T; L^2(0,L))$, $||p(0)||$ is interpreted as a temporal trace [32], with $||p(0)|| \lesssim ||p||_{H^1(0,T;L^2(0,L))}$. Hence we conclude that

$$
||w^n_{tt}(0)|| \leq f\left(||p||_{H^1(0,T;L^2(0,L))}, ||w_0||_{\mathcal{D}(\mathcal{A})}\right). \tag{2.5.10}
$$

Step 4 - Energy Level 1: Our goal now is to form the $E_1(t)$ energy which will correspond to time differentiation of the stiffness dynamics. We note that time differentiation does not affect the boundary conditions for $w^n(x,t) = \sum_{i=1}^n q_i(t)s_i(x)$. Hence, after proceeding with appropriate integration by parts, isolating conserved quantities, and gathering similar terms, we obtain the a priori identity:

$$
\begin{aligned}
&\frac{1}{2}\frac{d}{dt}\left[||w_{tt}||^2 + D||w_{xxt}||^2 + D||w_{xx}w_{xt}||^2 + D||w_{xxt}w_x||^2\right] \qquad (2.5.11)\\
&\quad = -\frac{d}{dt}\Big[4D(w_x w_{xx}, w_{xt}w_{xxt})\Big] + (p_t, w_{tt}) + 3D(w_{xx}w_{xxt}, w_{xt}^2) + 3D(w_x w_{xt}, w_{xxt}^2).
\end{aligned}
$$

We have omitted the superscript n here and in the estimation below for ease of presentation. The identity above is integrated in time on $(0,t)$, with an eye to utilize a version of Grönwall's inequality.

Remark 2.5.2. As an a priori estimate, the equality above holds for approximate solutions, which are appropriately smooth; this can be seen by operating directly on the ODE system (2.5.5), differentiating in time, multiplying by q_j'' and integrating in time.

Accordingly, we define the energy $E_1^n(t)$ precisely, corresponding to smoother norms for a solution:

$$E_1^n(t) = \frac{1}{2}\left[||w_{tt}^n||^2 + D||w_{xxt}^n||^2 + D||w_{xt}^n w_{xx}^n||^2 + D||w_x^n w_{xxt}^n||^2\right]. \tag{2.5.12}$$

Now, we must bound/absorb the unsigned quantities in the energy identity (2.5.11) above. We first note some important intermediate inequalities. (We have freely used: Young's and Poincaré's inequalities, Sobolev interpolation, and the continuous embedding $H^{1/2^+}(0,L) \hookrightarrow L^\infty(0,L)$.)

1. $3D\left|(w_{xx}w_{xxt}, w_{xt}^2)\right| \leq 3D||w_{xt}||^2_{L^\infty}||w_{xx}||\ ||w_{xxt}|| \lesssim ||w_{xx}||^4 + ||w_{xxt}||^4$

2. $3D\left|(w_x w_{xt}, w_{xxt}^2)\right| \leq 3D||w_x||_{L^\infty}||w_{xt}||_{L^\infty}||w_{xxt}||^2 \lesssim ||w_{xx}||^4 + ||w_{xxt}||^4$

3. $$\begin{aligned}4D\left|(w_x w_{xx}, w_{xt}w_{xxt})\right| &\leq \varepsilon_1||w_x w_{xxt}||^2 + C_{\varepsilon_1}||w_{xx}w_{xt}||^2 \\ &\leq \varepsilon_1||w_x w_{xxt}||^2 + C_{\varepsilon_1}||w_{xt}||^2_{L^\infty}||w_{xx}||^2.\end{aligned}$$

To continue our estimation of 3 above, we interpolate the term $||w_{xt}||^2_{L^\infty}$ as follows:

$$||w_{xt}||^2_{L^\infty} \lesssim ||w_t||^2_{3/2+\epsilon} \lesssim ||w_t||^{1/2-\epsilon}\ ||w_{xxt}||^{3/2+\epsilon}.$$

Substituting the above in 3 and then utilizing Young's inequality in the (p, q) setting we obtain:

$$4D\,|(w_x w_{xx}, w_{xt} w_{xxt})| \leq \varepsilon_1 ||w_x w_{xxt}||^2 + C_{\varepsilon_1} ||w_t||^{1/2-\epsilon}\ ||w_{xxt}||^{3/2+\epsilon}\ ||w_{xx}||^2 \quad (2.5.13)$$
$$\leq \varepsilon_1 ||w_x w_{xxt}||^2 + C_{\varepsilon_1} C_{\varepsilon_p} ||w_t||^{(1/2-\epsilon)q}\ \ ||w_{xx}||^{2q} + C_{\varepsilon_1} \varepsilon_p ||w_{xxt}||^{(3/2+\epsilon)p}.$$

We choose $p > 1$ such that $(3/2 + \epsilon)p = 2$. Hence, by fixing $\epsilon = 1/4$, we obtain $p = 8/7$ and $q = 8$. Inequality in (2.5.13) becomes:

$$4D\,|(w_x w_{xx}, w_{xt} w_{xxt})| \leq \varepsilon_1 ||w_x w_{xxt}||^2 + C_{\varepsilon_1} C_{\varepsilon_p} ||w_t||^4 + C_{\varepsilon_1} C_{\varepsilon_p} ||w_{xx}||^{32} + C_{\varepsilon_1} \varepsilon_p ||w_{xxt}||^2.$$

Choosing ε_1 and ε_p sufficiently small, we can absorb terms by $E_1^n(t)$ on the LHS of (2.5.11). Thus, using (2.5.3) in passing to the limit on the RHS, and invoking the result from (2.5.10), we arrive at the estimate:

$$E_1^n(t) \leq f_1\left(p_t, ||w_0||_{\mathcal{D}(\mathcal{A})}, ||w_1||_{H^2_*}\right) + f_2\left(p, ||w_0||_{\mathcal{D}(\mathcal{A})}, ||w_1||_{H^2_*}\right) t + C \int_0^t \left[E_1^n(\tau)\right]^2 d\tau. \quad (2.5.14)$$

Note that $C > 0$ above *does not depend* on w_0, w_1 or p. The functions f_1 and f_2 are smooth, real-valued functions, increasing in their arguments. In particular, the function f_2 is obtained after we apply (2.5.7) to the norms $||w_{xx}||^4, ||w_t||^4$ and $||w_{xx}||^{32}$ that appear on the RHS of the estimates (1)–(4). Dependence on p we take to mean dependence on the norm $||p||_{L^2(0,t;L^2(0,L))}$ (mutatis mutandis for p_t), as in the previous step.

Hence, using the *nonlinear* version of Grönwall's inequality [27], we obtain a local-in-time estimate:

$$E_1^n(t) \leq \frac{f_1 + f_2 t}{1 - C\left[f_1 t + f_2 t^2\right]} \equiv M_1(t), \quad 0 \leq t < T^* \text{ where } T^* = \sup_{t>0}\left\{C\left[f_1 t + f_2 t^2\right] < 1\right\}. \tag{2.5.15}$$

Remark 2.5.3. Following the assumptions of Theorem 2.5.1, requiring $p \in H^2_{loc}(0,\infty;L^2)$ is done here since the version of Grönwall we utilize for (2.5.14) requires f_1 and f_2 to be continuous functions in time.

Then, for any fixed $T < T^*$, we have that (2.5.15) constitutes a uniform-in-n a priori bound on $E_1^n(t) < M_1^*(T), \quad t \in [0,T]$, where

$$M_1^*(T) = \max_{t\in[0,T]} M_1(t); \tag{2.5.16}$$

this quantity depends only on fixed norms of the data and T.

Remark 2.5.4. It is also important to note that, for a fixed t, $M_1(t)$ is an *increasing* function in $||(w_0,w_1)||_{\mathscr{H}_s}$ that vanishes when $p = w_0 = w_1 = 0$; this is used for continuous dependence.

From (2.5.15), we conclude that the Galerkin approximations satisfy a local-in-time bound by the data on any interval $[0,T]$ with $T < T^*$[4]).

[4]Conversely, given $T > 0$, there is a ball of data small in the sense of $\sum E_i(0)$ for which solutions exist up to T.

Whenever the initial data $(w_0, w_1) \in \mathscr{H}$, as well as p, are fixed, then T^* is fixed; *hence, for the existence portion of the proof of Theorem 2.5.1, we take* $T < T^*$ *fixed and consider* $t \in [0, T]$.

Step 5 - Additional Spatial Regularity: Unlike the standard approach, we cannot obtain the needed additional boundedness of $\partial_x^4 w$ by going back through the equation (with additional regularity of w_{tt} established). To obtain further regularity of solutions, spatial differentiation is used.

Remark 2.5.5. Owing to the high order boundary conditions, one must take care in this process. We note energy identities associated with one spatial differentiation result in problematic trace terms that cannot be controlled by the conservative energetic terms. Moreover, as spatial differentiation produces mixed time-space terms, we do not proceed to obtain an energy estimate in this scenario; rather, we utilize an equipartition multiplier and integrate in space-time, which will provide control of the term

$$||\partial_x^4 w||^2_{L^2(0,t;L^2(0,L))} - ||w_{xxt}||^2_{L^2(0,t;L^2(0,L))}$$

the latter term is controlled by the estimate in the previous step.

To obtain the a priori bound, we multiply the equation by $\partial_x^4 w$ and estimate.

$$\left(w_{tt}, \partial_x^4 w\right) + D\left(\partial_x^4 w, \partial_x^4 w\right) - D\left(\partial_x [w_{xx}^2 w_x], \partial_x^4 w\right) + D\left(\partial_x^2 [w_{xx} w_x^2], \partial_x^4 w\right) = \left(p, \partial_x^4 w\right). \tag{2.5.17}$$

Note that as in Step 3, this can be justified by multiplying the weak ODE form

(2.5.5) by $\lambda_j q_j$ (see [48]). We integrate the above in time on $(0,t)$. For the first term of (2.5.17) we integrate by parts:

$$\int_0^t \left(w_{tt}, \partial_x^4 w\right) d\tau = \int_0^t (w_{xxtt}, w_{xx}) = (w_{xxt}, w_{xx})\Big|_0^t - \int_0^t ||w_{xxt}||^2.$$

For the remaining of the terms in (2.5.17) we identify positive quantities and gather terms.

$$\begin{aligned} &D\int_0^t \left[||\partial_x^4 w||^2 + ||w_x \partial_x^4 w||^2\right] d\tau - \int_0^t ||w_{xxt}||^2 d\tau \\ &= \int_0^t \left[\left(p, \partial_x^4 w\right) - D\left(w_{xx}^3, \partial_x^4 w\right) - 4D\left(w_x w_{xx} w_{xxx}, \partial_x^4 w\right)\right] d\tau - (w_{xxt}, w_{xx})\Big|_0^t. \end{aligned} \tag{2.5.18}$$

We now bound the expressions that appear on the RHS above.

1. $\left|(w_{xxt}, w_{xx})\Big|_0^t\right| \leq ||w_{xxt}(t)||\ ||w_{xx}(t)|| + ||w_{xxt}(0)||\ ||w_{xx}(0)||$

2. $\left|\left(p, \partial_x^4 w\right)\right| \leq\ C_\varepsilon ||p||^2 + \varepsilon ||\partial_x^4 w||^2$

3. $$\begin{aligned} D\left|(w_{xx}^3, \partial_x^4 w)\right| &\leq \delta ||\partial_x^4 w||^2 + C_\delta ||w_{xx}||_{L^6}^6 \\ &\leq \delta ||\partial_x^4 w||^2 + C_\delta ||w_{xx}||_{L^\infty}^4 ||w_{xx}||^2 \\ &\leq \delta ||\partial_x^4 w||^2 + C_\delta ||w_{xx}||_{1/2+\epsilon}^4 ||w_{xx}||^2 \\ &\leq \delta ||\partial_x^4 w||^2 + C_\delta \Big[||w||_4^{1+2\epsilon} ||w_{xx}||^{3-2\epsilon}\Big] ||w_{xx}||^2 \quad \text{(take } \epsilon = 1/4) \\ &\leq \delta ||\partial_x^4 w||^2 + C_\delta \delta_p ||w||_4^{(3/2)p} + C_{\delta_1,\delta_p} ||w||_2^{(9/2)q} \quad \text{(take } p = 4/3) \\ &\leq\ (\delta + C_\delta \delta_p)\, ||\partial_x^4 w||^2 + C_{\delta,\delta_p} ||w_{xx}||^{18} \end{aligned}$$

4. $4D\left|(w_x w_{xx} w_{xxx}, \partial_x^4 w)\right|$

$$\leq \eta||\partial_x^4 w||^2 + C_\eta ||w_x||_{L^\infty}^2 ||w_{xx}||_{L^\infty}^2 ||w_{xxx}||^2$$

$$\leq \eta||\partial_x^4 w||^2 + C_\eta ||w_{xx}||^2 \left[||w_{xx}||^{3/2-\epsilon} ||w||_4^{1/2+\epsilon}\right] [||w_{xx}||\ ||w||_4] \quad (\text{take } \epsilon = 1/4)$$

$$\leq \eta||\partial_x^4 w||^2 + C_\eta \eta_p ||w||_4^{(7/4)p} + C_{\eta,\eta_p} ||w_{xx}||^{(17/4)q} \quad (\text{take } p = 8/7)$$

$$\leq\ (\eta + C_\eta \eta_p)\, ||\partial_x^4 w||^2 + C_{\eta,\eta_p} ||w_{xx}||^{34}.$$

We choose $\varepsilon, \delta, \delta_p, \eta, \eta_p$ so that, upon integration, $\int_0^t ||\partial_x^4 w||^2 d\tau$ is absorbed by the LHS of (2.5.18). Hence, by denoting

$$V(t) = D\left|\left|\partial_x^4 w\right|\right|^2 + D\left|\left|w_x \partial_x^4 w\right|\right|^2,$$

and $V^n(t)$ the above functional evaluated on w^n, we estimate (2.5.18) as:

$$\int_0^t V^n(\tau) d\tau \leq f_3\left(t, p, E_0^n(0), E_1^n(0), E_0^n(t), E_1^n(t)\right) \quad \text{for all } t \in [0,T], \qquad (2.5.19)$$

where we have invoked the estimates from the previous level (2.5.7) and (2.5.15), and $T < T^*$. Again, f_3 is increasing in its arguments, and dependence on p is taken as in the previous sections.

Remark 2.5.6. Note that (2.5.19) *is not a true energy estimate* in the sense of pointwise-in-time control of an "energy". The estimate above highlights the need to first close the higher time estimate for solutions in order to use the equipartition approach.

Based on the boundedness of of $E_0^n(0)$ and $E_1^n(0)$, along with the combination of (2.5.7),(2.5.15), (2.5.19), we deduce that

$$\int_0^t V^n(\tau)d\tau \leq f_3\left(t, p, p_t, ||w_0||_{\mathcal{D}(\mathcal{A})}, ||w_1||_{H^2_*}, M_1^*(T)\right) \quad \text{for all } t \in [0,T]. \quad (2.5.20)$$

Combining (2.5.15) and (2.5.20), we arrive at the final energy estimate for boundedness of

$$||w^n||_{L^2(0,T;\mathcal{D}(\mathcal{A}))} + ||w_t^n||_{L^\infty(0,T;\mathscr{D}(\mathcal{A}^{1/2}))} + ||w_{tt}^n||_{L^\infty(0,T;L^2(0,L))} \leq C(\text{data}, T), \quad (2.5.21)$$

where $T < T^*$ as in (2.5.15) and the dependence on "data" is as in the RHS of (2.5.20). This bound holds for the associated subsequential weak limit points and provides additional compactness below.

Remark 2.5.7. Denoting w as the function corresponding to the weak/weak-* limit above, we see that $w \in L^2(0,T;H^4(0,L))$ and $w_t \in L^2(0,T;H^2_*)$; hence we obtain in the standard way [32] the auxiliary bound for $w \in C([0,T];H^3(0,L))$.

Step 6 - Limit Passage and Weak Solution: With higher a priori bounds in hand for smooth data $w_0 \in \mathcal{D}(\mathcal{A}),\ w_1 \in H^2_*$, we proceed to pass with the limit and construct a weak solution satisfying (2.4.13) with $k_2 = \iota = 0$ and $\sigma = 1$ on any $[0,T]$ for $T < T^*(w_0, w_1, p)$.

From (2.5.21), the Banach–Alaoglu theorem yields existence of a subsequence $\{w^{n_k}\}_{k=1}^\infty$ and associated weak limit point

$$w \in L^2\left(0,T;H^4(0,L)\right) \cap H^1\left(0,T;H^2_*\right) \cap H^2\left(0,T;L^2(0,L)\right), \quad \text{such that} \quad (2.5.22)$$

$$w^{n_k} \rightharpoonup w \in L^2\left(0,T;\mathcal{D}(\mathcal{A})\right); \;\; w_t^{n_k} \rightharpoonup w_t \in L^2\left(0,T;H_*^2\right); \;\; w_{tt}^{n_k} \rightharpoonup w_{tt} \in L^2\left(0,T;L^2\right), \tag{2.5.23}$$

with compactness of the Sobolev embeddings and Aubin–Lions ensuring strong convergence for w_{n_k} in $L^2(0,T;H_*^2)$.

Now, based on Definition 1, in order to identify w as a *weak solution*, it must satisfy the weak formulation (2.4.13) with $k_2 = \iota = 0$ and $\sigma = 1$. Identification for linear terms in (2.4.13) immediately follows from the above weak convergence, whereas the two [**NL Stiffness**] terms require more attention. For $\phi \in H_*^2$, adding and subtracting mixed terms, we obtain (omitting temporal integration):

$$\begin{aligned}
\left([w_x^{n_k}]^2 w_{xx}^{n_k} - w_x^2 w_{xx}, \phi_{xx}\right) &\le \left([w_x^{n_k}]^2 (w_{xx}^{n_k} - w_{xx}), \phi_{xx}\right) + \left(w_{xx}([w_x^{n_k}]^2 - w_x^2), \phi_{xx}\right) \\
&\le ||w_x^{n_k}||_{L^\infty}^2 \left(w_{xx}^{n_k} - w_{xx}, \phi_{xx}\right) + ||\phi_{xx}||\; ||w_{xx}||\; ||[w_x^{n_k}]^2 - w_x^2||_{L^\infty} \\
&\le ||w_{xx}^{n_k}||^2 \left(w_{xx}^{n_k} - w_{xx}, \phi_{xx}\right) + ||\phi_{xx}||\; ||w_{xx}||\; ||w_x^{n_k} + w_x||_{L^\infty} ||w_x^{n_k} - w_x||_{L^\infty} \\
&\le ||w_{xx}||^2 \left(w_{xx}^{n_k} - w_{xx}, \phi_{xx}\right) + 2\; ||\phi_{xx}||\; ||w_{xx}||^3 ||w_x^{n_k} - w_x||_{1/2+\epsilon} \\
&\to 0 \;\; \text{as} \;\; k \to \infty.
\end{aligned}$$

The above calculation requires no additional regularity of solutions, and follows from bounds at the baseline energy level E_0, i.e., $w, w^n \in L^\infty(0,T;H_*^2) \cap W^{1,\infty}(0,T;L^2(0,L))$. Below, we isolate the problematic nonlinear difference, and critically use additional regularity gained in the preceding steps.

$$\begin{aligned}\Big([w_{xx}^{n_k}]^2 w_x^{n_k} - w_{xx}^2 w_x, \phi_x\Big) &\le \Big([w_{xx}^{n_k}]^2 (w_x^{n_k} - w_x), \phi_x\Big) + \Big(w_x([w_{xx}^{n_k}]^2 - w_{xx}^2), \phi_x\Big) \\ &\le ||\phi_x||_{L^\infty} ||w_{xx}^{n_k}||^2 ||w_x^{n_k} - w_x||_{L^\infty} + ||\phi_x||_{L^\infty} ||w_x||_{L^\infty} ||[w_{xx}^{n_k}]^2 - w_{xx}^2|| \\ &\le ||\phi_{xx}||\ ||w_{xx}^{n_k}||^2 ||w_{xx}^{n_k} - w_{xx}|| + ||\phi_{xx}||\ ||w_{xx}||\ ||w_{xx}^{n_k} + w_{xx}||_{L^\infty} ||w_{xx}^{n_k} - w_{xx}|| \\ &\le ||\phi_{xx}||\ ||w_{xx}||^2 ||w_{xx}^{n_k} - w_{xx}|| + 2\ ||\phi_{xx}||\ ||w_{xx}||\ ||w_{xxx}||\ ||w_{xx}^{n_k} - w_{xx}|| \\ &\to 0 \ \text{ as } \ k \to \infty.\end{aligned}$$

We emphasize the need for strong convergence for $w_{xx}^{n_k}$ in $L^2(0,T;L^2(0,T))$ obtained through compactness of the higher estimates.

Remark 2.5.8. Algebraic manipulations of the difference $[w_{xx}^{n_k}]^2 w_x^{n_k} - w_{xx}^2 w_x$ reveal a clear compactness gap for limit passage at the level of only $||w_{xx}^{n_k}||$ boundedness. An alternative approach for the identification of limit points for $\{[w_{xx}^{n_k}]^2 w_x^{n_k}\}_{k=1}^\infty$ (which uniformly bounded in L^1), would be to utilize the Dunford–Pettis weak compactness criterion in L^1. However, associated multiplier estimates bring about non-trivial commutators corresponding to the quasilinear nature of [**NL Stiffness**].

We conclude that the limit point w, as above, satisfies the weak formulation (2.4.13) with $k_2 = \iota = 0$ and $\sigma = 1$, and thus, it is a *weak solution*.

Step 7 - Strong Solution and Free Boundary Condition: With a weak solution $w(x,t)$ in hand corresponding to smooth initial data, we have immediately that the solution is strong, by Definition 3 and the regularity afforded by (2.5.23). This concludes the proof of Theorem 2.5.1. □

Naturally, we would like to show that the strong solution constructed above satisfies the PDE pointwise, as well as the higher order boundary conditions.

Corollary 2.5.2. *Strong solutions $w(x,t)$ as described in Definition 3, satisfy equation* (2.4.1) *with $\sigma = 1$ and $\iota = k_2 = 0$ almost everywhere in space and in time. Additionally, they satisfy the free boundary conditions: $w_{xx}(L,t) = w_{xxx}(L,t) = 0$ for all $0 \leq t \leq T$.*

Proof of Corollary 2.5.2. The weak limit w constructed above satisfies:

$$(w_{tt}, \phi) + D(w_{xx}, \phi_{xx}) + D(w_{xx}^2 w_x, \phi_x) + D(w_x^2 w_{xx}, \phi_{xx}) = (p, \phi), \quad \forall \phi \in H_*^2, \quad a.e.\ t. \tag{2.5.24}$$

Having in hand the regularity given in (2.5.22), we undo integration by parts in (2.5.24) evaluated on test functions to obtain the strong form of the PDE. That is:

$$\Big(w_{tt} + D\partial_x^4 w - D\partial_x\Big[w_{xx}^2 w_x\Big] + D\partial_{xx}\Big[w_{xx} w_x^2\Big] - p, \phi\Big) = 0, \quad \forall \phi \in C_0^\infty(0,L).$$

Via density, we have:

$$w_{tt} + D\partial_x^4 w - D\partial_x\Big[w_{xx}^2 w_x\Big] + D\partial_{xx}\Big[w_{xx} w_x^2\Big] = p \quad a.e.\ x, \quad a.e.\ t, \tag{2.5.25}$$

and thus the PDE in (2.4.1) is satisfied *a.e.* x pointwise for *a.e.* t.

Since $w \in H_*^2$ by construction, we must verify the free boundary conditions. Undoing the integration by parts procedure and invoking (2.5.25) results the following boundary terms:

$$\phi_x(L)\left(w_{xx}(L)+w_x^2(L)w_{xx}(L)\right)-\phi(L)\left(w_{xxx}(L)+w_x(L)w_{xx}^2(L)+w_x^2(L)w_{xxx}(L)\right)=0, \tag{2.5.26}$$

for all $\phi \in H_*^2$, holding *a.e.* in t. But, as in Remark 2.5.7, $w \in C([0,T];H^3(0,L))$, and so we can write:

$$\phi(L)(1+w_x^2(L))w_{xxx}(L)=\phi_x(L)\left(w_{xx}(L)+w_x^2(L)w_{xx}(L)\right)-\phi(L)w_x(L)w_{xx}^2(L),$$

where the RHS is continuous function of time. Now, consider the subclass of $\phi \in H_0^1 \cap H_*^2 \subseteq H_*^2$. Then,

$$w_{xx}(L)\left(1+w_x^2(L)\right)\phi_x(L)=0 \ \text{ for all such } \phi.$$

By the surjectivity of the trace theorem, there exists one function so that $\phi_x(L) \neq 0$, and thus

$$w_{xx}(L)\left(1+w_x^2(L)\right)=0 \implies w_{xx}(L)=0.$$

Now, consider $\phi \in H_*^2$. Again, by the surjectivity of the trace theorem, there exists at least one ϕ so that $\phi(L) \neq 0$. Using this ϕ and the fact that $w_{xx}(L)=0$, (2.5.26) yields:

$$w_{xxx}(L)\left(1+w_x^2(L)\right)=0 \implies w_{xxx}(L)=0.$$

Thus, we have verified that the free boundary terms $w_{xx}(L)=w_{xxx}(L)=0$

are satisfied. $\square$

Remark 2.5.9. It is particularly important that strong solutions remain in $\mathscr{H}_s \equiv \mathcal{D}(\mathcal{A}) \times \mathscr{D}(\mathcal{A}^{1/2})$ for data (w_0, w_1) emanating therefrom—namely, exhibiting regularity and satisfying all four boundary conditions. This, for instance, allows us to use the Poincaré inequality repeatedly on the solution, so, for a strong solution w, we have the norm equivalences: $||\partial_x^4 w|| \sim ||w||_{H^4(0,L)} \sim ||w||_{\mathcal{D}(\mathcal{A})}$.

2.5.3.2 Uniqueness and Continuous Dependence

Now, consider two strong solutions, w and v whose difference $z = w - v$ satisfies:

$$z_{tt} + D\partial_x^4 z - D\partial_x \left(w_{xx}^2 w_x - v_{xx}^2 v_x\right) + D\partial_x^2 \left(w_{xx} w_x^2 - v_{xx} v_x^2\right) = 0, \tag{2.5.27}$$

as well as the strong form of the boundary conditions at $x = 0$ and $x = L$ and associated initial conditions $z_0 = w_0 - v_0$ and $z_1 = w_1 - v_1$. We consider the dynamics above on $t \in [0, T]$, where $T < T^* = \min\{T^*(w_0, w_1),\ T^*(v_0, v_1)\}$. We multiply (2.5.27) by z_t and integrate over $x \in (0, L)$.

For linear terms we have standard conserved quantities, $||z_t||^2$; $D||z_{xx}||^2$. We now take a closer look at the nonlinear differences. Note that the regularity of strong solutions in Definition 3 is sufficient—specifically $w_t \in L^2(0, T; H_*^2)$—to permit the calculations below.

1. $\left(\partial_x^2\left[w_{xx}w_x^2\right], z_t\right) - \left(\partial_x^2\left[v_{xx}v_x^2\right], z_t\right)$

$$= \left(w_{xx}w_x^2 - w_x^2 v_{xx}, z_{xxt}\right) + \left(w_x^2 v_{xx} - v_{xx}v_x^2, z_{xxt}\right).$$

Examining each of the resulting terms above yields:

(i) $\left(w_{xx}w_x^2 - w_x^2 v_{xx}, z_{xxt}\right) = \left(w_x^2, z_{xx}z_{xxt}\right) = \dfrac{1}{2}\dfrac{d}{dt}||w_x z_{xx}||^2 - \left(w_x w_{xt}, z_{xx}^2\right)$

(ii) $\left(w_x^2 v_{xx} - v_{xx}v_x^2, z_{xxt}\right) = \left(v_{xx}\left[w_x^2 - v_x^2\right], z_{xxt}\right) = \left(v_{xx}\left[w_x + v_x\right], z_x z_{xxt}\right).$

2. $-\left(\partial_x\left[w_{xx}^2 w_x\right], z_t\right) + \left(\partial_x\left[v_{xx}^2 v_x\right], z_t\right) = \left(w_{xx}^2 w_x - w_{xx}^2 v_x, z_{xt}\right) + \left(w_{xx}^2 v_x - v_{xx}^2 v_x, z_{xt}\right)$

Like before, we examine each term separately:

(i) $\left(w_{xx}^2 w_x - w_{xx}^2 v_x, z_{xt}\right) = \left(w_{xx}^2, z_x z_{xt}\right) = \dfrac{1}{2}\dfrac{d}{dt}||w_{xx}z_x||^2 - \left(w_{xx}w_{xxt}, z_x^2\right)$

(ii) $\left(w_{xx}^2 v_x - v_{xx}^2 v_x, z_{xt}\right) = \left(v_x\left[w_{xx}^2 - v_{xx}^2\right], z_{xt}\right) = \left(v_x\left[w_{xx} + v_{xx}\right], z_{xx}z_{xt}\right).$

Combining the linear terms along with 1 and 2 we obtain:

$$\begin{aligned}
&\frac{1}{2}\frac{d}{dt}\left[||z_t||^2 + D||z_{xx}||^2 + D||w_x z_{xx}||^2 + D||w_{xx}z_x||^2\right] \\
&\quad = D\left(w_x w_{xt}, z_{xx}^2\right) - D\left(v_{xx}\left[w_x + v_x\right], z_x z_{xxt}\right) \\
&\quad + D\left(w_{xx}w_{xxt}, z_x^2\right) - D\left(v_x\left[w_{xx} + v_{xx}\right], z_{xx}z_{xt}\right).
\end{aligned} \tag{2.5.28}$$

The expression above cannot be directly estimated, but we exploit symmetry in the polynomial nature of the nonlinearity by swapping the roles of w and v in the previous calculation (equivalent to subtracting v from w), adding the two identities, yielding the (now) symmetric identity:

$$
\begin{aligned}
\frac{d}{dt}\Big[||z_t||^2 + D||z_{xx}||^2\Big] + \frac{D}{2}\frac{d}{dt}\Big[||w_x z_{xx}||^2 + ||v_x z_{xx}||^2 + ||w_{xx} z_x||^2 + ||v_{xx} z_x||^2\Big] \\
= D\Big(w_x w_{xt} + v_x v_{xt}, z_{xx}^2\Big) + D\Big(w_{xx} w_{xxt} + v_{xx} v_{xxt}, z_x^2\Big) \\
-D\Big(\left[w_{xx} + v_{xx}\right]\left[w_x + v_x\right], z_x z_{xxt} + z_{xx} z_{xt}\Big).
\end{aligned} \tag{2.5.29}
$$

Now, the third term in the above line sees z-regularity higher than that appearing in the "energetic" (i.e., positive, conservative) portion of the identity. The key step is to rewrite this term, moving time derivatives onto individual trajectories treated as coefficients—so as to exploit bounds in higher norms for individual trajectories, as well as the particular quadratic factorization appearing here.

$$
\begin{aligned}
D\Big(\left[w_{xx} + v_{xx}\right]\left[w_x + v_x\right], z_x z_{xxt} + z_{xx} z_{xt}\Big) = D\frac{d}{dt}\Big(\left(w_{xx} + v_{xx}\right)\left(w_x + v_x\right), z_x z_{xx}\Big) \\
- D\Big(\partial_t\left[(w_{xx} + v_{xx})(w_x + v_x)\right], z_x z_{xx}\Big).
\end{aligned}
$$

Denote:

$$
E(t) = ||z_t||^2 + D||z_{xx}||^2 + \frac{D}{2}\Big[||w_x z_{xx}||^2 + ||v_x z_{xx}||^2 + ||w_{xx} z_x||^2 + ||v_{xx} z_x||^2\Big].
$$

Then, (2.5.29) becomes upon temporal integration:

$$
\begin{aligned}
E(t) = E(0) &- D\left(\left(w_{xx}+v_{xx}\right)\left(w_x+v_x\right), z_x z_{xx}\right)\Big|_0^t \\
&+ \int_0^t \Big[D\left(w_x w_{xt} + v_x v_{xt}, z_{xx}^2\right) + D\left(w_{xx} w_{xxt} + v_{xx} v_{xxt}, z_x^2\right) \\
&+ D\Big([w_{xxt}+v_{xxt}][w_x+v_x], z_x z_{xx}\Big) + D\Big([w_{xx}+v_{xx}][w_{xt}+v_{xt}], z_x z_{xx}\Big)\Big] d\tau.
\end{aligned}
$$

The RHS terms are estimated in the following way, using the Sobolev embeddings and Poincaré inequality, with an eye to use Grönwall's inequality:

1. $$
\begin{aligned}
D\left|\left(w_x w_{xt} + v_x v_{xt}, z_{xx}^2\right)\right| &\leq ||w_x w_{xt} + v_x v_{xt}||_{L^\infty} ||z_{xx}||^2 \\
&\lesssim \Big(||w_{xx}||\,||w_{xxt}|| + ||v_{xx}||\,||v_{xxt}||\Big)||z_{xx}||^2
\end{aligned}
$$

2. $$
\begin{aligned}
D\left|\left(w_{xx} w_{xxt} + v_{xx} v_{xxt}, z_x^2\right)\right| &\leq ||z_x||_{L^\infty}^2 \Big(||w_{xx}||\,||w_{xxt}|| + ||v_{xx}||\,||v_{xxt}||\Big) \\
&\lesssim \Big(||w_{xx}||\,||w_{xxt}|| + ||v_{xx}||\,||v_{xxt}||\Big)||z_{xx}||^2
\end{aligned}
$$

3. $$
\begin{aligned}
D\left|\left([w_{xxt}+v_{xxt}][w_x+v_x], z_x z_{xx}\right)\right| &\leq ||w_x+v_x||_{L^\infty}\,||z_x||_{L^\infty}\,||w_{xxt}+v_{xxt}||\,||z_{xx}|| \\
&\lesssim \left(||w_{xx}|| + ||v_{xx}||\right)\left(||w_{xxt}|| + ||v_{xxt}||\right)||z_{xx}||^2
\end{aligned}
$$

4. $$
\begin{aligned}
D\left|\left([w_{xx}+v_{xx}][w_{xt}+v_{xt}], z_x z_{xx}\right)\right| &\leq ||w_{xx}+v_{xx}||\,||z_x||_{L^\infty}\,||w_{xt}+v_{xt}||_{L^\infty}\,||z_{xx}|| \\
&\lesssim \left(||w_{xx}|| + ||v_{xx}||\right)\left(||w_{xxt}|| + ||v_{xxt}||\right)||z_{xx}||^2
\end{aligned}
$$

5. $D\,|([w_{xx}+v_{xx}][w_x+v_x]z_x, z_{xx})|$

$\le C_{\varepsilon_1}(w,v)||z_x||^2 + \varepsilon_1||z_{xx}||^2$

$\lesssim C_{\varepsilon_1}(w,v)||z||\,||z_{xx}|| + \varepsilon_1||z_{xx}||^2$

$\le C_{\varepsilon_1,\varepsilon_2}(w,v)||z||^2 + (\varepsilon_1+\varepsilon_2)||z_{xx}||^2$

$\lesssim C_{\varepsilon_1,\varepsilon_2}(w,v)\left[\int_0^t ||z_t||^2 d\tau + ||z(0)||^2\right] + (\varepsilon_1+\varepsilon_2)||z_{xx}||^2,$

where above we have used interpolation and H^2_* norm equivalence in the second inequality, and the fundamental theorem of calculus in the fourth line. The dependence of C above is in the sense that $C(w,v) \equiv C\left(||w_{xxx}+v_{xxx}||\,||w_{xx}+v_{xx}||\right) \le C\left(\sup_{0\le t\le T}\left[||w(t)||_3^2 + ||v(t)||_3^2\right]\right)$.

Thus, choosing $\varepsilon_1, \varepsilon_2$ sufficiently small, and putting 1–5 together, we obtain:

$$E(t) \le c(1+C(w,v))E(0) + C(w,v)\int_0^t E(\tau)d\tau + \int_0^t K(w,v)E(\tau)d\tau. \qquad (2.5.30)$$

We again note the dependence of $K(w,v)$ in the sense of:

$$K(w,v) \equiv K\Big(||w_{xx}+v_{xx}||\,||w_{xxt}+v_{xxt}||\Big) \le K\Big(||w||_2^2, ||w_t||_2^2, ||v||_2^2, ||v_t||_2^2\Big).$$

The constant c in (2.5.30) does not depend on the initial data, nor the trajectories w, v.

Finally, we note the $C([0,T])$ boundedness (for $T < T^*(\text{data}_w, \text{data}_v)$) of the quantities $C(w,v),\ K(w,v)$ from the regularity of strong solutions, along with Remark 2.5.7 on the individual trajectories, $(w, w_t),\ (v, v_t)$. Taking $\sup_{[0,T]}$, we obtain:

$$E(t) \leq \mathcal{C}_1 E(0) + \mathcal{C}_2 \int_0^t E(\tau) d\tau,$$

where $t \in [0,T]$ and we have the dependencies

$$\mathcal{C}_i\Big(||(w_0, w_1)||_{\mathscr{H}_s}, ||(v_0, v_1)||_{\mathscr{H}_s}, ||p||_{H^1(0,T;L^2(0,L))} \Big).$$

The standard Grönwall lemma yields:

$$E(t) \leq \mathcal{C}_1 E(0) e^{\mathcal{C}_2 t}, \quad t \in [0,T]. \tag{2.5.31}$$

Uniqueness of strong solutions follows immediately, since if $(w_0, w_1) = (v_0, v_1)$, the times of existence are identified and $E(0) = 0$ gives $z = 0$ in the sense of $L^2(0,T; L^2(0,L))$ for all valid T.

Continuous dependence also follows from (2.5.31), but is somewhat more subtle. Upon inspection, the constants above $\mathcal{C}_i$ are continuous, real-valued, positive functions of their arguments. Namely, the $\mathcal{C}_i(\cdots),\ i = 1,2$ are bounded when restricting to $\overline{B_R(\mathscr{H}_s)}$—see Remark 2.5.4. Hence, for $(w_n, w_{n,t}), (w, w_t) \in \overline{B_R(\mathscr{H}_s)}$ we see that $z_n = w - w_n$ has the property that

$$(z_n(0), z_{n,t}(0)) \to (0,0) \in \mathscr{H} \implies (z_n, z_{n,t}) \to (0,0) \in C([0,T]; \mathscr{H}).$$

2.6 The Case with Nonlinear Inertia: $\sigma = \iota = 1$, $k_2 > 0$

2.6.1 Precise Statement of the Theorem

Theorem 2.6.1. *Take $\sigma = \iota = 1$ and $k_2 > 0$, and consider $p \in H^3_{loc}(0,\infty; L^2(0,L))$. For initial data $(w_0, w_1) \in \mathcal{D}(\mathcal{A}^2)^2$, strong solutions exist up to some time $T^*(w_0, w_1, p)$ and are unique on their existence interval. For all $t \in [0, T^*)$, a solution obeys the energy identity*

$$E(t) + k_2 \int_0^t ||w_{xxt}||^2_{L^2(0,L)} = E(0) + \int_0^t (p, w_t)_{L^2(0,L)} d\tau,$$

where $E(t)$ is as in (2.4.5) with $\sigma = \iota = 1$.

Restricting to $B_R(\mathscr{D}(\mathcal{A}^2)^2)$, for any $T < T^*(R,p)$ solutions depend continuously on the data in the sense of $C([0,T]; \mathscr{H})$ with an estimate on the difference of two trajectories, $z = w^1 - w^2$:

$$\sup_{t \in [0,T]} \Big|\Big|(z(t), z_t(t))\Big|\Big|_{\mathscr{H}} \leq C(R,T) \Big|\Big|\Big(z(0), z_t(0)\Big)\Big|\Big|_{\mathscr{H}}, \quad \forall\, t \in [0,T].$$

Remark 2.6.1. The dependence $T^* = T^*\Big(||(w_0, w_1)||_{\mathcal{D}(\mathcal{A}^2) \times \mathcal{D}(\mathcal{A}^2)}, ||p||_{H^3(0,T;L^2(0,L))}\Big)$.

2.6.2 Proof Outline

For this proof we utilize a modified strategy from the previous section, as the presence of inertia (and damping) change the sequence of multipliers. Indeed, with the addition of damping (as per the discussion above), we can obtain a sequence of true energy estimates at various levels, and again exploit the techniques in the proof of the *Theorem* 2.5.1 after closing estimates. Due to the structure of [**NL Inertia**], even in the presence of velocity-regularizing Kelvin–Voigt damping, further additional regularity (hence higher estimates) will be needed in the construction of solutions and their uniqueness.

2.6.3 Proof of Theorem 2.6.1

2.6.3.1 Existence

The setup here is the same as in Section 2.5.3.1. Since the inertial term and damping ($\iota = 1$ and $k_2 > 0$) are additional terms to the stiffness equation, we will proceed through the relevant calculations corresponding only to [**NL Inertia**] ([**NL Stiffness**] calculations are unchanged). *Kelvin–Voigt damping* appears in the final estimates with no discussion, owing to its linearity.

Step 1 - Approximants: Again, consider smooth data, $w_0 \in \mathcal{D}(\mathcal{A}^2)$ and $w_1 \in \mathcal{D}(\mathcal{A}^2)$, and take Fourier partial sums as $\{w_0^n\}_{n=1}^{\infty}$ and $\{w_1^n\}_{n=1}^{\infty}$. Then, as before, we have:

$$w_0^n \to w_0 \ \text{ in } \mathcal{D}(\mathcal{A}^2); \quad w_1^n \to w_1 \ \text{ in } \mathcal{D}(\mathcal{A}^2) \tag{2.6.1}$$

and

$$w^n(x,t) \coloneqq \sum_{j=1}^{n} q_j(t) s_j(x),$$

for $q_j(t)$ smooth functions of time. Throughout this section we freely use $u^n =$

$-(1/2)\int_0^x [w_x^n]^2 d\xi$.

From the weak form, (2.4.13) (this time taken with $\iota = 1$ and $k_2 > 0$), we construct the corresponding matrix system using $\mathcal{S}_{ijkl}$ from (2.5.4) and

$$\mathcal{I}_{ijkl} = \left(\int_0^x \phi_{i,x}\phi_{j,x} d\xi, \int_0^x \phi_{k,x}\phi_{l,x} d\xi \right). \tag{2.6.2}$$

Remark 2.6.2. The following calculation connects $\mathcal{I}_{ijkl}$ back to the weak form (2.4.13):

$$\begin{aligned}\mathcal{I}_{ijkl} &= -\int_0^L \left[\left(\partial_x \int_x^L \int_0^\xi \phi_{i,x}\phi_{j,x} d\xi_2 d\xi \right) \int_0^x \phi_{k,x}\phi_{l,x} d\xi \right] dx \\ &= \int_0^L \left[\left(\int_x^L \int_0^\xi \phi_{i,x}\phi_{j,x} d\xi_2 d\xi \right) \phi_{k,x}\phi_{l,x} \right] dx.\end{aligned}$$

Analogously to (2.5.5), we then have the separated form of the ODE system:

$$\begin{aligned} q_i''(s_i, s_j) + \left[q_i''(q_i)^2 + (q_i')^2 q_i \right] \mathcal{I}_{iiij} + k_2 q_i' \left[\delta_i^4(s_i, s_j) \right] \\ + D q_i \left[k_i^4(s_i, s_j) \right] + D q_i^3 \left[\mathcal{S}_{iiij} + \mathcal{S}_{jiii} \right] = (p, s_j). \end{aligned} \tag{2.6.3}$$

Although this ODE system is not a traditional evolution (it is quasilinear in time), it is polynomially nonlinear in the q_i's. Thus, via the implicit function theorem and for sufficiently small data, we have *local* solvability for q_i'' in terms of the other quantities and lower order terms in q (this is due to the invertibility of the "mass matrix"). Therefore, local-in-time, there are $C^4(0, t^*(n))$ solutions, again noting the regularity assumption on p.

Step 2 - Energy Level 0: For this step we examine the inertial term that corresponds to **Level 0** which was described in **Step 2** of Section 2.5.3.1 for the stiffness-only equation ($\iota = k_2 = 0$). We note that in the upcoming calculations we will omit the differential of the variable in the integral if this is obvious by the limits of the integration.

$$\left(\partial_x \left[w_x \int_x^L u_{tt}\right], w_t\right) = -\left(\int_x^L u_{tt}, w_x w_{xt}\right) = -\left(\int_x^L u_{tt}, \partial_x \int_0^x w_x w_{xt}\right)$$
$$= (u_{tt}, u_t) = \frac{1}{2}\frac{d}{dt}||u_t||^2.$$

Denote $\mathcal{E}_0^n(t) = E_0^n(t) + I_0^n(t) \geq 0$, where $I_0^n(t) = \frac{1}{2}||u_t^n||^2$ and $E_0^n(t)$ is as in (2.5.6). Estimating conservatively, we have:

$$\mathcal{E}_0^n(t) + k_2 \int_0^t ||w_{xxt}^n||^2 d\tau \leq \mathcal{E}_0^n(0) + \frac{1}{2}\int_0^t ||p||^2 + \frac{1}{2}\int_0^t \mathcal{E}_0^n(\tau) d\tau \quad \text{for all} \quad t > 0. \tag{2.6.4}$$

From (2.6.1) and $u_t = -\int_0^x w_x w_{xt}$, so $||u_t|| \lesssim ||w||_{\mathscr{D}(\mathcal{A}^{1/2})}||w_t||_{\mathscr{D}(\mathcal{A}^{1/2})}$. It is immediate that $\{\mathcal{E}_0^n(0)\}_{n=1}^\infty$ is uniform-in-n controlled by $||(w_0, w_1)||_{\mathscr{D}(\mathcal{A}^{1/2})}$. Hence, the standard Grönwall inequality yields:

$$\mathcal{E}_0^n(t) \leq g_0\left(p, ||w_0||_{\mathcal{D}(\mathcal{A})}, ||w_1||_{H_*^2}\right) e^{t/2} \quad \text{for all} \quad t > 0. \tag{2.6.5}$$

The function g_0 is analogous as that described in (2.5.7).

Step 3 - Uniform Boundedness of Initial Inertia: To utilize the additional a priori bound described in the next step, we need the quantity $||w_{tt}^n(0)||^2 + ||u_{tt}^n(0)||^2$ to be uniformly bounded by appropriate norms on w_0 and w_1. Our proof of uniform $L^2(0, L)$ boundedness $\{w_{tt}^n(0)\}_{n=1}^\infty$ in **Step 3** in the proof of *Theorem* 2.5.1 *cannot be* *invoked for this calculation*, since additional terms now appear in the equation for $\iota = 1,\ k_2 > 0$.

From the equation, approximate solutions satisfy the relation

$$\begin{aligned} &||w_{tt}^n||^2 + D(\partial_x^4 w^n, w_{tt}^n) + k_2\left(\partial_x^4 w_t^n, w_{tt}^n\right) - D(\partial_x([w_{xx}^n]^2 w_x^n), w_{tt}^n) \\ &\quad + D(\partial_{xx}([w_x^n]^2 w_{xx}^n), w_{tt}^n) + \left(\partial_x\left[w_x^n \int_x^L u_{tt}^n\right], w_{tt}^n\right) = (p, w_{tt}^n). \end{aligned} \tag{2.6.6}$$

Examining the inertial term:

$$\left(\partial_x\left[w_x^n \int_x^L u_{tt}^n\right], w_{tt}^n\right) = -\left(u_{tt}^n, \int_0^x w_x^n w_{xtt}^n\right) = ||u_{tt}^n||^2 + \left(u_{tt}^n, \int_0^x [w_{xt}^n]^2\right),$$

where we used the expansion of u_{tt} in terms of w as in (2.4.4). Combining everything, we have the identity:

$$\begin{aligned} ||w_{tt}^n||^2 + ||u_{tt}^n||^2 = {} & (p, w_{tt}^n) - \left(u_{tt}^n, \int_0^x [w_{xt}^n]^2\right) - k_2\left(\partial_x^4 w_t^n, w_{tt}^n\right) \\ & - D(\partial_x^4 w^n, w_{tt}^n) + D(\partial_x([w_{xx}^n]^2 w_x^n), w_{tt}^n) - D(\partial_{xx}([w_x^n]^2 w_{xx}^n), w_{tt}^n). \end{aligned} \tag{2.6.7}$$

Since approximate solutions (and p) are continuous in time, we take the time-trace at $t = 0$ in (2.6.7) and use Young's inequality to obtain the estimate:

$$\begin{aligned} ||w_{tt}^n(0)||^2 + ||u_{tt}^n(0)||^2 \le {} & \delta||u_{tt}^n(0)||^2 + c_\delta||w_{xxt}^n(0)||^4 + \varepsilon||w_{tt}^n(0)||^2 \\ & + c_\varepsilon\Big[||p(0)||^2 + ||\partial_x^4 w_t^n(0)||^2 + ||\partial_x^4 w^n(0)||^4||w_{xxx}^n(0)||^2 \\ & + ||w_{xx}^n(0)||^2||w_{xxx}^n(0)||^4 + \left(1 + ||w_{xx}^n(0)||^4\right)||\partial_x^4 w^n(0)||^2\Big]. \end{aligned}$$

Choosing sufficiently small δ and ε, and using (2.6.1), we can finally conclude that

$$||w_{tt}^n(0)||^2 + ||u_{tt}^n(0)||^2 \le C\left(||w_0||_{\mathcal{D}(\mathcal{A})}, ||w_1||_{\mathcal{D}(\mathcal{A})}, p(0)\right). \tag{2.6.8}$$

This fact will be used below in the next energy level.

Step 4 - Energy Level 1: In this step we proceed with examining the inertial term from the *Energy Level 1* estimate described in **Step 3** of Section 2.5.3.1. Our aim is to control the conserved quantity $||u_{tt}||^2$, corresponding to a (formal) time differentiation of the equations. Differentiating the inertial term in time and multiplying by w_{tt} we form:

$$\begin{aligned}\left(\partial_{xt}\left[w_x\int_x^L u_{tt}\right], w_{tt}\right) &= -\left(w_{xt}\int_x^L u_{tt}, w_{xtt}\right) - \left(w_x\int_x^L u_{ttt}, w_{xtt}\right)\\ &\equiv \qquad\quad \mathcal{I}_1 \qquad\quad + \qquad\quad \mathcal{I}_2.\end{aligned}$$

For $\mathcal{I}_2$, we have $\mathcal{I}_2 = -\left(\int_x^L u_{ttt}, w_x w_{xtt}\right) = -\left(u_{ttt}, \int_0^x w_x w_{xtt}\right)$. Recalling $u_{tt}(x) = -\int_0^x \left[w_{xt}^2 + w_x w_{xtt}\right] d\xi$, we obtain:

$$\mathcal{I}_2 = (u_{ttt}, u_{tt}) + \left(u_{ttt}, \int_0^x w_{xt}^2\right) = \frac{1}{2}\frac{d}{dt}||u_{tt}||^2 + \frac{d}{dt}\left(u_{tt}, \int_0^x w_{xt}^2\right) - 2\left(u_{tt}, \int_0^x w_{xt}w_{xtt}\right).$$

The second term above will be estimated so that it can be absorbed by pointwise-in-time conserved quantities. The third term is identical to $\mathcal{I}_1$, and

$$\mathcal{I}_1 = \left(\int_0^x \left[w_{xt}^2 + w_x w_{xtt}\right], \int_0^x w_{xt}w_{xtt}\right) = \frac{1}{4}\frac{d}{dt}\left|\left|\int_0^x w_{xt}^2\right|\right|^2 + \left(\int_0^x w_x w_{xtt}, \int_0^x w_{xt}w_{xtt}\right).$$

Combining these calculations, we obtain:

$$\frac{d}{dt}\left[\frac{1}{2}||u_{tt}||^2 + \frac{3}{4}\left|\left|\int_0^x w_{xt}^2\right|\right|^2 + \left(u_{tt}, \int_0^x w_{xt}^2\right)\right] = -3\left(\int_0^x w_x w_{xtt}, \int_0^x w_{xt} w_{xtt}\right). \tag{2.6.9}$$

Utilizing once more the approximate inextensibility relation, we can rewrite:

$$\begin{aligned}&\frac{d}{dt}\left[\frac{1}{2}||u_{tt}||^2 + \frac{3}{4}\left|\left|\int_0^x w_{xt}^2\right|\right|^2 + \left(u_{tt}, \int_0^x w_{xt}^2\right)\right]\\ =&3\left(u_{tt}, \int_0^x w_{xt} w_{xtt}\right) + 3\left(\int_0^x w_{xt}^2, \int_0^x w_{xt} w_{xtt}\right).\end{aligned}$$

Poincaré inequality and the Sobolev embedding into L^∞ yields:

$$\begin{aligned}&\frac{d}{dt}\left[\frac{1}{2}||u_{tt}||^2 + \frac{3}{4}\left|\left|\int_0^x w_{xt}^2\right|\right|^2 + \left(u_{tt}, \int_0^x w_{xt}^2\right)\right]\\ \leq C_{\varepsilon_1}&\left[||u_{tt}||^4 + \left|\left|\int_0^x w_{xt}^2\right|\right|^4\right] + C_{\varepsilon_2}||w_{xxt}||^4 + (\varepsilon_1 + \varepsilon_2)\,||w_{xxtt}||^2.\end{aligned} \tag{2.6.10}$$

For the unsigned, conservative term on the LHS we utilize Young's inequality with precise coefficients:

$$\left|\left(u_{tt}, \int_0^x w_{xt}^2\right)\right| \leq \frac{3}{8}||u_{tt}||^2 + \frac{2}{3}\left|\left|\int_0^x w_{xt}^2\right|\right|^2,$$

which is sufficient for absorption on the LHS of (2.6.10).

Now, let us introduce more notation for the estimate resulting from the above formal calculations:

$$I_1^n(t) = \frac{1}{2}||u_{tt}^n||^2 + \frac{3}{4}\left|\left|\int_0^x \left[w_{xt}^2\right]^n\right|\right|^2 \quad \text{and} \quad \mathcal{E}_1^n(t) = E_1^n(t) + I_1^n(t), \tag{2.6.11}$$

with $E_1^n(t)$ given in the stiffness analysis by (2.5.12). Compiling everything together and absorbing damping terms on the RHS, we then have that the approximate solutions w^n satisfy:

$$\begin{aligned} \mathcal{E}_1^n(t) + k_2\int_0^t ||w_{xxtt}^n||^2 \leq g_1\left(p_t, ||w_0||_{\mathcal{D}(\mathcal{A})}, ||w_1||_{\mathcal{D}(\mathcal{A})}\right) + g_2\left(p, ||w_0||_{\mathcal{D}(\mathcal{A})}, ||w_1||_{H_*^2}\right)t \\ + C\int_0^t \left[\mathcal{E}_1^n(\tau)\right]^2 d\tau. \end{aligned} \tag{2.6.12}$$

The dependencies for g_1 and g_2 follow after the application of (2.6.5) and (2.6.8). Note that $C > 0$ here *does not depend* on w_0, w_1 or p. Dependence on p is taken in the sense of (2.5.14).

Step 5 - Energy Level 2: In contrast to what was done in the stiffness-only estimate for **Step 5** of Section 2.5.3, we proceed to obtain an actual *energy estimate* for higher spatial regularity. Indeed, the inclusion of the strong damping $k_2 > 0$ allows us to consider improved regularity of the solution by employing the multiplier $\partial_x^4 w_t$, not permissible when $k_2 = 0$. Thus the calculations for the from Section 2.5.3 are modified below.

We proceed by multiplying the equation by $\partial_x^4 w_t$ and spatially integrating, with appropriate integration by parts. Here it is important to take note of the boundary conditions associated to eigenfunctions in Section 2.4.5 and hence to approximants w^n and all of their time derivatives as well.

Isolating conserved quantities and gathering terms yields:

$$\frac{1}{2}\frac{d}{dt}\left[||w_{xxt}||^2 + D||\partial_x^4 w||^2 + D||w_x\partial_x^4 w||^2\right] + k_2||\partial_x^4 w_t||^2$$
$$= \left(p, \partial_x^4 w_t\right) - 4D\left(w_x w_{xx} w_{xxx}, \partial_x^4 w_t\right) - D\left(w_{xx}^3, \partial_x^4 w_t\right) - \left(\partial_x\left[w_x \int_x^L u_{tt}\right], \partial_x^4 w_t\right).$$

We first estimate quantities associated with stiffness using (as before) interpolation, the Sobolev embeddings, and Young's inequality:

1. $4D\left|\left(w_x w_{xx} w_{xxx}, \partial_x^4 w_t\right)\right| \leq \; C_{\delta_1}||w_{xx}||^8 + C_{\delta_1}||\partial_x^4 w||^4 + \delta_1||\partial_x^4 w_t||^2$

2. $D\left|\left(w_{xx}^3, \partial_x^4 w_t\right)\right| \leq C_{\delta_2}||w_{xx}||_{L^\infty}^4||w_{xx}||^2 + \delta_2||\partial_x^4 w_t||^2$
$$\leq C_{\delta_2}\left(||w_{xx}||_{L^\infty}^{16/3} + ||w_{xx}||^8\right) + \delta_2||\partial_x^4 w_t||^2.$$

where we have used Young's inequality $p = 4/3$ and $q = 4$. Subsequently, we interpolate $||w_{xx}||_{L^\infty}^{16/3}$ as:

$$||w_{xx}||_{L^\infty}^{16/3} \leq ||w_{xx}||_{1/2+\epsilon}^{16/3} \leq ||w_{xx}||^{10/3}||w_{xx}||_2^2 \lesssim ||w_{xx}||^{20/3} + ||\partial_x^4 w||^4, \qquad (2.6.13)$$

where we chose $\epsilon = 1/4$ and used Young's inequality again with $p = 2$ and $q = 2$.

According to the above, we introduce the notation:

$$E_2^n(t) = ||w_{xxt}^n||^2 + D||\partial_x^4 w^n||^2 + D||w_x^n \partial_x^4 w^n||^2. \qquad (2.6.14)$$

We now estimate the *inertial* contribution above, aiming to control the term

$||u_{xxt}||^2$:

$$\left(\partial_x\left[w_x\int_x^L u_{tt}\right],\partial_x^4 w_t\right)=\left(w_{xx}\int_x^L u_{tt},\partial_x^4 w_t\right)-\left(w_x u_{tt},\partial_x^4 w_t\right)$$
$$\equiv \qquad \mathcal{J}_1 \qquad + \qquad \mathcal{J}_2.$$

We can directly bound $\mathcal{J}_1$ as follows:

$$|\mathcal{J}_1|\le C_{\delta_3}||w_{xx}||_{L^\infty}^2||u_{tt}||^2+\delta_3||\partial_x^4 w_t||^2\le C_{\delta_3}||\partial_x^4 w||^4+C_{\delta_3}||u_{tt}||^4+\delta_3||\partial_x^4 w_t||^2.$$

For $\mathcal{J}_2$, we note that $u_{xxt}=-w_x w_{xxt}-w_{xx}w_{xt}$, and use this expression to integrate by parts twice:

$$\mathcal{J}_2=-\left(u_{tt},w_{xxx}w_{xxt}\right)-2\left(u_{xxt},w_{xx}w_{xxt}\right)+\frac{1}{2}\frac{d}{dt}||u_{xxt}||^2+\left(u_{xxtt},w_{xx}w_{xt}\right). \quad (2.6.15)$$

We estimate the remaining unsigned terms:

1. $-2\left(u_{xtt},w_{xx}w_{xxt}\right)=2\left(u_{tt},w_{xxx}w_{xxt}\right)+2\left(u_{tt},w_{xx}w_{xxxt}\right),$

   we can combine the first term on the RHS with the first in (2.6.15), then control each term:

   (i) $|(u_{tt},w_{xxx}w_{xxt})|\lesssim||u_{tt}||^4+||\partial_x^4 w||^4+||w_{xxt}||^4$

   (where we used Young's inequality with 1 for the u_{tt} term)

   (ii) $|(u_{tt},w_{xx}w_{xxxt})|=|(w_{xx}u_{tt},w_{xxxt})|\le C_{\delta_4}||\partial_x^4 w||^4+C_{\delta_4}||u_{tt}||^4+\delta_4||\partial_x^4 w_t||^2.$

2. $(u_{xxtt}, w_{xx}w_{xt}) = (\partial_t[u_{xxt}], w_{xx}w_{xt})$

$$= \frac{d}{dt}\left(u_{xxt}, w_{xx}w_{xt}\right) - (u_{xxt}, w_{xxt}w_{xt}) - (u_{xxt}, w_{xx}w_{xtt}),$$

where each term is bounded as follows:

(i) $|(u_{xxt}, w_{xxt}w_{xt})| \lesssim ||u_{xxt}||^4 + ||w_{xt}||^2_{L^\infty}||w_{xxt}||^2 \lesssim ||u_{xxt}||^4 + ||w_{xxt}||^4$

(ii) $|(u_{xxt}, w_{xx}w_{xtt})| = |(w_{xx}u_{txx}, w_{xtt})| \leq C_{\varepsilon_3}||\partial_x^4 w||^4 + C_{\varepsilon_3}||u_{xxt}||^4 + \varepsilon_3||w_{xxtt}||^2$

(iii) $|(u_{xxt}, w_{xx}w_{xt})| \leq \varepsilon||u_{xxt}||^2 + C_\varepsilon||w_{xt}||^2_{L^\infty}||w_{xx}||^2$

$$\leq \varepsilon||u_{xxt}||^2 + C_\varepsilon||w_{xt}||^{9/4}_{L^\infty} + C_\varepsilon||w_{xx}||^{18},$$

where we used Young's inequality with $p = 9/8$ and $q = 9$. Then we use interpolation for $||w_{xt}||^{9/4}_{L^\infty}$:

$$||w_{xt}||^{9/4}_{L^\infty} \leq ||w_t||^{9/4}_{3/2+\epsilon} \leq ||w_t||^{9/32}||w_{xxt}||^{63/32} \leq C_{\varepsilon_p}||w_t||^{18} + \varepsilon_p||w_{xxt}||^2, \tag{2.6.16}$$

where we chose $\epsilon = 1/4$ and Young's inequality with $p = 64$ and $q = 64/63$.

By choosing ε and ε_p sufficiently small, the above terms can be absorbed. Additionally, we note that from the previous energy bounds, (2.6.5), $||w_t^n||$ and $||w_{xx}^n||$ are bounded in any power in which they appear.

Denoting:

$$I_2^n(t) = \frac{1}{2}||u_{xxt}^n||^2 \quad \text{and} \quad \mathcal{E}_2^n(t) = E_2^n(t) + I_2^n(t),$$

where $E_2^n(t)$ is given by (2.6.14), we can obtain a clean estimate. It is true from (2.6.1) that, as before, $\{\mathcal{E}_2^n(0)\}_{n=1}^\infty$ is uniformly bounded in terms of $||(w_0, w_1)||_{\mathscr{D}(\mathcal{A})^2}$.

Thus, combining (2.6.12) with a compilation of the calculations described in this step and absorbing damping terms on the RHS, we have the estimate

$$\begin{aligned}\mathcal{E}_1^n(t) + \mathcal{E}_2^n(t) + k_2 \int_0^t \left[||w_{xxtt}^n||^2 + ||\partial_x^4 w_t^n||^2 \right] d\tau \\ \lesssim g_3 \left(p_t, ||w_0||_{\mathcal{D}(\mathcal{A})}, ||w_1||_{\mathcal{D}(\mathcal{A})} \right) + g_4 \left(p, ||w_0||_{\mathcal{D}(\mathcal{A})}, ||w_1||_{H_*^2} \right) t \\ + \int_0^t \left[\mathcal{E}_1^n(\tau) + \mathcal{E}_2^n(\tau) \right]^2 d\tau. \qquad (2.6.17)\end{aligned}$$

We point out once again that the $C > 0$ associated to '$\lesssim$' above *does not depend* on w_0, w_1 or p and that the denoted dependence on p (and its derivative) is taken in the sense of (2.5.14).

Hence, disregarding the damping integral and invoking *nonlinear* Grönwall [27], we obtain:

$$\mathcal{E}_1^n(t) + \mathcal{E}_2^n(t) \leq \frac{g_3 + g_4 t}{1 - C\left[g_3 t + g_4 t^2\right]} \equiv M_2(t) \quad 0 \leq t < T_1^*, \qquad (2.6.18)$$

where $T_1^* = \sup_t \left\{ C\left[g_3 t + g_4 t^2\right] < 1 \right\}$. From (2.6.18), we deduce that the Galerkin approximations w^n satisfy a uniform-in-n a priori bound on $[0, T]$ for any $T < T_1^*$:

$$0 \leq \mathcal{E}_1^n(t) + \mathcal{E}_2^n(t) \leq M_2^*(T) \equiv \max_{t \in [0,T]} M_2(t).$$

This, along with (2.6.5), provides uniform-in-n boundedness in the associated norms of $\mathcal{E}_0$, $\mathcal{E}_1$ and $\mathcal{E}_2$ for a finite time depending on the initial data.

Step 6 - Boundedness of Initial Jerk: It is apparent from the expression of the [**NL Inertia**] in (2.4.4) that the existence of strong solutions requires higher regularity of w_{tt}. We obtain this via yet another energy level, corresponding to two temporal differentiations of the equations. To begin, we again need uniform estimates of $t = 0$ quantities appearing in the energy estimates. We remark that the resulting regularity of solutions obtained here is requisite also in the latter proof of uniqueness. Lastly, we note that in order to obtain this estimate (as well as that in the previous sections for $\mathcal{E}_1^n$ and $\mathcal{E}_2^n$) with $\iota = 1$, the presence of the damping term $k_2 > 0$ is critical.

For the upcoming energy inequality for $\mathcal{E}_3^n(t)$, we must justify boundedness in n of $\{||w_{ttt}^n(0)||\}_{n=1}^{\infty}$, $\{||u_{ttt}^n(0)||\}_{n=1}^{\infty}$. To that end, the weak equations of motion (2.4.13) hold on approximants w^n and can be differentiated in time for any fixed test function ϕ. Then, by choosing $\phi = s_j(x)$, multiplying (2.4.13) by $q_j^{'''}(t)$ and summing over $j = 1, 2, \dots, n$, we obtain:

$$\begin{aligned}&||w_{ttt}^n||^2 + D\left(\partial_x^4 w_t^n, w_{ttt}^n\right) + k_2\left(\partial_x^4 w_{tt}^n, w_{ttt}^n\right) - D\left(\partial_{xt}\left[(w_{xx}^n)^2 w_x^n\right], w_{ttt}^n\right)\\ &+ D\left(\partial_{xxt}\left[w_{xx}^n (w_x^n)^2\right], w_{ttt}^n\right) + \left(\partial_{xt}\left[w_x^n \int_x^L u_{tt}^n\right], w_{ttt}^n\right) - (p_t, w_{ttt}^n) = 0. \qquad (2.6.19)\end{aligned}$$

Differentiating directly, we have $u_{ttt} = -\int_0^x \left[3w_{xt}w_{xtt} + w_x w_{xttt}\right] d\xi$, which yields:

$$\begin{aligned}\left(\partial_{xt}\left[w_x^n \int_x^L u_{tt}^n\right], w_{ttt}^n\right) &= -\left(\partial_t\left[w_x^n \int_x^L u_{tt}^n\right], w_{xttt}^n\right)\\ &= -\left(w_{xt}^n \int_x^L u_{tt}^n, w_{xttt}^n\right) - \left(w_x^n \int_x^L u_{ttt}^n, w_{xttt}^n\right)\\ &\equiv \qquad \mathcal{K}_1 \qquad + \qquad \mathcal{K}_2.\end{aligned}$$

For $\mathcal{K}_1$ we proceed by undoing the integration by parts which yields:

$$\mathcal{K}_1 = \left(w^n_{xxt} \int_x^L u^n_{tt}, w^n_{ttt} \right) - \left(w^n_{xt} u^n_{tt}, w^n_{ttt} \right).$$

These two terms can now be transferred to the right hand side and be estimated. For $\mathcal{K}_2$ we recall the expression for u_{ttt} above, and by adding and subtracting appropriate terms we have:

$$\mathcal{K}_2 = - \left(u^n_{ttt}, \int_0^x w^n_x w^n_{xttt} \right) = ||u^n_{ttt}||^2 + 3 \left(u^n_{ttt}, \int_0^x w^n_{xt} w^n_{xtt} \right).$$

Grouping everything together, and absorbing $||w^n_{ttt}(0)||^2$ and $||u^n_{ttt}(0)||^2$ from the RHS, we obtain:

$$||w^n_{ttt}(0)||^2 + ||u^n_{ttt}(0)||^2 \leq h_1 \left(p_t(0), \partial_x^k w^n(0), \partial_x^l w^n_t(0), \partial_x^4 w^n_{tt}(0) \right), \quad k, l = 1, 2, 3, 4, \tag{2.6.20}$$

with h_1 is polynomial in its slots. As we can see from the above expression, it is now crucial to establish the boundedness of the sequence $\{\partial_x^4 w^n_{tt}(0)\}_{n=1}^{\infty}$ in $L^2(0, L)$ in terms of the data, $(w_0, w_1) \in \mathscr{D}(\mathcal{A}^2)$.

To achieve this bound, we revisit the weak form (2.4.13) and test with $\phi = \partial_x^8 s_j(x)$, then multiplying by $q''_j(t)$ and summing over $j = 1, 2, \ldots, n$, yielding (after some integration by parts):

$$||\partial_x^4 w_{tt}^n||^2 + \left(\partial_x^5\left[w_x^n\int_x^L u_{tt}^n\right], \partial_x^4 w_{tt}^n\right) = \left(p, \partial_x^4 w_{tt}^n\right) - D\left(\partial_x^8 w^n, \partial_x^4 w_{tt}^n\right) - k_2\left(\partial_x^8 w_t^n, \partial_x^4 w_{tt}^n\right)$$

$$+D\left(\partial_x^5\left[(w_{xx}^n)^2 w_x^n\right], \partial_x^4 w_{tt}^n\right) - D\left(\partial_x^6\left[w_{xx}^n (w_x^n)^2\right], \partial_x^4 w_{tt}^n\right).$$

Brute force yields:

$$\partial_x^5\left[w_x^n\int_x^L u_{tt}^n\right] = \partial_x^6 w^n \int_x^L u_{tt}^n - 5[\partial_x^5 w^n u_{tt}^n + w_{xx}^n u_{xxxtt}^n]$$

$$-10[\partial_x^4 w^n u_{xtt}^n + w_{xxx}^n u_{xxtt}^n] - w_x^n \partial_x^4 u_{tt}^n.$$

Next, we utilize the last term of the above expression to create the quantity $||\partial_x^4 u_{tt}||^2$:

$$\partial_x^4 u_{tt} = -\left[6w_{xxt}w_{xxxt} + 2w_{xt}\partial_x^4 w_t + \partial_x^4 w w_{xtt} + 3w_{xxx}w_{xxtt} + 3w_{xx}w_{xxxtt} + w_x\partial_x^4 w_{tt}\right].$$

We also have:

$$-\left(w_x^n\partial_x^4 u_{tt}^n, \partial_x^4 w_{tt}^n\right) = \left(\partial_x^4 u_{tt}^n, -w_x^n\partial_x^4 w_{tt}^n\right)$$

$$= ||\partial_x^4 u_{tt}^n||^2 + 6\left(\partial_x^4 u_{tt}^n, w_{xxt}^n w_{xxxt}^n\right) + 2\left(\partial_x^4 u_{tt}^n, w_{xt}^n \partial_x^4 w_t^n\right)$$

$$+\left(\partial_x^4 u_{tt}^n, \partial_x^4 w^n w_{xtt}^n\right) + 3\left(\partial_x^4 u_{tt}^n, w_{xxx}^n w_{xxtt}^n\right) + 3\left(\partial_x^4 u_{tt}^n, w_{xx}^n w_{xxxtt}^n\right).$$

Combining the terms above, we can extract $||\partial_x^4 w_{tt}^n||^2$ and $||\partial_x^4 u_{tt}^n||^2$ on the LHS. We group the RHS terms into different categories based on the actions that are necessary to control them. ***Type 1*** is first:

$$T_1 \equiv \left(p, \partial_x^4 w_{tt}^n\right) - D\left(\partial_x^8 w^n, \partial_x^4 w_{tt}^n\right) - k_2\left(\partial_x^8 w_t^n, \partial_x^4 w_{tt}^n\right) + D\left(\partial_x^5\left[(w_{xx}^n)^2 w_x^n\right], \partial_x^4 w_{tt}^n\right)$$
$$-D\left(\partial_x^6\left[w_{xx}^n (w_x^n)^2\right], \partial_x^4 w_{tt}^n\right) - \left(\partial_x^6 w^n \int_x^L u_{tt}^n, \partial_x^4 w_{tt}^n\right) + 5\left(\partial_x^5 w^n u_{tt}^n, \partial_x^4 w_{tt}^n\right)$$
$$-6\left(\partial_x^4 u_{tt}^n, w_{xxt}^n w_{xxxt}^n\right) - 2\left(\partial_x^4 u_{tt}^n, w_{xt}^n \partial_x^4 w_t^n\right),$$

where for these terms, it is clear that

$$|T_1| \leq h_2\left(p, \partial_x^i w^n, \partial_x^j w_t^n, u_{tt}^n\right) + \varepsilon_1 ||\partial_x^4 w_{tt}^n||^2 + \delta_1 ||\partial_x^4 u_{tt}^n||^2, \quad i, j = 1, 2, \ldots, 8, \quad (2.6.21)$$

where h_2 depends on ε_1, δ_1 and is polynomial in its slots. ***Type 2*** is next:

$$T_2 \equiv 10\left(\partial_x^4 w^n u_{xtt}^n, \partial_x^4 w_{tt}^n\right) + 10\left(w_{xxx}^n u_{xxtt}^n, \partial_x^4 w_{tt}^n\right) + 5\left(w_{xx}^n u_{xxxtt}^n, \partial_x^4 w_{tt}^n\right). \quad (2.6.22)$$

For this category we will exploit the fact that $||\partial_x^4 u_{tt}^n||^2$ appears in the LHS and that $\{u_{tt}^n(0)\}_{n=1}^\infty$ is bounded in $L^2(0, L)$ as shown in (2.6.8) which will be used in interpolation for the terms $\partial_x^i u_{tt},\ i = 1, 2, 3$. We show how to control one of the terms appearing in (2.6.22).

$$\begin{aligned}\left|\left(w_{xx}^n u_{xxxtt}^n, \partial_x^4 w_{tt}^n\right)\right| &\leq C_\varepsilon ||w_{xxx}^n||^2 ||u_{xxxtt}^n||^2 + \varepsilon ||\partial_x^4 w_{tt}^n||^2 \\ &\leq C_\varepsilon ||w_{xxx}^n||^{10} + C_\varepsilon ||u_{xxxtt}^n||^{5/2} + \varepsilon ||\partial_x^4 w_{tt}^n||^2,\end{aligned}$$

where we used Young's inequality with $p = 5$ and $q = 5/4$. Then we use interpolation for $||u^n_{xxxtt}||^{5/2}$:

$$||u^n_{xxxtt}||^{5/2} \le ||u^n_{tt}||^{5/8}||\partial_x^4 u^n_{tt}||^{15/8} \le C_{\varepsilon_p}||u^n_{tt}||^{10} + \varepsilon_p||\partial_x^4 u^n_{tt}||^2,$$

where employed Young's inequality once again with $p = 16$ and $q = 16/15$.

Remark 2.6.3. We can see from the explicit expression of $\partial_x^i u^n_{tt}$, $i = 0, 1, 2, 3$, that

$$u^n_{tt}(0) = u^n_{xtt}(0) = u^n_{xxtt}(L) = u^n_{xxxtt}(L) = 0.$$

Hence, Poincaré's inequality guarantees that $||u^n_{tt}||_i \sim ||\partial_x^i u^n_{tt}||$ for $i = 1, 2, 3$.

The remaining ***Type 2*** are bounded analogously, yielding:

$$|T_2| \le h_3\left(\partial_x^i w^n, u^n_{tt}\right) + \varepsilon_2||\partial_x^4 w^n_{tt}||^2 + \delta_2||\partial_x^4 u^n_{tt}||^2, \quad i = 1, 2, \ldots, 5. \tag{2.6.23}$$

Finally, we have ***Type 3***:

$$T_3 \equiv -\left(\partial_x^4 u^n_{tt}, \partial_x^4 w^n w^n_{xtt}\right) - 3\left(\partial_x^4 u^n_{tt}, w^n_{xxx} w^n_{xxtt}\right) - 3\left(\partial_x^4 u^n_{tt}, w^n_{xx} w^n_{xxxtt}\right).$$

For this category, we interpolate the terms $\partial_x^i w_{tt}$, $i = 1, 2, 3$, exploiting the fact that $\{w^n_{tt}(0)\}_{n=1}^{\infty}$ is bounded in $L^2(0, L)$ as shown in (2.6.8). We omit these details, as the calculations are identical to those described for ***Type 2***. We obtain the bound:

$$|T_3| \le h_4\left(\partial_x^i w^n, w^n_{tt}\right) + \varepsilon_3||\partial_x^4 w^n_{tt}||^2 + \delta_3||\partial_x^4 u^n_{tt}||^2, \quad i = 1, 2, \ldots, 5. \tag{2.6.24}$$

Combining (2.6.21), (2.6.23) and (2.6.24), absorbing with ε_k, δ_k small, and taking the (valid on approximants) time trace at $t = 0$, we produce the following estimate:

$$||\partial_x^4 w_{tt}^n(0)||^2 + ||\partial_x^4 u_{tt}^n(0)||^2 \leq h\left(p(0), \partial_x^i w^n(0), \partial_x^j w_t^n(0), w_{tt}^n(0), u_{tt}^n(0)\right), \;\; i, j = 1, 2, \ldots, 8.$$

By combining (2.6.1) and (2.6.8), we can *finally* write (2.6.20) as:

$$||w_{ttt}^n(0)||^2 + ||u_{ttt}^n(0)||^2 \leq C\left(p(0), p_t(0), ||w_0||_{\mathcal{D}(\mathcal{A}^2)}, ||w_1||_{\mathcal{D}(\mathcal{A}^2)}\right). \tag{2.6.25}$$

Step 7 - Energy Level 3: With the initial jerk bounded, we proceed with the higher energy estimate corresponding to two time differentiations of the equation. The formal identity (applying ∂_t^2 to (2.4.1) and multiplying by w_{ttt}) is:

$$\begin{aligned}
&\frac{1}{2}\frac{d}{dt}\left[||w_{ttt}||^2 + D||w_{xxtt}||^2 + D||w_x w_{xxtt}||^2 + D||w_{xx}w_{xtt}||^2\right] + k_2||w_{xxttt}||^2 \\
&\quad = D(w_x w_{xt}, w_{xxtt}^2) + D(w_{xx}w_{xxt}, w_{xtt}^2) - 4D(w_{xx}w_{xxt}w_{xt}, w_{xttt}) - 2D(w_x w_{xxt}^2, w_{xttt}) \\
&\qquad - 2D(w_x w_{xx} w_{xxtt}, w_{xttt}) - 4D(w_{xxt}w_x w_{xt}, w_{xxttt}) - 2D(w_{xx}w_{xt}^2, w_{xxttt}) \\
&\qquad - 2D(w_{xx}w_x w_{xtt}, w_{xxttt}) - \left(\partial_{xtt}\left[w_x \int_x^L u_{tt}\right], w_{ttt}\right).
\end{aligned}$$

We bound the RHS, in line with previous sections, using the Sobolev embeddings and Young's inequality; the estimates from stiffness terms are straightforward. Inertia is handled as in previous estimates. After two temporal differentiation we have:

$$
\begin{aligned}
&\left(\partial_{xtt}\left[w_x\int_x^L u_{tt}\right], w_{ttt}\right)\\
&= -\left(\partial_{tt}\left[w_x\int_x^L u_{tt}\right], w_{xttt}\right)\\
&= -\left(w_{xtt}\int_x^L u_{tt}, w_{xttt}\right) - 2\left(w_{xt}\int_x^L u_{ttt}, w_{xttt}\right) - \left(w_x\int_x^L u_{tttt}, w_{xttt}\right)\\
&\equiv \qquad \mathcal{L}_1 \qquad + \qquad \mathcal{L}_2 \qquad + \qquad \mathcal{L}_3.
\end{aligned}
$$

We bound $\mathcal{L}_1$ and $\mathcal{L}_2$ as:

1. $|\mathcal{L}_1| \lesssim ||w_{xtt}||_{L^\infty}||u_{tt}||\ ||w_{xttt}|| \leq C_{\varepsilon_7}||u_{tt}||^4 + C_{\varepsilon_7}||w_{xxtt}||^4 + \varepsilon_7||w_{xxttt}||^2$

2. $|\mathcal{L}_2| \lesssim ||w_{xt}||_{L^\infty}||u_{ttt}||\ ||w_{xttt}|| \leq C_{\varepsilon_8}||w_{xxt}||^4 + C_{\varepsilon_8}||u_{ttt}||^4 + \varepsilon_8||w_{xxttt}||^2.$

The term $\mathcal{L}_3$ creates the desired conserved quantity (again using the explicit representation of u_{ttt}):

$$
\mathcal{L}_3 = (u_{tttt}, u_{ttt}) + 3\left(u_{tttt}, \int_0^x w_{xt}w_{xtt}\right) = \frac{1}{2}\frac{d}{dt}||u_{ttt}||^2 + 3\left(\int_x^L u_{tttt}, w_{xt}w_{xtt}\right).
$$

The additional term that was produced above can be manipulated as follows:

$$
\begin{aligned}
\left(u_{tttt}, \int_0^x w_{xt}w_{xtt}\right) =& \frac{d}{dt}\left(u_{ttt}, \int_0^x w_{xt}w_{xtt}\right) - \left(u_{ttt}, \int_0^x w_{xtt}^2\right) - \left(u_{ttt}, \int_0^x w_{xt}w_{xttt}\right)\\
\equiv& \qquad \frac{d\mathcal{M}_1}{dt} \qquad + \qquad \mathcal{M}_2 \qquad + \qquad \mathcal{M}_3.
\end{aligned}
$$

Now, $\mathcal{M}_2$ and $\mathcal{M}_3$ will be moved to the right hand side and estimated as follows:

1. $|\mathcal{M}_2| \lesssim ||u_{ttt}||^2 + ||w_{xtt}^2||^2 \lesssim ||u_{ttt}||^2 + ||w_{xtt}||^2_{L^\infty}||w_{xtt}||^2 \lesssim ||u_{ttt}||^2 + ||w_{xxtt}||^4$

2. $$|\mathcal{M}_3| = \left|\left(w_{xt}\int_x^L u_{ttt}, w_{xttt}\right)\right| \leq ||w_{xt}||_{L^\infty}||u_{ttt}||\ ||w_{xttt}||$$
$$\leq C_{\varepsilon_9}||w_{xxt}||^4 + C_{\varepsilon_9}||u_{ttt}||^4 + \varepsilon_9||w_{xxttt}||^2.$$

The $\mathcal{M}_1$ is more delicate, since it must be absorbed by conservative quantities:

$$|\mathcal{M}_1| \leq \varepsilon||u_{ttt}||^2 + C_\varepsilon||w_{xtt}||^2_{L^\infty}||w_{xt}||^2 \leq \varepsilon||u_{ttt}||^2 + C_\varepsilon||w_{xtt}||^{9/4}_{L^\infty} + C_\varepsilon||w_{xt}||^{18}$$
$$\leq \varepsilon||u_{ttt}||^2 + C_{\varepsilon,\varepsilon_p}||w_{tt}||^{18} + C_\varepsilon\varepsilon_p||w_{xxtt}||^2 + C_\varepsilon||w_{xt}||^{18},$$

accomplished as in (2.6.16).

Moving on, we compile the above calculations into an energy estimate, taking

$$E_3(t) = \frac{1}{2}\left[||w_{ttt}||^2 + D||w_{xxtt}||^2 + D||w_x w_{xxtt}||^2 + D||w_{xx}w_{xtt}||^2\right], \quad I_3(t) = \frac{1}{2}||u_{ttt}||^2,$$

and subsequently $\mathcal{E}_3(t) = E_3(t) + I_3(t)$. Thus, by invoking (2.6.1) and (2.6.25) to guarantee the uniform boundedness of $\mathcal{E}_3^n(0)$, we obtain:

$$\begin{aligned}\mathcal{E}_3^n(t) + k_2\int_0^t ||w^n_{xxttt}||d\tau \leq & g_5\left(p, p_t, p_{tt}, ||w_0||_{\mathcal{D}(\mathcal{A}^2)}, ||w_1||_{\mathcal{D}(\mathcal{A}^2)}\right) \\ & + g_6\left(p, ||w_0||_{\mathcal{D}(\mathcal{A})}, ||w_1||_{H^2_*}, M_2^*\right)t + \sum_{j=1}^{9}\varepsilon_j\int_0^t ||w^n_{xxttt}||^2 d\tau \\ & + C\int_0^t \left[\mathcal{E}_3^n(\tau)\right]^2 d\tau \quad \text{for all } t\in[0,T],\end{aligned}$$

where $T < T_1^*$ and $M_2^*(T)$ are as in (2.6.18). In addition, $C > 0$ *does not depend* on w_0, w_1 or p. Absorbing the damping terms, we finally obtain through another application nonlinear Grönwall's inequality:

$$\mathcal{E}_3^n(t) \leq \frac{g_5 + g_6 t}{1 - C\left[g_5 t + g_6 t^2\right]} \quad 0 \leq t < T_2^*, \tag{2.6.26}$$

where $T_2^* = \min_t \left(\sup_t \left\{C\left[g_3 t + g_4 t^2\right] < 1\right\}, T_1^*\right)$. As before, this yields a uniform-in-n a priori bound on solutions in the topology corresponding to $\mathcal{E}_3$ on any $[0,T]$ for $T < T_2^*$. We remark once again that the regularity of p considered in theorem (2.6.1) is necessary for ensuring that the functions $g_1, g_2, \ldots, g_6$ are continuous functions in time, as required by the version of the Grönwall lemma we employ.

Step 8 - Sufficient Regularity for w_t:

Regularity for the damping (with smooth data) proceeds standardly, through the equation:

$$\begin{aligned} ||\partial_x^4 w_t^n|| \lesssim \ & ||p|| + ||w_{tt}^n|| + ||w_{xxx}^n|| \ ||\partial_x^4 w^n||^2 + ||w_{xx}^n|| \ ||w_{xxx}^n||^2 \\ & + \left(1 + ||w_{xx}^n||^2\right) ||\partial_x^4 w^n|| + ||w_{xx}^n|| \ ||u_{tt}^n||. \end{aligned}$$

Using (2.6.18) we can deduce that

$$||\partial_x^4 w_t^n|| \text{ is bounded in } L^\infty(0,T;L^2(0,L)), \tag{2.6.27}$$

for any $T < T_2^*$. Thus, combining (2.6.18) and (2.6.26) and (2.6.27), we can finally obtain a priori bounds:

$$||w^n||_{L^\infty(0,T;\mathcal{D}(\mathcal{A}))} + ||w_t^n||_{L^\infty(0,T;\mathcal{D}(\mathcal{A}))} + ||w_{tt}^n||_{L^\infty(0,T;H_*^2)} \leq C(\text{data}, T), \tag{2.6.28}$$

(among other controlled norms), where "data" indicates dependence on (w_0, w_1) measured in norms up to that of $\mathscr{D}(\mathcal{A}^2)^2$.

Step 9 - Limit Passage and Weak Solution: With our a priori bounds in hand for smooth data $w_0 \in \mathcal{D}(\mathcal{A}^2)$, $w_1 \in \mathcal{D}(\mathcal{A}^2)$, we proceed to pass with the limit and construct a weak solution satisfying (2.4.13) with $\sigma = \iota = 1$ and $k_2 > 0$. The boundedness of the terms in (2.6.28) yields to the existence of a subsequence $\{w^{n_k}\}_{k=1}^{\infty}$ and a limit point $w \in H^1(0,T;\mathcal{D}(\mathcal{A})) \cap H^2(0,T;H_*^2)$, such that

$$w^{n_k} \rightharpoonup w \in L^2(0,T;\mathcal{D}(\mathcal{A}))\,; \;\; w_t^{n_k} \rightharpoonup w_t \in L^2(0,T;\mathcal{D}(\mathcal{A}))\,; \;\; w_{tt}^{n_k} \rightharpoonup w_{tt} \in L^2\left(0,T;H_*^2\right).$$

We must show that w satisfies the weak form (2.4.13), in this case with $\sigma = \iota = 1$ and $k_2 > 0$. The details corresponding to limit point identification for [**NL Stiffness**] are identical to those in **Step 6** of Section 2.5.3, thus we focus on [**NL Inertia**] terms.

We first show that $u_{tt}^{n_k} \to u_{tt}$ in $L^2(0,T;L^2(0,L))$. To that end, we consider the differences:

$$||u_{tt}^{n_k} - u_{tt}|| \leq \left|\left|\int_x^L \left([w_{xt}^{n_k}]^2 - w_{xt}^2\right)\right|\right|^2 + \left|\left|\int_x^L (w_x^{n_k} w_{xtt}^{n_k} - w_x w_{xtt})\right|\right|^2 \equiv \mathcal{Y}_1 + \mathcal{Y}_2.$$

We will show that both $\mathcal{Y}_1$ and $\mathcal{Y}_2$ go to zero as $k \to \infty$.

$$\mathcal{Y}_1 \lesssim ||w_{xt}^{n_k} + w_{xt}||_{L^\infty}^2 ||w_{xt}^{n_k} - w_{xt}||^2 \lesssim ||w_{xxt}||^2 ||w_{xt}^{n_k} - w_{xt}||^2 \quad \to 0 \;\text{ as }\; k \to \infty.$$

$$
\begin{aligned}
\mathcal{Y}_2 &\leq ||w_x^{n_k}(w_{xtt}^{n_k} - w_{xtt})||^2 + ||w_{xtt}(w_x^{n_k} - w_x)||^2 \\
&\leq ||w_x^{n_k}||_{L^\infty}^2 ||w_{xtt}^{n_k} - w_{xtt}||^2 + ||w_{xtt}||_{L^\infty}^2 ||w_x^{n_k} - w_x||^2 \\
&\lesssim ||w_{xx}||^2 ||w_{xtt}^{n_k} - w_{xtt}||^2 + ||w_{xxtt}||^2 ||w_x^{n_k} - w_x||^2 \\
&\quad \to 0 \quad \text{as} \quad k \to \infty.
\end{aligned}
$$

Now, in order to pass to the limit for the [**NL Inertia**] term we need to show that

$$
\left(w_x^{n_k} \int_x^L u_{tt}^{n_k}, \phi_x \right) \to \left(w_x \int_x^L u_{tt}, \phi_x \right) \qquad \text{for all } \phi \in H_*^2.
$$

This holds since:

$$
\begin{aligned}
&\left| \left(w_x^{n_k} \int_x^L u_{tt}^{n_k} - w_x \int_x^L u_{tt}, \phi_x \right) \right| \\
&\leq \left| \left(w_x^{n_k} \int_x^L [u_{tt}^{n_k} - u_{tt}], \phi_x \right) + \left((w_x^{n_k} - w_x) \int_x^L u_{tt}, \phi_x \right) \right| \\
&\leq ||\phi_x||_{L^\infty} ||w_x^{n_k}|| \; ||u_{tt}^{n_k} - u_{tt}|| + ||\phi_x||_{L^\infty} ||u_{tt}|| \; ||w_x^{n_k} - w_x|| \\
&\leq ||\phi_x||_{L^\infty} ||w_x|| \; ||u_{tt}^{n_k} - u_{tt}|| + ||\phi_x||_{L^\infty} ||u_{tt}|| \; ||w_x^{n_k} - w_x|| \\
&\quad \to 0 \quad \text{as} \quad k \to \infty.
\end{aligned}
$$

Hence, w satisfies the weak formulation (2.4.13) with $\sigma = \iota = 1$ and $k_2 > 0$. With a weak solution $w(x,t)$ in hand corresponding to smooth data, we have by Definition 4 that the solution is strong, via the estimate (2.6.28) that provides the necessary regularity for $w,\ w_t,\ w_{tt}$.

And thus we have proven theorem 2.6.1.

Corollary 2.6.2. *Strong solutions w, described in Definition 4, satisfy equation (2.4.1) with $\sigma = \iota = 1$ and $k_2 > 0$ in the sense of $L^2(0,T;L^2(0,L))$. Additionally, they satisfy $w_{xx}(L,t) = w_{xxx}(L,t) = 0$ for all $0 \le t \le T$.*

Proof of Corollary 2.6.2. The weak form is now satisfied by the constructed limit:

$$(w_{tt},\phi) + D(w_{xx},\phi_{xx}) + k_2(w_{xxt},\phi_{xx}) + D(w_{xx}^2 w_x,\phi_x) + D(w_x^2 w_{xx},\phi_{xx}) \\ - \left(w_x \int_x^L u_{tt},\phi_x\right) = (p,\phi), \quad \forall \phi \in H_*^2, \quad a.e.\ t. \tag{2.6.29}$$

Reversing integration by parts, yields (on test functions):

$$\left(w_{tt} + D\partial_x^4 w + k_2 \partial_x^4 w_t - D\partial_x\Big[w_{xx}^2 w_x\Big] + D\partial_{xx}\Big[w_{xx}w_x^2\Big] + \partial_x\left[w_x \int_x^L u_{tt}\right] - p,\phi\right) = 0,$$

for all $\phi \in C_0^\infty(0,L)$. By density, we have the equation holding in $L^2(0,L)$, as desired:

$$w_{tt}+D\partial_x^4 w+k_2\partial_x^4 w_t-D\partial_x\Big[w_{xx}^2 w_x\Big]+D\partial_{xx}\Big[w_{xx}w_x^2\Big]+\partial_x\left[w_x \int_x^L u_{tt}\right] = p \quad a.e.\ x,\ \ a.e.\ t. \tag{2.6.30}$$

The solution resides in H_*^2, but we must show the natural boundary conditions $w_{xx}(L,t) = w_{xxx}(L,t) = 0$. The argument proceeds as before, invoking (2.6.30) and yielding, upon integration by parts:

$$\begin{aligned}&\phi_x(L)\left((1+w_x^2(L))w_{xx}(L)+w_{xxt}(L)\right)\\&\quad-\phi(L)\Big((1+w_x^2(L))w_{xxx}(L)+w_x(L)w_{xx}^2(L)+w_{xxxt}(L)\Big)=0,\quad\forall\phi\in H_*^2,\end{aligned}\tag{2.6.31}$$

where we interpret the time derivatives above distributionally. Considering $\phi \in H_0^1 \cap H_*^2 \subseteq H_*^2$, we see $\phi_x(L)\left((1+w_x^2(L))w_{xx}(L)+w_{xxt}(L)\right)=0$. There exists one such function so that $\phi_x(L) \neq 0$, and thus

$$w_{xxt}(L)+\left(1+w_x^2(L)\right)w_{xx}(L)=0.$$

Now, since $w \in H^1(0,T;\mathscr{D}(\mathcal{A}))$ for smooth solutions, we have $w \in C([0,T];\mathscr{D}(\mathcal{A}))$. Hence $w_{xx}(L,t)$, $w_{xxx}(L,t)$ are continuous functions of time, so we have a linear ODE of the form $f'(t)+g(t)f(t)=0$, with classical solution

$$w_{xx}(L,t)=w_{xx}(L,0)e^{-\int_0^t(1+w_x^2(L,s))ds}.$$

As $w_0 \in \mathcal{D}(\mathcal{A})$, $w_{xx}(L,0)=0$ and thus $w_{xx}(L,t)=0$ for all $t \in (0,T)$.

The same argument now applies for $\phi \in H_*^2$, yielding

$$w_{xxxt}(L)+\left(1+w_x^2(L)\right)w_{xxx}(L)=0,$$

from which we deduce that $w_{xxx}(L,t)=0$ for all $t \in (0,T)$. $\square$

2.6.3.2 Uniqueness and Continuous Dependence

Consider w and v to be two strong solutions of (2.4.1) with $\sigma = \iota = 1$ and $k_2 > 0$ and let $z \equiv w - v$. Using the multiplier z_t on (2.4.1) we obtain:

$$\begin{aligned}\frac{1}{2}\frac{d}{dt}&\Big[||z_t||^2 + D||z_{xx}||^2 + D||w_x z_{xx}||^2 + D||w_{xx} z_x||^2\Big] \\ &+ k_2||z_{xxt}||^2 + \left(\partial_x\left[w_x \int_x^L \overline{u}_{tt} - v_x \int_x^L \hat{u}_{tt}\right], z_t\right) \\ &= D\left(w_x w_{xt}, z_{xx}^2\right) - D\left(v_{xx}\left[w_x + v_x\right], z_x z_{xxt}\right) \\ &+ D\left(w_{xx} w_{xxt}, z_x^2\right) - D\left(v_x\left[w_{xx} + v_{xx}\right], z_{xx} z_{xt}\right),\end{aligned} \tag{2.6.32}$$

where

$$\overline{u}_{tt}(x) = -\int_0^x \left[w_{xt}^2 + w_x w_{xtt}\right] d\xi \quad \text{and} \quad \hat{u}_{tt}(x) = -\int_0^x \left[v_{xt}^2 + v_x v_{xtt}\right] d\xi.$$

The presence of strong damping allows us to estimate the RHS in a straightforward manner (without the subtlety needed in Section 2.5.3.2):

1. $D\left|(w_x w_{xt}, z_{xx}^2)\right| \lesssim ||w_{xx}||\ ||w_{xxt}||\ ||z_{xx}||^2$

2. $D\left|(v_{xx}\left[w_x + v_x\right], z_x z_{xxt})\right| \le C_{\varepsilon_1}||v_{xx}||^2||w_{xx} + v_{xx}||^2||z_{xx}||^2 + \varepsilon_1||z_{xxt}||^2$

3. $D\left|\left(w_{xx} w_{xxt}, z_x^2\right)\right| \lesssim ||w_{xx}||\ ||w_{xxt}||\ ||z_{xx}||^2$

4. $D\left|(v_x\left[w_{xx} + v_{xx}\right], z_{xx} z_{xt})\right| \le C_{\varepsilon_2}||v_{xx}||^2||w_{xxx} + v_{xxx}||^2||z_{xx}||^2 + \varepsilon_2||z_{xxt}||^2.$

For the inertial term, we have:

$$\begin{aligned}
&\left(\partial_x \left[w_x \int_x^L \overline{u}_{tt} - v_x \int_x^L \hat{u}_{tt}\right], z_t\right) \\
&= -\left((w_x - v_x)\int_x^L \overline{u}_{tt}, z_{xt}\right) - \left(v_x \int_x^L \left[\overline{u}_{tt} - \hat{u}_{tt}\right], z_{xt}\right) \\
&\equiv \qquad\qquad \mathcal{N} \qquad\qquad + \qquad\qquad \mathcal{O}.
\end{aligned}$$

Firstly:

$$|\mathcal{N}| = \left|\left(\overline{u}_{tt}, \int_0^x z_x z_{xt}\right)\right| \lesssim ||z_{xt}||_{L^\infty}||\overline{u}_{tt}||\ ||z_x|| \leq \varepsilon_3 ||z_{xxt}||^2 + c_{\varepsilon_3}||\overline{u}_{tt}||^2||z_{xx}||^2.$$

The second term $\mathcal{O}$ yields:

$$\begin{aligned}
\mathcal{O} &= -\left(\overline{u}_{tt} - \hat{u}_{tt}, \int_0^x v_x z_{xt}\right) \\
&= \left(\int_0^x \left[w_{xt}^2 - v_{xt}^2\right], \int_0^x v_x z_{xt}\right) + \left(\int_0^x \left[w_x w_{xtt} - v_x v_{xtt}\right], \int_0^x v_x z_{xt}\right) \\
&\equiv \qquad\qquad \mathcal{O}_1 \qquad\qquad + \qquad\qquad \mathcal{O}_2,
\end{aligned}$$

where

$$\begin{aligned}
\mathcal{O}_2 = \left(\int_0^x \left[z_x w_{xtt} + v_x z_{xtt}\right], \int_0^x v_x z_{xt}\right) &= \frac{1}{2}\frac{d}{dt}\left|\left|\int_0^x v_x z_{xt}\right|\right|^2 - \left(\int_0^x v_{xt} z_{xt}, \int_0^x v_x z_{xt}\right) \\
&\quad + \left(\int_0^x z_x w_{xtt}, \int_0^x v_x z_{xt}\right).
\end{aligned}$$

The conserved d/dt quantity will remain on the LHS, with the rest moved to the RHS and estimated:

$$\left|\left(\int_0^x v_{xt}z_{xt}, \int_0^x v_x z_{xt}\right)\right| \leq \varepsilon_4 ||v_{xt}||^2_{L^\infty} ||z_{xt}||^2 + c_{\varepsilon_4} \left|\left|\int_0^x v_x z_{xt}\right|\right|^2$$

$$\leq \varepsilon_4 ||v_{xxt}||^2 \; ||z_{xxt}||^2 + c_{\varepsilon_4} \left|\left|\int_0^x v_x z_{xt}\right|\right|^2$$

$$\left|\left(\int_0^x z_x w_{xtt}, \int_0^x v_x z_{xt}\right)\right| \lesssim ||w_{xtt}||^2 ||z_{xx}||^2 + \left|\left|\int_0^x v_x z_{xt}\right|\right|^2.$$

Remark 2.6.4. The above calculation demonstrates the necessity of forming an energy identity (namely the **Energy Level 3** formed in the proof of *Theorem* 2.6.1) that provides higher spatial regularity for w_{tt}.

Lastly we have:

$$|\mathcal{O}_1| \leq \left|\left(\int_0^x (w_{xt} + v_{xt})\, z_{xt}, \int_0^x v_x z_{xt}\right)\right| \leq \varepsilon_5 \left(||w_{xxt} + v_{xxt}||\right)^2 ||z_{xxt}||^2 + c_{\varepsilon_5} \left|\left|\int_0^x v_x z_{xt}\right|\right|^2.$$

Defining:

$$\mathcal{E}(t) = \frac{1}{2}\left[||z_t||^2 + D||z_{xx}||^2 + D||w_x z_{xx}||^2 + D||w_{xx} z_x||^2 + \left|\left|\int_0^x v_x z_{xt}\right|\right|^2\right],$$

combining estimates for $\mathcal{N}$ and $\mathcal{O}$, and recalling $\overline{u}_{tt}(x) = -\int_0^x \left[w_{xt}^2 + w_x w_{xtt}\right]$, we obtain:

$$\mathcal{E}(t) + k_2 \int_0^t ||z_{xxt}||^2 \leq \mathcal{E}(0) + \int_0^t K(w,v)\mathcal{E}(\tau) d\tau + \sum_{i=1}^{5} \varepsilon_i \int_0^t C(w,v)||z_{xxt}||^2, \tag{2.6.33}$$

where the above dependencies are of the following sense:

$$K(w,v) = K\left(||w||_3^2, ||w_t||_2^2, ||v||_3^2, ||w_{tt}||_1^2\right) \quad \text{and} \quad C(w,v) = \left(||w||_2^2, ||w_t||_2^2\right).$$

The regularity of strong solutions in the inertial case with data in $\mathcal{D}(\mathcal{A}^2)^2$ (see e.g., (2.6.26)) provide $w_{ttt} \in L^\infty(0,T;L^2(0,T))$ (with a bound in terms of the data), and with $w_{tt} \in L^\infty(0,T;H_*^2)$; thus we have $w_{tt} \in C([0,T];H^1(0,L))$. From this, and the energy estimate for inertial solutions ((2.6.28) with Remark 2.5.7), we obtain $C([0,T])$ boundedness (for $T < T^*(\text{data}_w, \text{data}_v)$) of the quantities $C(w,v),\ K(w,v)$ the individual trajectories $(w,w_t),\ (v,v_t)$. Taking $\sup_{[0,T]}$ and choosing ε_i sufficiently small (depending on the data), we obtain:

$$\mathcal{E}(t) \le \mathcal{C}_1\mathcal{E}(0) + \mathcal{C}_2\int_0^t \mathcal{E}(\tau)d\tau,$$

where $t \in [0,T]$ and we have the dependencies

$$\mathcal{C}_i\Big(||(w_0,w_1)||_{\mathscr{H}_s^I}, ||(v_0,v_1)||_{\mathscr{H}_s^I}, ||p||_{H^2(0,T;L^2(0,L))}\Big).$$

The standard Grönwall lemma yields:

$$\mathcal{E}(t) \le \mathcal{E}(0)e^{\mathcal{C}_1 t}, \quad t \in [0,T].$$

Uniqueness and continuous dependence follow as in Section 2.5.3.2 for stiffness-only dynamics, i.e., in the sense that $||z||_2^2 + ||z_t||^2 \lesssim \mathcal{E}(t)$.

2.7 Global Solutions for Sufficiently Small Data

2.7.1 Precise Statement of the Theorem

Theorem 2.7.1. *Suppose $\iota = \sigma = 1$ with $k_2 > 0$, and take $p \equiv 0$. Then there exists a number $Q > 0$ such that if $||(w_0, w_1)||_{\mathscr{D}(\mathcal{A}^2)\times\mathscr{D}(\mathcal{A}^2)} \leq Q$, then the corresponding strong solution (w, w_t) of* (2.4.1)–(2.4.2) *has time of existence $T^*(w_0, w_1) = +\infty$ and there exist $M, \omega > 0$ depending only on Q such that*

$$||(w(t), w_t(t))||^2_{\mathscr{D}(\mathcal{A}^2)\times\mathscr{D}(\mathcal{A}^2)} \leq M \exp(-\omega t).$$

We note that the above theorem will obtain unproblematically in the case of $\iota = 0$ and $k_2 > 0$, i.e., when nonlinear inertia is neglected and Kelvin–Voigt damping is included. On the other hand, it is clear the result should be possible with weaker damping. See the second point in Section 2.8.

2.7.2 Outline of Proof

We proceed as in [43, 52] to obtain global existence indirectly via the *Barrier method*, which exploits the superlinearity in the problem. Using the damping, we will employ stabilization type multipliers at every energy level to obtain an inequality of the form in the theorem below, which we take from [43]:

Theorem 2.7.2. *Suppose that $X : [0, \infty) \to [0, \infty)$ is a continuous function such* *that there is a* $T > 0$ *so that* $X(T) < \infty$ *and*

$$X(T)+C_1\int_0^T X(s)ds \leq C_2X(0)+C_3\sum_{i=1}^{N_1} X^{\alpha_i}(0)+C_4\sum_{i=1}^{N_2} X^{\beta_i}(T)+C_5\sum_{i=1}^{N_3}\int_0^T X^{\gamma_i}(s)ds, \tag{2.7.1}$$

where $\alpha_i > 1,\ i = 1, 2, \ldots, N_1,\ \beta_j > 1,\ j = 1, 2, \ldots, N_2$ *and* $\gamma_k > 1, k = 1, 2, \ldots, N_3$. *Then there exists a* $\mathscr{C}$ *depending on* $C_i, N_i, \alpha_i, \beta_i$ *so that if* $X(0) \leq \epsilon \leq \mathscr{C}$, *then*

$$X(t) \leq \frac{\epsilon}{\mathscr{C}} \exp\left(-\mathscr{C}t\right).$$

For us, $X(t)$ will be the sum of (the majority of) the norms appearing in the formal energy identities we have constructed thus far. Any continuous function that satisfies the integral inequality has the desired property: exponential decay for sufficiently small initial conditions $X_i(0)$, which in turn yields global-in-time existence [43].

To form an inequality of the form (2.7.1) we will utilize the previous calculations we have obtained for the energy estimates in Section 2.6, along with additional estimates based on equipartition multipliers at each level. We will attempt to form (2.7.1) for *each* $X_i(t),\ i = 0, 1, 2, 3$ separately, where X_i's correspond to each energy level we have defined before, and sum the results. To streamline exposition of comparable calculations in the earlier sections, we demonstrate the detailed calculations for $X_0(t)$. For $X_i(T),\ i = 1, 2, 3$, we will only highlight deviations from the details in the proof of theorems 2.5.1 and 2.6.1.

2.7.3 Proof of Theorem 2.7.1

Step 1 - Inequality for X_0: Recalling the estimate for $\mathcal{E}_0$ in **Step 2** of Section 2.6, we redefine:

$$X_0(t) = ||w_t(t)||^2 + ||w_{xx}(t)||^2 + ||w_x w_{xx}(t)||^2 + ||u_t(t)||^2$$

and we have immediately the inequality:

$$X_0(T) + k_2 \int_0^T ||w_{xxt}||^2 \leq X_0(0). \tag{2.7.2}$$

It is crucial to retain the inertial term to appear under the integral sign, thus we augment (2.7.2) to obtain:

$$X_0(T) + \int_0^T \left[k_2 ||w_{xxt}||^2 + ||u_t||^2\right] \leq X_0(0) + \int_0^T ||u_t||^2. \tag{2.7.3}$$

The inertial term appearing on the RHS will now have to be estimated. Note that if *we bound it above by* $X_0(0)$, it will appear under the time integral and such a bound would be inconsistent with the form of inequality (2.7.1). Rather, we estimate as:

$$||u_t||^2 \lesssim ||w_x w_{xt}||^2 \lesssim ||w_{xx}||^2 ||w_{xt}||^2 \lesssim ||w_{xx}||^6 + ||w_{xt}||^3, \tag{2.7.4}$$

where we've used Young's inequality with $p = 3$ and $q = 3/2$. We interpolate $||w_{xt}||^3$

as follows:

$$||w_{xt}||^3 \leq ||w_t||^{3/2}||w_{xxt}||^{3/2} \leq c_{\varepsilon_1}||w_t||^6 + \varepsilon_1||w_{xxt}||^2, \tag{2.7.5}$$

again using Young's inequality with $p = 4$ and $q = 4/3$. Thus we have the ε for absorption, and we obtain:

$$X_0(T) + c_1 \int_0^T \left[||w_{xxt}||^2 + ||u_t||^2\right] \leq X_0(0) + c_2 \int_0^T \left[||w_{xx}||^6 + ||w_t||^6\right]. \tag{2.7.6}$$

Invoking norm equivalence between $H^2(0, L)$ and H^2_*, (2.7.6) becomes:

$$X_0(T) + c_1 \int_0^T \left[||w_t||^2 + ||u_t||^2\right] \leq X_0(0) + c_2 \int_0^T \left[||w_{xx}||^6 + ||w_t||^6\right]. \tag{2.7.7}$$

Now, the equipartition (stability) multiplier for this level is w; multiplying (2.4.1) by the solution and integrating by parts in space and time, we obtain:

$$\begin{aligned}\frac{k_2}{2}||w_{xx}(T)||^2 + D\int_0^T \left[||w_{xx}||^2 + 2||w_x w_{xx}||^2\right] - \int_0^T \left[||w_t||^2 + ||u_t||^2\right] \\ = \frac{k_2}{2}||w_{xx}(0)||^2 - \int_0^L ww_t\Big|_0^T - 2\int_0^L uu_t\Big|_0^T.\end{aligned}$$

We note that from $u(x,t) = -\frac{1}{2}\int_0^x w_x^2(\xi, t)d\xi$, we have:

$$||u(t)||^2 \lesssim \Big|\Big|\int_0^x w_x(\xi, t)\left[\int_0^\xi w_{xx}(\zeta, t)d\zeta\right]d\xi\Big|\Big|^2 \lesssim ||w_x(t)w_{xx}(t)||^2 \lesssim X_0(t),$$

via Fubini and Jensen's inequality, having then extended the integrals to $x \in [0, L]$.

Hence, $||u(T)||^2 + ||u(0)||^2 \leq c_3 X_0(0)$. The RHS can then be estimated straightforwardly, yielding:

$$\frac{k_2}{2}||w_{xx}(T)||^2 + D\int_0^T \left[||w_{xx}||^2 + 2||w_x w_{xx}||^2\right] - \int_0^T \left[||w_{xxt}||^2 + ||u_t||^2\right] \leq c_3 X_0(0). \tag{2.7.8}$$

We then take an appropriate linear combination of (2.7.7) and (2.7.8) (with constants depending on the damping coefficient k_2), and eliminate the negative terms appearing in (2.7.8). Then, by possible adjustments of the constants, we have:

$$X_0(T) + C_1\int_0^T X_0 \leq C_2 X_0(0) + C_3\int_0^T X_0^6. \tag{2.7.9}$$

Step 2 - Inequality for X_1 and X_2: In this step we will proceed by forming the inequality that corresponds to $X_1 + X_2$. As we will see later, there will be terms in the X_2 estimate that will need to by absorbed by some appearing in X_1. We define:

$$X_1(t) = ||w_{tt}(t)||^2 + ||w_{xxt}(t)||^2 + ||w_{xt}(t)w_{xx}(t)||^2 + ||w_x(t)w_{xxt}(t)||^2 + ||u_{tt}(t)||^2.$$

Remark 2.7.1. Note X_1 does not include the quantity $||\int_0^x w_{xt}^2||^2$, as $\mathcal{E}_1$ does. As it can be seen from the following calculations, the aforementioned norm is not needed in obtaining (2.7.1).

Following similar calculations as in **Step 4** in the proof of Theorem 2.6.1, we obtain:

$$\left(\partial_{xt}\left[w_x\int_x^L u_{tt}\right]\ ,w_{tt}\right) = \frac{1}{2}\frac{d}{dt}||u_{tt}||^2 + \frac{d}{dt}\left(u_{tt}, \int_0^x w_{xt}^2\right) - 3\left(u_{tt}, \int_0^x w_{xt}w_{xtt}\right). \tag{2.7.10}$$

The conserved quantity of (2.7.10) will remain to the LHS, while the remaining terms will be moved to the RHS and be estimated, after we proceed with integration in time, as follows:

1. $\left|\left(u_{tt}(T), \int_0^x w_{xt}^2(T)\right)\right| \leq \delta_1||u_{tt}(T)||^2 + c_{\delta_1}||w_{xxt}(T)||^4$
2. $\left|\left(u_{tt}(0), \int_0^x w_{xt}^2(0)\right)\right| \lesssim ||u_{tt}(0)||^2 + ||w_{xxt}(0)||^4$
3. $\left|\left(u_{tt}, \int_0^x w_{xt}w_{xtt}\right)\right| \leq \delta_2||u_{tt}||^2 + c_{\delta_2}||w_{xxt}||^6 + c_{\delta_2,\varepsilon_1}||w_{tt}||^6 + c_{\delta_2}\varepsilon_1||w_{xxtt}||^2.$

In addition to the above calculations, we add the term $\int_0^T ||u_{tt}||^2$ to both sides of the inequality. On the RHS it will be estimated via:

$$||u_{tt}||^2 \lesssim ||w_{xxt}||^2||w_{xt}||^2 + ||w_{xxt}||^2||w_x||\ ||w_{xtt}|| + ||w_{xx}||^2||w_{xtt}||^2.$$

Using Young's inequality and interpolation, as in (2.7.4) and (2.7.5), and directly invoking the stiffness calculations in **Step 4** in the proof of Theorem 2.5.1, we arrive at:

$$X_1(T) + \int_0^T \left[k_2||w_{xxtt}||^2 + ||u_{tt}||^2\right] \leq c_1 \left(X_1(0) + X_1^2(0) + X_0^2(0) + X_0^{16}(0)\right) + c_2 X_1^2(T)$$
$$+c_3 \int_0^T \left[X_1^2 + X_1^3 + X_1^4 + X_0^2 + X_0^3\right] + \delta \int_0^T ||u_{tt}||^2 + \varepsilon \int_0^T ||w_{xxtt}||^2, \tag{2.7.11}$$

where ε and δ collect the various ε_i's and δ_i's corresponding to earlier applications of Young's inequality.

For the time-differentiated version of the equations, w_t acts as the equipartition multiplier. After the appropriate calculations, and straightforward estimation, we obtain:

$$\frac{k_2}{2}||w_{xxt}(T)||^2 + D \int_0^T \left[||w_{xxt}||^2 + ||w_{xt}w_{xx}||^2 + ||w_x w_{xxt}||^2\right] - \int_0^T \left[||w_{tt}||^2 + ||u_{tt}||^2\right]$$
$$\leq c_1(X_1(0) + X_0(0)) + \varepsilon_1 ||w_{tt}(T)||^2 + \delta_1 ||u_{tt}(T)||^2 + c_2 \int_0^T \left[X_1^2 + X_1^0\right] + \delta_2 \int_0^T ||u_{tt}||^2. \tag{2.7.12}$$

Now, we define:

$$X_2(t) = ||w_{xxt}(t)||^2 + ||\partial_x^4 w(t)||^2 + ||w_x(t)\partial_x^4 w(t)||^2 + ||u_{xxt}(t)||^2.$$

Then, duplicating the calculations in **Step 5** in the proof of Theorem 2.6.1 and adding $\int_0^T ||u_{xxt}||^2$ to both sides we have:

$$X_2(T) + \int_0^T \left[k_2||\partial_x^4 w_t||^2 + ||u_{xxt}||^2\right] \le c_1 \left(X_2(0) + X_0^9(0)\right)$$
$$+c_2 \int_0^T \left[X_2^2 + X_1^2 + X_0^{10/3} + X_0^4\right] + \varepsilon_2 \int_0^T ||w_{xxtt}||^2. \qquad (2.7.13)$$

Remark 2.7.2. The term $||w_{xxtt}||^2$ appearing on the RHS of the above inequality is the reason why we chose to have the calculations of X_1 and X_2 combined.

To complete the estimate for $X_2(t)$, we proceed by employing $\partial_x^4 w$ as a multiplier. The calculations corresponding to stiffness are described in **Step 5** in the proof of Theorem 2.5.1. Inertial terms are handled through differentiation and spatial integration by parts:

$$\int_0^T \left(\partial_x \left[w_x \int_x^L u_{tt}\right], \partial_x^4 w\right)$$
$$= \int_0^T \left(w_{xx} \int_x^L u_{tt}, \partial_x^4 w\right) - \int_0^T \left(w_x u_{tt}, \partial_x^4 w\right)$$
$$= \int_0^T \left(w_{xx} \int_x^L u_{tt}, \partial_x^4 w\right) - \int_0^T (u_{tt}, w_{xx} w_{xxx}) - 2\int_0^T \left(u_{ttx}, w_{xx}^2\right) - \int_0^T (u_{ttxx}, w_x w_{xx}).$$

The only non-trivial term to estimate is the last; integrate by parts *in* t and note $\partial_t (-w_x w_{xx}) = u_{xxt}$:

$$-\int_0^T (u_{ttxx}, w_x w_{xx}) = -w_x w_{xx} u_{xxt}\Big|_0^T - \int_0^T ||u_{xxt}||^2.$$

Combining, we obtain:

$$\frac{k_2}{2}||\partial_x^4 w(T)||^2 + D\int_0^T \left[||\partial_x^4 w||^2 + ||w_x\partial_x^4 w||^2\right] - \int_0^T \left[||w_{xxt}||^2 + ||u_{xxt}||^2\right]$$
$$\leq c_1\left(X_2(0) + X_1(0) + X_0(0) + X_0^2(0)\right) + \varepsilon_3||w_{xxt}(T)||^2 + \delta_3||u_{xxt}(T)||^2$$
$$+ c_2\int_0^T \left[X_2^2 + X_1^2 + X_0^2 + X_0^9 + X_0^{17}\right] + \varepsilon_4\int_0^T ||\partial_x^4 w||^2. \qquad (2.7.14)$$

As before, we add (2.7.11) to (2.7.13), and we add (2.7.12) to (2.7.14); we then choose an appropriate linear combination of the sums for absorption of negative integral terms; we then choose ε_i, δ_i appropriately, and invoke norm equivalence for H_*^2, yielding the estimate for $X_1 + X_2$:

$$X_2(T) + X_1(T) + C_1\int_0^T [X_2 + X_1]$$
$$\leq C_2\Big(X_2(0) + X_1(0) + X_1^2(0) + X_0(0) + X_0^2(0) + X_0^9(0) + X_0^{16}(0)\Big)$$
$$+ C_3X_1^2(T) + C_4\int_0^T \left[X_2^2 + X_2^4 + X_1^2 + X_1^3 + X_1^4 + X_0^2 + X_0^3 + X_0^9 + X_0^{17}\right]. \qquad (2.7.15)$$

Step 3 - Inequality for X_3: Define:

$$X_3(t) = ||w_{ttt}(t)||^2 + ||w_{xxtt}(t)||^2 + ||w_x w_{xxtt}(t)||^2 + ||w_{xx}(t)w_{xtt}(t)||^2 + ||u_{ttt}(t)||^2.$$

The estimate corresponding to *two time* differentiations of (2.4.1) with the multiplier w_{ttt} can be directly formed from the existing calculations for **Step 7** in the proof of

Theorem (2.6.1).

$$
\begin{aligned}
X_3(T) &+ c_1 \int_0^T \left[||w_{ttt}||^2 + ||u_{ttt}||^2\right] \\
&\leq c_2 \left(X_3(0) + X_2^9(0) + X_1^9(0)\right) + c_3 \left(X_2^9(T) + X_1^9(T)\right) \\
&+ c_4 \int_0^T \left[X_3^2 + X_2^2 + X_2^4 + X_1^2 + X_1^3 + X_1^4 + X_0^2 + X_0^3 + X_0^4\right], \qquad (2.7.16)
\end{aligned}
$$

where we added $\int_0^T ||u_{ttt}||^2$ to both sides and proceeded as in earlier estimates.

In this case, w_{tt} is the equipartition multiplier, and calculations corresponding to stiffness are duplicated from **Step 7** in the proof of *Theorem* (2.6.1). The inertial term calls for a slightly altered approach:

$$
\begin{aligned}
\left(\partial_{xtt}\left[w_x \int_x^L u_{tt}\right], w_{tt}\right) = -\left(w_{xtt} \int_x^L u_{tt}, w_{xtt}\right) - 2\left(w_{xt} \int_x^L u_{ttt}, w_{xtt}\right) \\
-\left(w_x \int_x^L u_{tttt}, w_{xtt}\right).
\end{aligned}
$$

The first two terms above can be treated similarly to $\mathcal{J}_i$ of **Step 5** in the proof of *Theorem* (2.6.1), and for the latter we write:

$$
\begin{aligned}
\int_0^T \left(u_{tttt}, -\int_0^x w_x w_{xtt}\right) = \int_0^T \left(u_{tttt}, u_{tt}\right) + \int_0^T \frac{d}{dt}\left(u_{ttt}, \int_0^x w_{xt}^2\right) \\
-2\int_0^T \left(u_{ttt}, \int_0^x w_{xt} w_{xtt}\right).
\end{aligned}
$$

The first term will be integrated by parts *in time* and the following two will be estimated as above.

Hence, assembling everything together we have:

$$\begin{aligned}\frac{k_2}{2}||w_{xxtt}(T)||^2 + c_1\int_0^T \left[||w_{xxtt}||^2 + ||w_x w_{xxtt}||^2 + ||w_{xx}w_{xtt}||^2\right] - c_2\int_0^T \left[||w_{ttt}||^2 + ||u_{ttt}||^2\right] \\ \leq c_3\left(X_3(0) + X_1^2(0) + X_1(0)\right) + c_4 X_1(T) + \varepsilon_1||w_{ttt}(T)||^2 + \varepsilon_2||u_{ttt}(T)||^2 \\ + c_5 X_1^2(T) + c_6\int_0^T \left[X_3^2 + X_2^2 + X_2^4 + X_1^2 + X_1^4 + X_0^2 + X_0^4\right].\end{aligned} \tag{2.7.17}$$

Combining (2.7.16) with (2.7.17) in an appropriate linear combination, we obtain:

$$\begin{aligned}X_3(T) + C_1\int_0^T X_3 \leq & C_2\left(X_3(0) + X_2^9(0) + X_1(0) + X_1^2(0) + X_1^9(0)\right) \\ & + C_3\left(X_1^9(T) + X_2^9(T)\right) + C_4 X_1(T) \\ & + C_5\int_0^T \left[X_3^2 + X_2^2 + X_2^4 + X_1^2 + X_1^3 + X_1^4 + X_0^2 + X_0^3 + X_0^4\right].\end{aligned} \tag{2.7.18}$$

Here we remark that the term $X_1(T)$ appearing above is bounded by (2.7.11).

Finally, we note that the bound above depends on the boundedness of the quantity $X_3(0)$ which contains the term $||w_{ttt}(0)||^2 + ||u_{ttt}(0)||^2$. This term does not explicitly appear as data, however, it is directly bounded by the data $||(w_0, w_1)||^2_{\mathscr{D}(\mathcal{A}^2)^2}$, which can be shown directly on approximate solutions, as was the focus of **Step 6** in Section 2.6.1.

Step 4 - Global Estimate: With the constituent inequalities in hand from **Steps**

1–3, we form:

$$X(T) = X_0(T) + X_1(T) + X_2(T) + X_3(T).$$

This quantity is nonnegative, and continuous due to the regularity of constructed solutions. We then add (2.7.9), (2.7.15) and (2.7.18), and with minor algebraic manipulations, we obtain:

$$X(T) + C_1 \int_0^T X(s)ds \leq C_2 X(0) + C_3 F_0 + C_4 \left(X^2(T) + X^9(T) \right) + C_5 \int_0^T F(s)ds, \tag{2.7.19}$$

where

$$F_0 = X^2(0) + X^9(0) + X^{16}(0)$$

and

$$F(s) = X^2(s) + X^3(s) + X^{10/3}(s) + X^4(s) + X^6(s) + X^9(s) + X^{17}(s).$$

This final estimate (2.7.19) is of the form in Theorem 2.7.2, which concludes the proof of Theorem 2.7.1 □

2.8 Comments and Open Problems

We briefly discuss open problems and directions for future work.

- **The existence of finite energy, weak solutions** seems to be a challenging one. It is clear that additional compactness is needed for the identification of limit points associated only to the stiffness portion of the dynamics. Compensated compactness requirements (e.g., those in L^1) might be adapted to the nonlinear structures, though it is unclear if such an approach would be more expedient than the higher order energy methods employed here.

- **The elimination or weakening of damping** seems a natural course. In our estimates, it is clear that the regularizing effects of Kelvin–Voigt damping are stronger than explicitly needed in the construction of solutions and estimation of inertial terms. On the other hand, weak damping of the form $k_0 w_t$ is clearly too weak to address inertial terms. Unfortunately, for cantilevered beams, the physical interpretation of $A^{1/2} w_t \sim k_1 \partial_x^2 w_t$ damping is unclear—see the discussions in [21] and [39]. Thus, it is a question for future work to utilize weaker (than Aw_t) damping to obtain global solutions with sufficiently small data for (2.4.1) with $\sigma, k_2 = 1$ and $\iota = 0$.

- Explicit **proof of blow up** for large data in this quasilinear system would nicely complement our local existence results. Currently, numerical evidence shows that large data quickly leads to non-physical solutions (kinking or pass-through).

- **The introduction of non-conservative forces** as discussed in the introduction (e.g., with application to piezoelectric energy harvesting) is a natural next step. The earlier work [21] addresses a piston-theoretic beam, as does the more recent [60, 61]. However, exploiting the superlinearity of the nonlinear stiffness to provide a rigorous framework for long-time behavior of trajectories is a desirable future goal.

Chapter 3: Simulation of Inextensible Cantilever Dynamics

3.1 Summary of the Chapter

This chapter is devoted to numerically simulating the inextensible cantilever dynamics that were introduce in Chapter 1. A modal approach is used to produce mathematically-oriented numerical results that provide insight into the features and limitations of the inextensible model.

3.2 Introduction

In this chapter we focus on (2.4.1)–(2.4.3) and make clear distinctions between linear dynamics $\sigma = \iota = 0$, [**NL Stiffness**] only dynamics ($\sigma = 1,\ \iota = 0$), and fully nonlinear dynamics—with [**NL Stiffness**] and [**NL Inertia**] ($\sigma = \iota = 1$).

We are interested in dynamical stability properties, as well as long-time, qualitative responses of the dynamics, to: distributed pressures (via piston theory, described in the next section), and varying initial conditions. We will measure displacements of the cantilever, and we will track things like the free end displacement curves $\Big(u(L,t), w(L,t)\Big)$, the arc-length of the beam as a function of time, and energies (see Section 2.4.3) as a function of time.

In Sections 3.2.1 and 3.2.2 we describe the method and approach to producing dynamic (modal) simulations. Subsequently, in Section 3.2.3, we show our numerical results and provide a detailed discussion. Finally, in Section 3.2.4, we provide an overview of numerical conclusions drawn from our simulations here.

3.2.1 Dynamical Driver: Piston Theory

In our simulations, we seek a simple way to test the model, affect beam stability, and "drive" the dynamics. In line with the applications relevant to cantilever large deflections, we consider a rudimentary means for simulating the flow of gas around the cantilever. Though there are various ways to consider flow-beam coupling, the simplest is to eliminate the fluid dynamic variables altogether. This has the benefit of reducing the flow-beam system to a single non-conservative beam dynamics. Such a reduction is a dramatic simplification of complex, multi-physics phenomena, but, focusing on a simple, un-coupled model allows us to perform a thorough numerical study that can be performed straight-forwardly. (More sophisticated related, flow-structure models are certainly explored in the rigorous mathematical literature—see, e.g., [15, 16].)

We consider beam dynamics interacting with a potential flow. For certain flow conditions, the dynamic pressure on the surface of the beam, $p(x,t)$, can be approximated point-wise in x by an expression written in the *down-wash* of the fluid $W = (\partial_t + U\partial_x)w$, where $w(x,t)$ is the transverse displacement of the beam, and U is the unperturbed axial flow velocity. This results in a nonlinear expression [3] in W

that is linearized to produce the *piston-theoretic* pressure $p(x,t)$ on the beam [76]:

$$p(x,t) = p_0(x) - \beta[w_t + Uw_x]. \tag{3.2.1}$$

Above, $p_0(x)$ is a static pressure on the surface of the beam (for the numerical portion of this paper we will take $p_0(x) = 0$). The parameter $\beta > 0$ is a fluid density parameter.[1] We consider both positive and negative values for U, corresponding to axial flow from clamped to free end ($U > 0$—flag-like configuration [2,41]), as well as from free to clamped end ($U < 0$—inverted flag configuration [46,70]). Note that the presence of aerodynamics provides both a stabilizing term—weak damping—scaled by $\beta > 0$, as well a destabilizing non-conservative term scaled by βU. (See [39] for more discussion.)

With (3.2.1) providing our dynamic driver, we can consider a simple non-conservative dynamics that can give rise to instability in our model, resulting in large deflections that "test" the inextensible nonlinear effects.

3.2.2 Modal Dynamics

Modal analysis, here, refers to a Galerkin method, based on the above weak formulation (2.4.13), whereby solutions are approximated by in vacuo structural eigenfunctions (modes) (e.g., [26, 42, 76]). Since the eigenfunctions of standard elasticity operators form a basis for the state space, a good well-posedness result for the full system justifies this type of approximation. The approximation can be dynamic, as

[1]See [76] for a discussion of the flow non-dimensionalization, and further discussion of characteristic parameter values.

in reducing an evolutionary PDE to a finite dimensional system of ODEs by truncation, or it can be stationary, reducing the problem of dynamic instability (for linear dynamics) to an algebraic equation.

3.2.2.1 Cantilever Modes

Critical to any modal analysis—see, for instance, [42]—are the in vacuo modes (eigenfunctions) associated to the configuration. We are working with the linear Euler–Bernoulli cantilever as our approximants in H^2_*, and the modes and associated eigenvalues can be computed in an elementary way. These functions are *complete* and *orthonormal* in $L^2(0,L)$, as well as complete and orthogonal in $H^2_*(0,L)$ (with respect to $(\cdot,\cdot)_{H^2_*}$).

The cantilever mode shapes of interest are:

$$s_n(x) \equiv c_n(\cos(\kappa_n x) - \cosh(\kappa_n x)) + C_n(\sin(\kappa_n x) - \sinh(\kappa_n x)),$$

where the C_n are obtained by solving the associated characteristic equation: $\cos(\kappa_n L)\cosh(\kappa_n L) = -1$. We have

$$C_n = \frac{-c_n\Big(\cos(\kappa_n L) + \cosh(\kappa_n L)\Big)}{\sin(\kappa_n L) + \sinh(\kappa_n L)},$$

and the c_n values are chosen to normalize the functions in the $L^2(0,L)$ sense.

The mode numbers $\kappa_n L$ are obtained by numerically solving the characteristic equation.

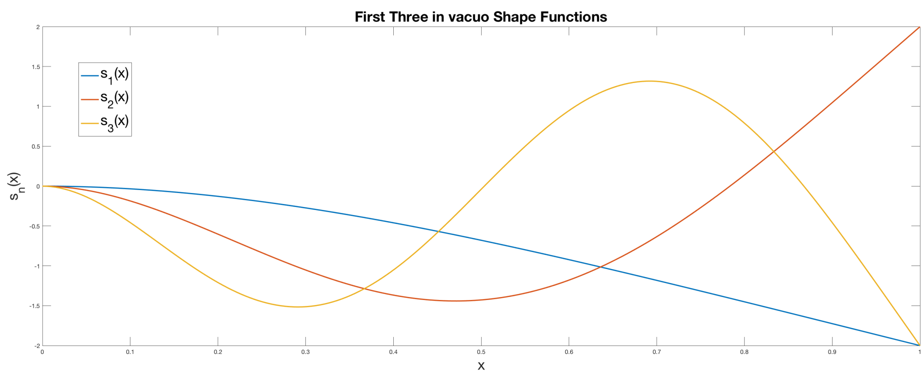

3.2.2.2 Calculating the Flutter Point: Reduction to Perturbed Eigenvalue Problem

Let us consider the Galerkin procedure for the full linear beam equation with linear piston theory and the possibility of imposed weak damping $k_0 \geq 0$:

$$w_{tt} + Dw_{xxxx} + (k_0 + \beta)w_t = -\beta U w_x \tag{3.2.2}$$

on $(0, L)$, with cantilever boundary conditions. We expand the solution via the in vacuo mode functions $\{s_j\}$ as $w(t,x) = \sum q_j(t)s_j(x)$. The $\{q_j\}$ represent smooth, *time-dependent coefficients*. Plugging this representation into the (3.2.2), multiply-

n	k_nL
1	1.8751
2	4.6941
3	7.8548
4	10.9955
5	14.1372
6	17.2788

Table 3.1: First 6 mode numbers for the cantilever (Clamped-Free, **CF**) configuration.

ing by s_n, and integrating over $(0, L)$ for each n we obtain:

$$\sum_m \left[\left[q''_m(t) + (\beta + k_0) q'_m(t) + D k_m^4 q_m(t) \right] (s_m, s_n) + \beta U (\partial_x s_m, s_n) q_m(t) \right] = 0, \tag{3.2.3}$$

with $'$ indicating ∂_t.

Orthonormality of the eigenfunctions can be invoked to produce *diagonal* terms, whereas the terms scaled by $\beta U(\partial_x s_m, s_n)$ are *off-diagonal* and give rise to the instability of the ODE system.

To simply determine the stability of the problem as a function of the given parameters, we can invoke a standard engineering ansatz [25, 76] (and references therein): *assume simple harmonic motion* according to some dominant (perturbed) frequency $\widetilde{\omega}$; we allow possible contribution from all functions s_n for $n = 1, 2, ..., N$ via coefficients labeled α_n:

$$w(t, x) \approx e^{-i\widetilde{\omega}t} \sum_{j=1}^{N} \alpha_j s_j(x), \tag{3.2.4}$$

where N is a chosen dimensional *truncation.* We multiply the modal equation by s_n, and then integration produces an eigenvalue problem in the perturbed frequency $\widetilde{\omega}$. With the off-diagonal entries $(\partial_x s_m, s_n)$ in hand (for $1 \leq m, n \leq N$ with $m \neq n$), we compute diagonal terms

$$\Omega_j(\widetilde{\omega}) = -\widetilde{\omega}^2 - i(\beta + k_0)\widetilde{\omega} + D k_j^4, \quad j = 1, 2, ..., N,$$

and we create the matrix for $1 \leq n, m \leq N$:

$$A = A(\widetilde{\omega}) = [a_{mn}], \quad \text{with} \;\; a_{mn} = \begin{cases} \Omega_m & \text{for} \;\; m = n \\ \\ \beta U(\partial_x s_n, s_m) & \text{for} \;\; m \neq n. \end{cases} \tag{3.2.5}$$

For chosen parameter values of D, k_0, β, U, L, we enforce the zero determinant condition for non-trivial solutions in $\widetilde{\omega}$:

$$\det\Big(A(\widetilde{\omega})\Big) = 0,$$

and solve for $\widetilde{\omega} = [\widetilde{\omega}_1, ..., \widetilde{\omega}_N]^T$. The associated complex roots allows us to track the stability response of the natural modes to the *perturbation* terms. This method is explored in-depth in [39] for beams across multiple configurations. In [39], however, this method is shown to be an accurate predictor of the onset of instability due to non-conservative piston-theoretic terms. Specifically, for the flow parameter U, we can define U_{crit} as a critical bifurcation parameter, such that for all other coefficients fixed, when $U < U_{\text{crit}}$ the linear dynamics exhibit bounded for-all-time trajectories; when $U > U_{\text{crit}}$, trajectories for the linear dynamics will exhibit unbounded growth (in time). We refer to this as the *onset* of instability due to the flow U.

In the simulations below, the modal method described above allows us to determine that for $D = L = k_0 = \beta = 1$, the onset of instability corresponding to the linear cantilever is $U_{\text{crit}} \approx 135.9$; this figure will arise repeatedly in our simulations below. We note that for $U > U_{\text{crit}}$, the linear dynamics have destabilized eigenvalue(s), and the linear dynamics (with no nonlinear elastic restoring force) will accordingly grow exponentially in time.

3.2.2.3 Nonlinear Modal Simulations

Now, as in Section 3.2.2.2, let us expand the solution to the nonlinear problem (2.4.1) as $w = \sum_i s_i q_i$, where again $s_i(x)$ are the in vacuo cantilever mode shapes, with and $q_i(t)$ being smooth functions of time. Plugging the solution into the weak form (2.4.13) gives us a corresponding "matrix" system in $\{q_t(t)\}$ by subsequently testing with $\phi = s_j$.

We define (corresponding respectively to [**NL Stiffness**] and [**NL Inertia**]):

$$\mathcal{S}_{ijkl} = (\phi_{i,xx}\phi_{j,xx}, \phi_{k,x}\phi_{l,x}) \tag{3.2.6}$$

$$\mathcal{I}_{ijkl} = \left(\int_0^x \phi_{i,x}\phi_{j,x}, \int_0^x \phi_{k,x}\phi_{l,x}\right). \tag{3.2.7}$$

Remark 3.2.1. The following calculation for $\mathcal{I}_{ijkl}$ back to the weak form (2.4.13):

$$\begin{aligned}
\mathcal{I}_{ijkl} &= \left(\int_0^x \phi_{i,x}\phi_{j,x}, \int_0^x \phi_{k,x}\phi_{l,x}\right) \\
&= -\int_0^L \left[\left(\partial_x \int_x^L \int_0^\xi \phi_{i,x}\phi_{j,x} d\xi_2 d\xi\right) \int_0^x \phi_{k,x}\phi_{l,x} d\xi\right] dx \\
&= \int_0^L \left[\left(\int_x^L \int_0^\xi \phi_{i,x}\phi_{j,x} d\xi_2 d\xi\right) \phi_{k,x}\phi_{l,x}\right] dx.
\end{aligned}$$

Employing Einstein notation, so that $q_i s_i$ is interpreted as the sum, we have the following separated form of (2.4.1)–(2.4.3) taken with the piston-theoretic RHS

(3.2.1):

$$q_i''(s_i,s_j) + \left[q_i''(q_i)^2 + (q_i')^2 q_i\right]\mathcal{I}_{iiij} + \beta q_i'(s_i,s_j) + Dq_i\left[k_i^4(s_i,s_j)\right] + Dq_i^3\left[\mathcal{S}_{iiij} + \mathcal{S}_{jiii}\right] = \beta U(\partial_x s_i, s_j). \tag{3.2.8}$$

This form, (3.2.8), constitutes the bi-infinite *modal form* of (2.4.13) with $\iota = \sigma = 1$ and $k_2 = 0$.

Remark 3.2.2. Note the *temporally* quasilinear term $q_i''(q_i)^2\mathcal{I}_{iiij}$, which may slow down time-stepping computations, as the equations are algebraically implicit in q''. The spatial nonlinearity—cubic type, and quasilinear—can be seen in the terms involving $\mathcal{S}$.

The summation in equation (3.2.8) is truncated to include just N mode functions after which we conduct a reduction of order. The resulting $2N \times 2N$ system of ODEs is solved using the `ode15i` function in MATLAB, which requires the ODE to be in the form $f(y, y_t) = 0$. To expand the summations, we use a Mathematica script and then a Python script to convert the output to valid MATLAB syntax. For the computation of $\mathcal{S}_{ijkl}$, the inbuilt function `integral` is used. The components of $\mathcal{I}_{ijkl}$, $\int_0^x s_{i,x}s_{j,x}$, $\int_0^x s_{k,x}s_{l,x}$, are computed using the inbuilt `integral` function and the final integral for the inner product is taken using Simpson's Rule. Once the ODE system is numerically solved, the final solution is computed by taking the corresponding linear combinations of the mode functions. Visual/graphical output can be produced as $(X, Y) = (u(x,t), w(x,t))$, where u is obtained from w through the effective inextensibility relation (2.4.3).

3.2.3 Qualitative Analysis of Numerical Simulations

For the simulations presented in this section we take the following conventions:

- The flags ι, σ take values of 0 or 1, depending on what is being discussed.
- Non-central parameters are taken to unity: $L = \beta = D = 1$.
- The stationary pressure, $p_0(x)$ in (3.2.1), is taken identically zero.
- Imposed damping is taken to be zero, i.e., $k_0 = k_2 = 0$.
- Unless stated otherwise, the number of modes used in each simulation was $N = 6$.

For these conventions, we mention that [39] and [40] discuss piston-theoretic and structural parameter values in more depth. It is worth commenting that, even when $\iota = 1$, *we do not invoke any damping* in our simulations below. In our theoretical results, we recall that $k_2 > 0$ is necessary for the existence proof to obtain when $\iota = 1$ (Theorem 2.6.1). We choose to focus these preliminary numerical simulations on the undamped case to understand the essence of the nonlinear effects. In particular, these results below indicate precisely how the [**NL Inertia**] effects produce issues.

Lastly, we now specify our initial data repository for simulations below:

- [**1st Mode ID**] $w(0,x) = s_1(x) = [\cos(\kappa_1 x) - \cosh(\kappa_1 x)] - \mathcal{C}_1[\sin(\kappa_1 x) - \sinh(\kappa_1 x)],\ w_t(0,x) = 0,$

where $\kappa_1 \approx 1.8751$ is the first Euler–Bernoulli cantilevered mode number (with $L = 1$) and $\mathcal{C}_1 \approx 0.7341$.

- **[2nd Mode ID]** $w(0,x) = s_2(x) = [\cos(\kappa_2 x) - \cosh(\kappa_2 x)] - \mathcal{C}_2[\sin(\kappa_2 x) - \sinh(\kappa_2 x)],\ w_t(0,x) = 0$,

  where $\kappa_2 \approx 4.6941$ is the second Euler–Bernoulli cantilevered mode number (with $L = 1$) and $\mathcal{C}_2 \approx 1.0185$.

- **[Polynomial ID]** $w(0,x) = -4x^5 + 15x^4 - 20x^3 + 10x^2,\ w_t(0,x) = 0$;

- **[Linear IV]** $w(0,x) = 0,\ w_t(0,x) = ax$, where the parameter $a > 0$ will be increased in size as a mechanism to increase the "size" of the initial data (in the sense of $L^2(0,1)$).

3.2.3.1 Conservation of Arc Length in Numerical Simulations

Since the inextensible dynamics are predicated on enforcing the inextensibility constraint, we posit that arc length should be approximately conserved throughout dynamic deflections. However, as we are enforcing an *effective* inextensibility constraint (2.4.3), we expect that approximation of the full constraint (2.3.1) produces errors that can be exaggerated by larger and larger deflections.

First, in Figure 3.1, we demonstrate that arc-length is faithfully conserved throughout deflection, across the varying initial conditions *for the in vacuo case* ($U = 0$, $\beta = 0$). These plots take active stiffness and inertia—$\iota = \sigma = 1$. In these simulations, the initial velocity multiplier a is set to 1.

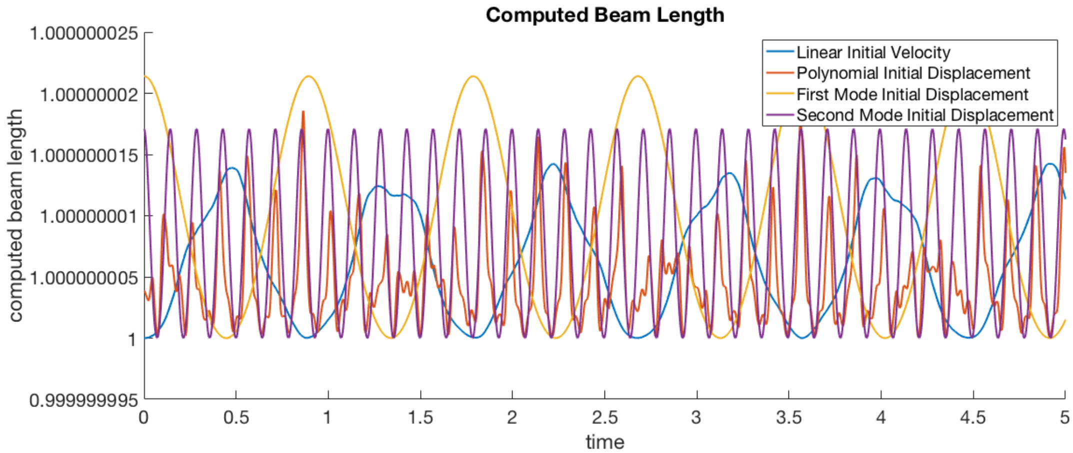

Figure 3.1: In vacuo computed arc length, varying initial conditions. Amplitude of oscillations are of the order of beam's length.

However, for [**Linear IV**] initial conditions, increasing values of the initial velocity multiplier a (with zero initial displacement) yields the degradation of arc-length conservation, as seen in Figure 3.2.

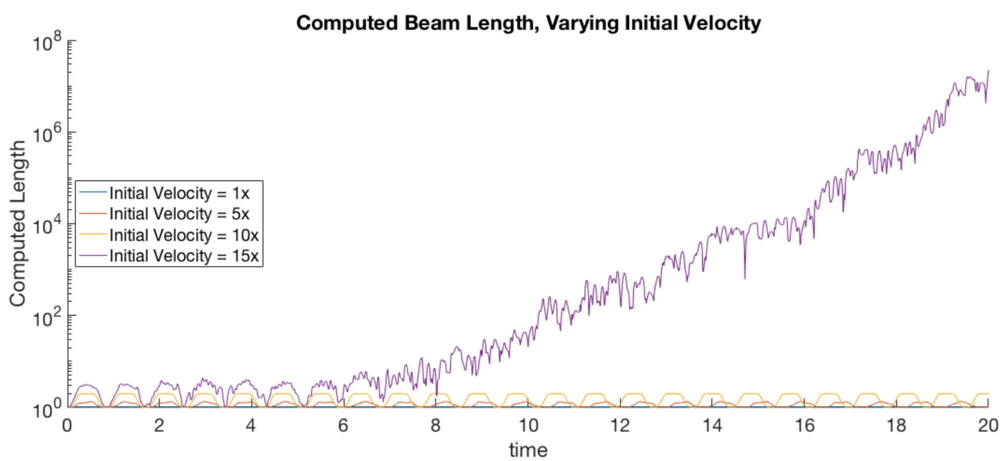

Figure 3.2: In vacuo computed arc length, varying initial velocity multiplier a.

We also see degradation in the conservation of arc length when the piston-theoretic flow is active. Figure 3.3 gives the computed arc length for the full non-linear beam $\sigma = \iota = 1$ for varying values of $U > 0$. The initial condition is [**Linear IV**] with $a = 1$.

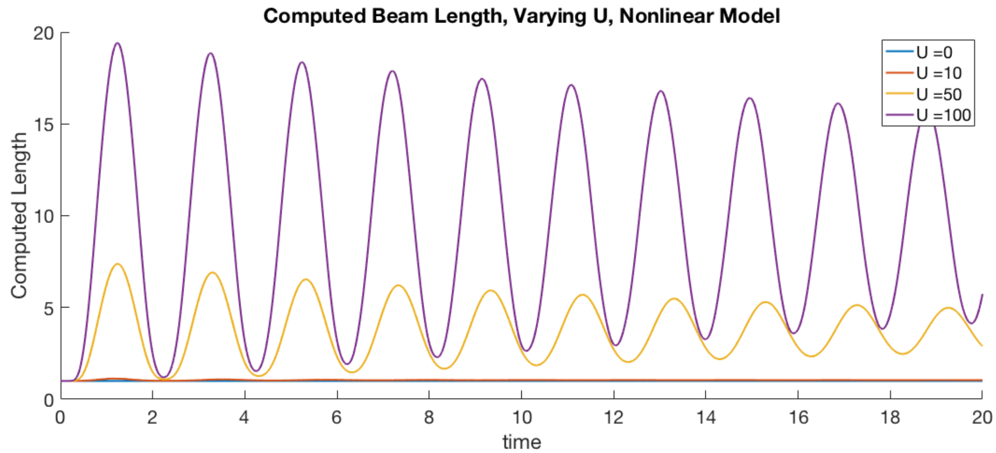

Figure 3.3: Full nonlinear model computed arc length, varying U, $\beta = 1$.

We note that as U increases, beam deflections are larger (owing to a stronger forcing), resulting in observed degradation. All flow velocities U here are below the linear *onset* critical value of $U_{\text{crit}} \approx 135.9$. The reason for this will become clear in the discussions that follow.

3.2.3.2 Computed Total Energies

In this section we compute the total (nonlinear) energies associated to various situations. We are interested in tracking the temporal evolution of $E(t)$: when in vacuo dynamics are considered ($U = 0$), we expect conservation of energy. When $U \neq 0$, we expect that energies will evolve, owing to the non-conservative flow effects of (3.2.1).

We first examine the computed total energies for the in vacuo, fully nonlinear beam ($\iota = \sigma = 1$), with varying initial velocity size in Figure 3.4.

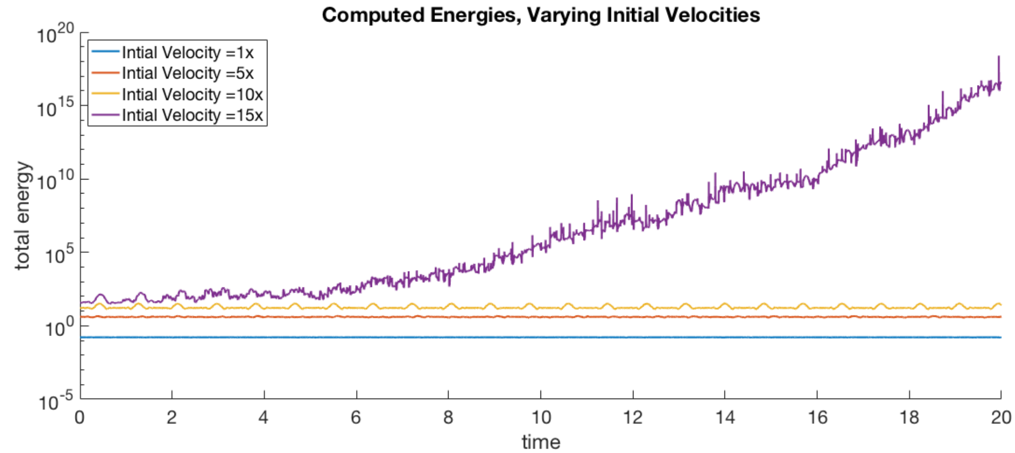

Figure 3.4: In vacuo total energies with [**Linear IV**] varying a.

When the size of the initial data is sufficiently small, we see near perfect conservation of energy, $E(t) = E(0)$, perhaps with slight periodic effects. However, when the initial data size is large, we see that energy conservation is lost.

For the linear model, with stiffness and inertia turned off ($\sigma = \iota = 0$), the in vacuo critical value is $U_{\text{crit}} = 135.9$. Figure 3.5 gives the computed energies for varying U values below and above U_{crit}.

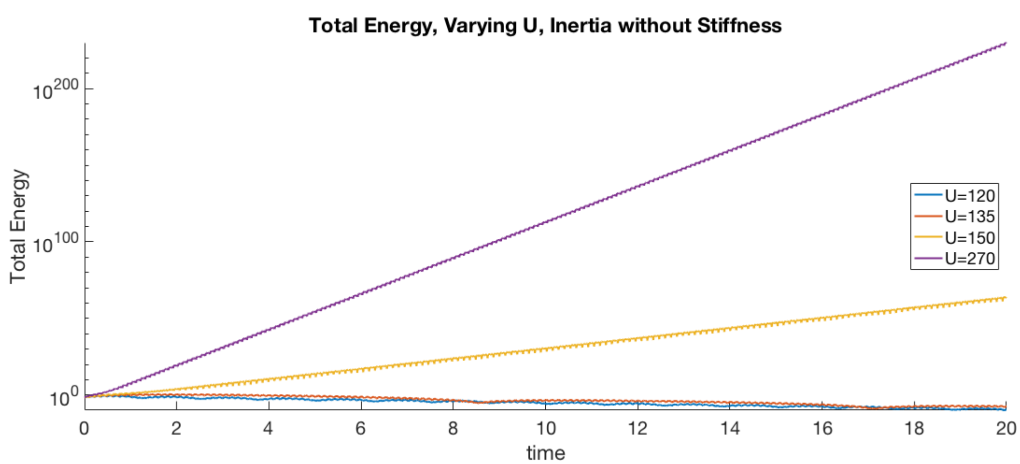

Figure 3.5: Total energies for the beam, varying U, $\beta = 1$, linear model.

We note that for $U > U_{\text{crit}}$, we observe exponential growth in time of energies, as expected [39]. Below U_{crit} we see exponential decay, as a function of the presence of damping in linear piston theory (3.2.1). We contrast this picture with the same simulations, with active nonlinear restoring forces. (See [39] and [40] for more in-depth study and discussion when an extensible beam is being considered.)

First, we include stiffness only ($\sigma = 1$, $\iota = 0$). The energy is modified accordingly—Section (2.4.3). Figure 3.6 shows that the nonlinear stiffness effect is enough to provide stability in the sense that for $U > U_{\text{crit}}$, the energy plateaus. Indeed, these post-onset dynamics converge to *limit cycle oscillations*. Below U_{crit}, the trajectories which were stable in Figure 3.5 remain so here.

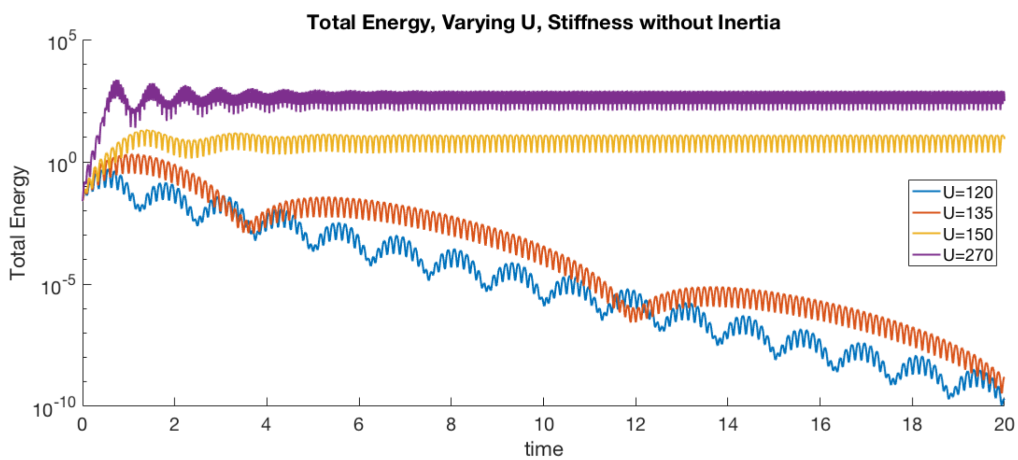

Figure 3.6: Energies for the beam, varying U, with $\beta = 1$, $\sigma = 1$, and $\iota = 0$.

We demonstrate a limit cycle oscillation in the post-onset regime $U > U_{\text{crit}}$ for stiffness only dynamics ($\sigma = 1$, $\iota = 0$) when $U = 140$. Figure 3.7 shows the beam vertical end point displacement for $U = 140$.

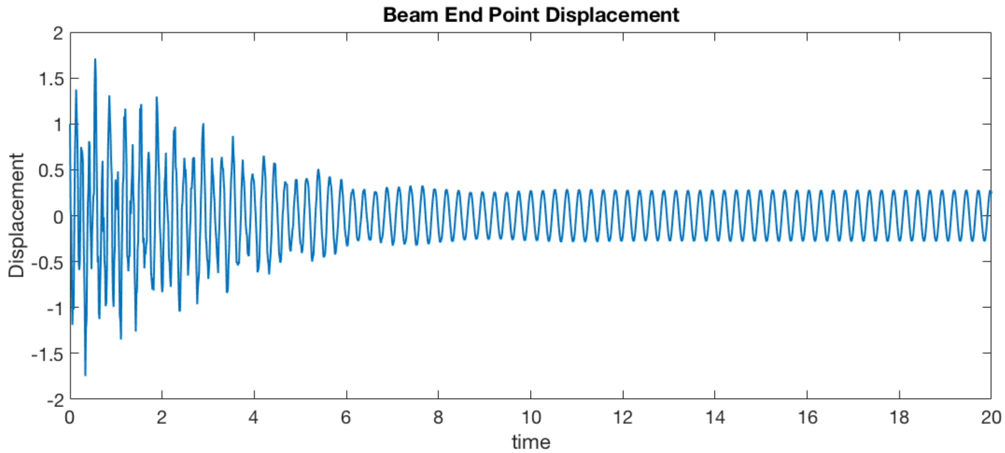

Figure 3.7: Limit Cycle Oscillation of beam vertical displacement, stiffness only, $U = 140$, $\beta = 1$.

The next question which naturally arises is: What happens to these stability (energy or displacement) plots when [**NL Inertia**] is present in the model? More specifically, we can ask two questions: (i) Does the presence of [**NL Stiffness**] and/or [**NL Inertia**] affect the linear critical onset value U_{crit}? (ii) In the post-onset regime, what do fully nonlinear ($\sigma = \iota = 1$) dynamics look like? For (i), we defer this complex question to future work, but we note that it does appear that the presence of [**NL Inertia**] does affect—lower—the critical value for instability, however this affect is highly dependent upon initial configuration; an interesting, if not wholly surprising, observation.

Indeed, with $\iota = 1$, no consistent limit cycle oscillation behavior could be observed through the linear piston-theoretic RHS. This is consistent with engineering literature [59, 61]. Again, outcomes are highly dependent on initial configuration. In Figure 3.8, both the stiffness and inertia terms are included in the model ($\sigma = \iota = 1$). Note that the [**NL Inertia**] term clearly destabilizes the computation after a sufficient amount of time, and as a result, we observe blowup of total energy for a range of U values, even those well below the linear critical onset value U_{crit}.

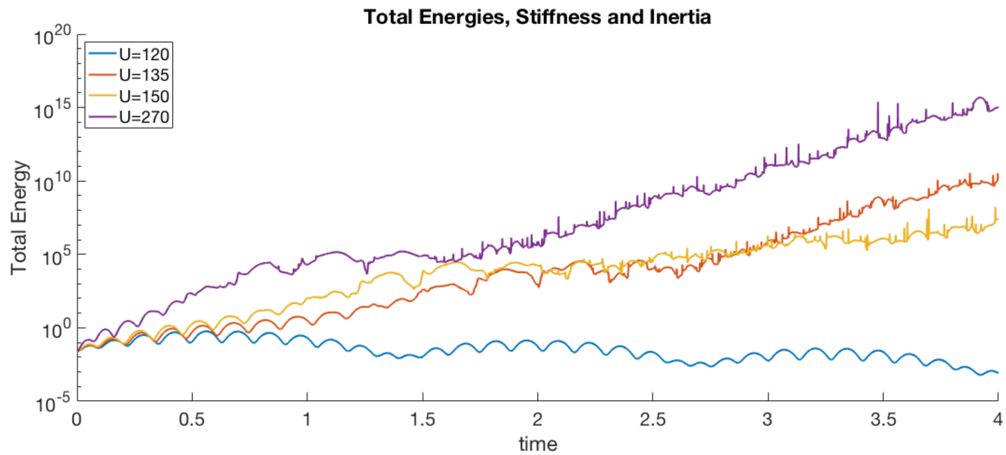

Figure 3.8: Total energies for the beam, varying U, $\beta = 1$, stiffness with inertia.

3.2.3.3 Inverted Flag Simulations

Interesting questions arise when the flow direction is inverted $U < 0$, yielding the so called inverted flag configuration [46]. With flow from free to clamped end, we can ask about critical values of U, as well as possible end behaviors.

In principle, the structural model is robust enough to support limit cycle oscillations in this configuration, but we were unable to observe this. Convergence to non-trivial steady states, however, was observed—sometimes referred to as buckling.

As $-U$ increases, the final steady state of the system transitions from equilibrium to a nontrivial deflected state, occurring around $\widehat{U}_{\text{crit}} = -6.3$. Figure 3.9 shows a nontrivial steady state for the inverted flag configuration when $U = -10$.

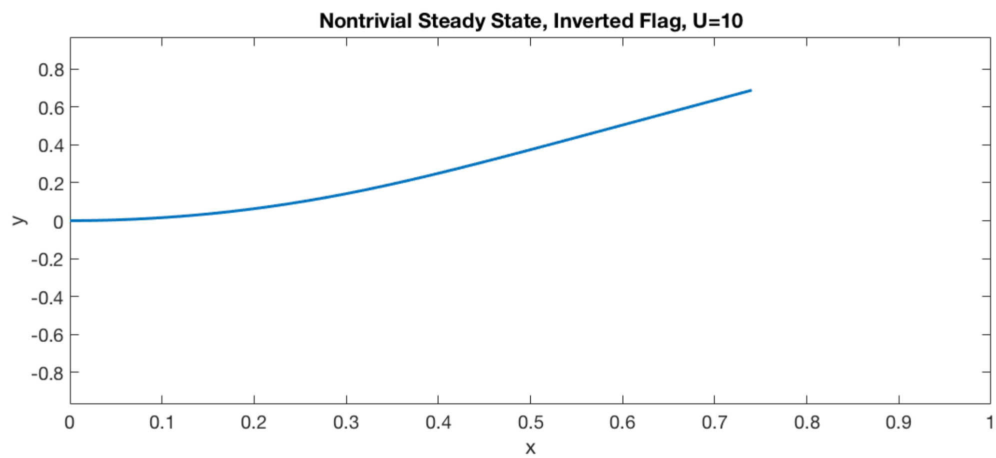

Figure 3.9: Nontrivial steady state displacement for the inverted flag, $U = -10$, $\beta = 1$.

Correspondingly, Figure 3.10 shows the different energy contributions for the inverted flag when $U = -10$. Note the steady decay in energy associated to [**NL Inertia**]. As we observe convergence to a steady state, it is clear that the energy $E(t) \to const.$

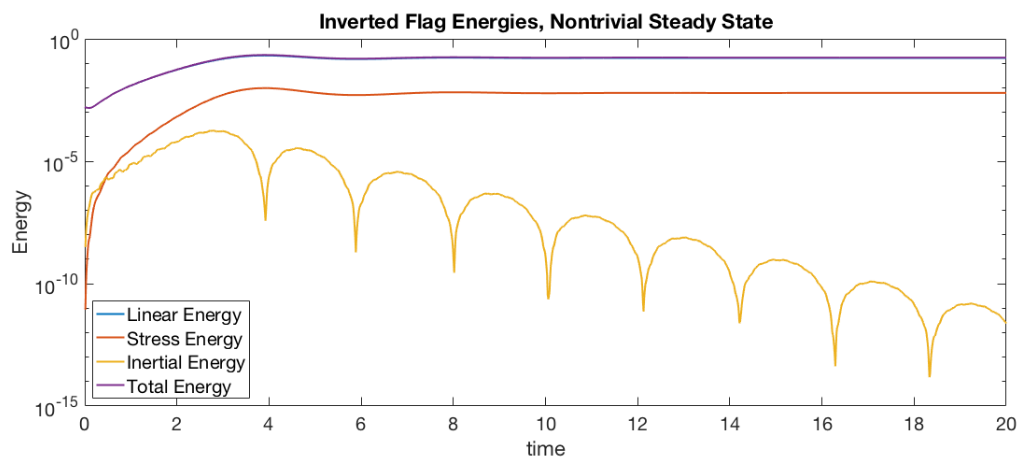

Figure 3.10: Nontrivial steady state energies for the inverted flag, $U = -10$, $\beta = 1$.

Figure 3.11 tracks the values of the coefficients q_i corresponding to each s_i for $i = 1, 2, 3, 4$ in the inverted flag dynamics for $U = -10$. Note that there is a contribution from both the first and second modes to the nontrivial steady state shown in Figure 3.9, however there is minimal contribution from the higher modes with decay evident from the aerodynamic damping coming from (3.2.1).

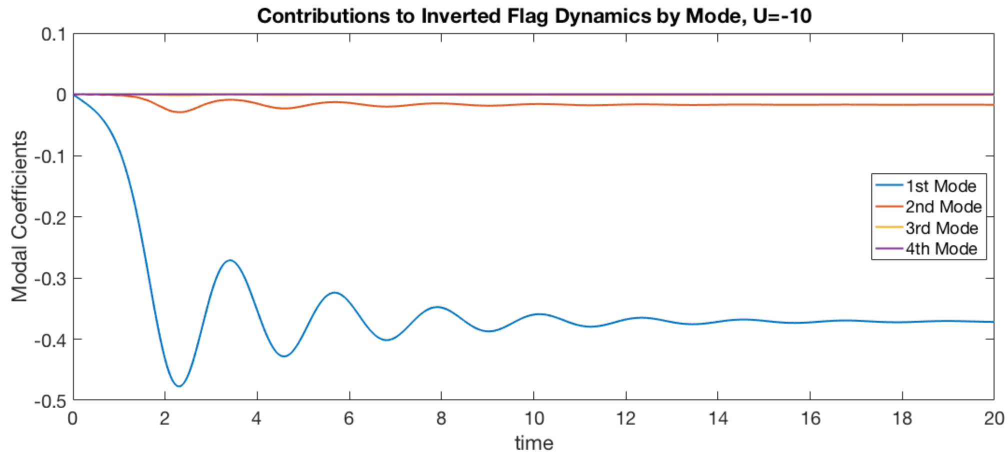

Figure 3.11: Modal coefficients, $U = -10$, $\beta = 1$.

Figure 3.12 shows how the U value, ranging from -6 to -7, influences the terminal modal coefficients at $T = 20$. Around $U = -6.3$ we see the deflected steady state emerge.

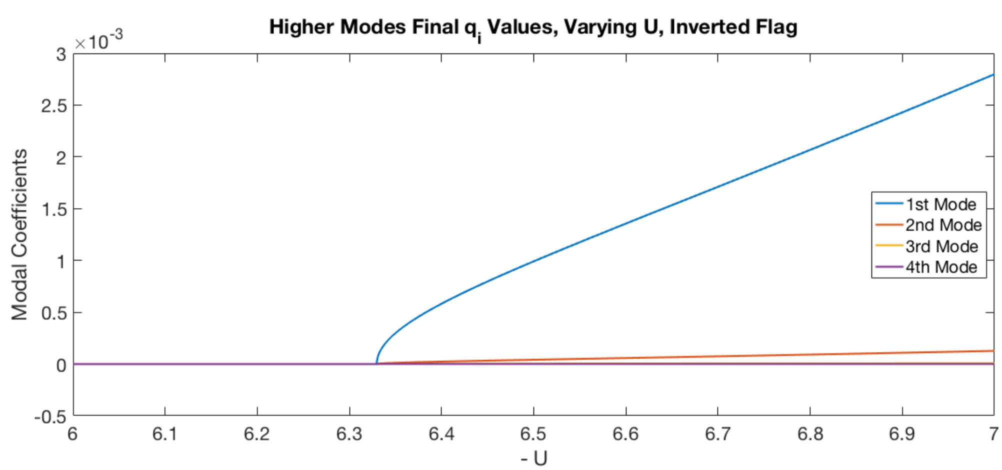

Figure 3.12: Modal coefficients, Varying $-6 \geq U \geq -7$, $\beta = 1$.

We note that the static end behavior of the piston-theoretic inverted flag has been noted for some time [24], but this conclusion was obtained via a *linear elastic* *model*. Hence, to our knowledge, this is the first confirmation that the presence of inextensible nonlinearity does not alter the established result.

3.2.3.4 Influence of Number of Modes on Simulations

Below is a plot of the total energy for $U = 130$, fully nonlinear model ($\iota = \sigma = 1$) *as we increase the number of modes in the simulation*. From the plot it is clear that varying the number of modes *does effect the onset of instability*, as the energy remains bounded for only 3 modes, but we see exponential growth with 6 modes. As far as we can tell, for this nonlinear model, U_{crit} is around 130, which means the presence of nonlinearity has decreased the onset of instability as compared to the linear model (which had $U_{\text{crit}} \approx 135.9$). We note that for semilinear models analyzed in [**?**]) *the presence of nonlinearity does not affect* U_{crit}.

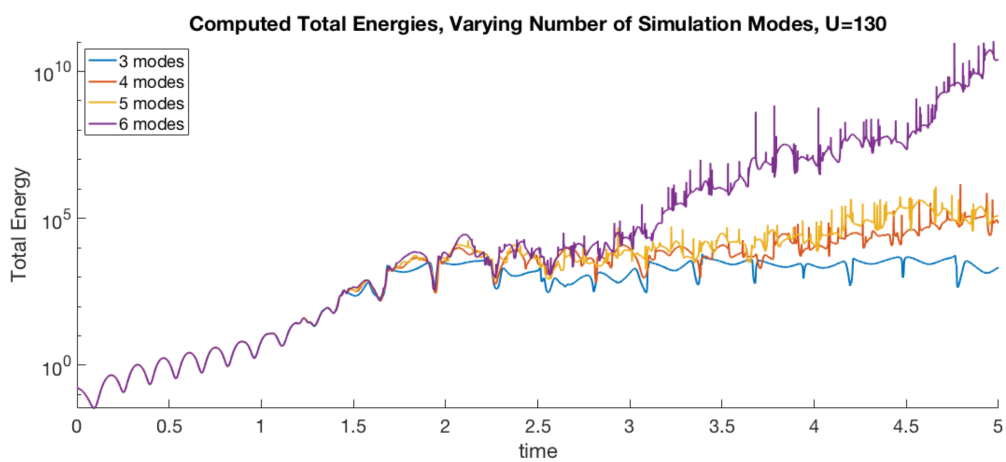

Figure 3.13: Energies for the fully nonlinear model, $U = 135.9$, $\beta = 1$.

For the inverted flag system ($U < 0$), the number of modes influences where the beam begins to transition to a deflected steady state, as shown in Figure 3.14.

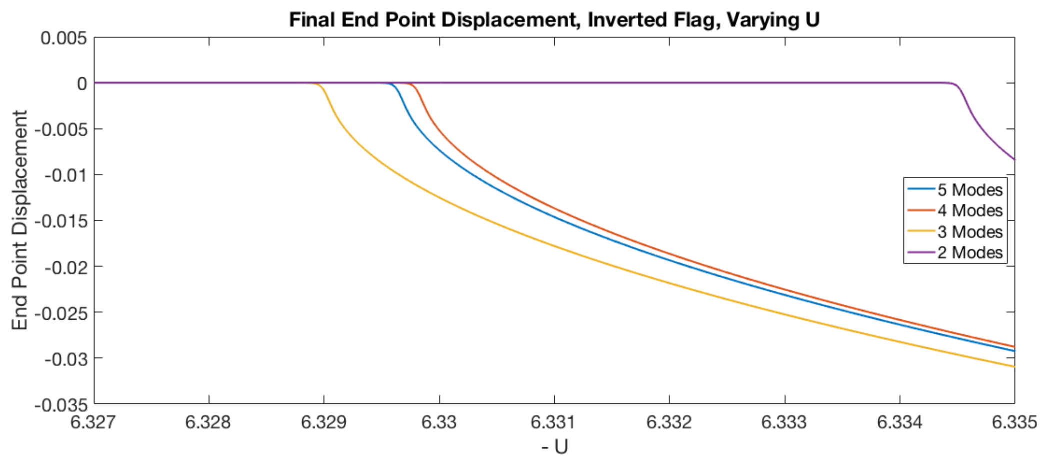

Figure 3.14: Final $x = L$ displacement, inverted flag, varying U and number of modes, $\beta = 1$.

3.2.4 Numerical Conclusions

We briefly provide conclusions drawn from the previous section.

- Arc length and energy conservation are reasonably satisfied for the inextensible beam dynamics, at least for solutions with small enough deflections. Both breakdown when deflections are sufficiently large, and we expect this is due to the violation of the assumption $u_x << 1$.

- [**NL Stiffness**] provides a strong enough (quasilinear) restoring force to bounded post-critical trajectories and provide limit cycles. This is similar to the situation for extensible beams, where the nonlinearity is semilinear (as in Krieger or von Karman type); see [16, 39].

- [**NL Inertia**] is the challenging term. With inertia in force, large deflections become problematic. Specifically, simulations break or become unphysical (for instance, with the beam bending back on itself or kinking.) Considering piston-theoretic pressures, no consistent prediction of onset of instability can be given when $\iota = 1$. Moreover, no consistent post-critical behavior was found; specifically, no stable limit cycles were observed when $\iota = 1$.

- For the full nonlinear model of the inextensible beam, we see many effects in the qualitative behavior that depend on the initial data size and type. Moreover, the quasilinear (in time and space) nature of the model seems to suggest that dependence on data is unavoidable for theoretical and numerical results.

- For the inverted flag configuration $U < 0$, non-trivial steady states were obtained in a post-critical regime. Again, no limit cycles were observed when $\sigma = 1$, regardless of the value of ι.

- The number of modes used in simulating the dynamics affects stability and qualitative properties. This is atypical, by engineering standards, where for structures that are non cantilevers, so called *modal convergence*, is observed fairly uniformly for $N \approx 4$. Owing the highly nonlinear nature of this model, as well as the large deflection nature and free boundary condition, modal convergence is not observed for such low mode numbers, and eventual behavior is dependent on N.

3.2.5 Obtaining Limit Cycle Oscillations for Full Inextensible Dynamics

In line with the work in the engineering literature making use of higher order piston theory, we hope to produce limit cycle oscillations for the dynamics *when inertia is active*. The first set of numerical tests to be run involve the impact of strong damping $k_2 > 0$ on controlling the "bad" behaviors of [**NL Inertia**]. Beyond the effect of damping (perhaps to permit limit cycles), we will attempt to simulate limit cycles by involving the more sophisticated *nonlinear piston theory*; recent work [59,61] has indicated that large deflection piston theory produces such limit cycle oscillations. Future work will also tackle the problem of determining U_{crit} with nonlinear effects active; specifically, how the linear $U_{\text{crit}} \approx 135.9$ would lower when $\sigma = 1$ and/or $\iota = 1$. Even formulating this problem is difficult, as the effect of nonlinearity here on stability seems to be highly dependent on initial conditions.

Chapter 4: Large Deflections of Inextensible Cantilevered Plates

4.1 Summary of the Chapter

In this chapter we consider some extensions to two spatial dimensions of the cantilevered beam configuration that was introduced in Chapter 1; namely inextensible plates. Our principal configuration is that of a thin, isotropic, homogeneous rectangular plate, clamped on one edge and free on the remaining three. We proceed through the geometric and elastic modeling for large deflections to obtain equations of motion via Hamilton's principle for the appropriately specified energies. We then enforce *effective* inextensibility constraints through Lagrange multipliers. Multiple plate analogs of the established 1D model are obtained, based on various assumptions. In total, we present three distinct nonlinear partial differential equation models, and, additionally, describe a class of "higher order" models. Each model has particular advantages and drawbacks for both mathematical and engineering analyses. We conclude with a discussion of the various models, as well as some analytical problems.

4.2 Introduction

In this chapter we aim to provide the equations of motion of the "natural" beam extension to a 2D inextensible plate. We specifically follow the approaches for the beam, coming from references [26, 58] and [21]. Apart from the intriguing mathematical challenges that this extension produces, we are also interested in this configuration since, in the context of energy harvesting, structures are truly two dimensional.

That being said, we will specifically consider a *plate* with three free edges and one edge clamped. Clearly along the clamped edge, the plate is not free to extend and must have strain in the direction parallel to the clamped edge. The purpose of this investigation is to explore several alternative models based on *a variety of assumptions* about the 2D mid-plane strain. As seen in the three principal nonlinear cantilever models derived below, the *issue of shear strain is quite subtle*. The most attractive *mathematical model*, which generalizes the well-accepted inextensible beam theory, will require an assumption of zero mid-plane shear strain, as well as zero mid-plane longitudinal strains.

As we shall see, there is no single, clear plate extension of the our beam model. Indeed, there are certain modeling and order choices, each of which yields a different system for the equations of motion. The presence of 2D shear effects is a critical aspect of the analysis here. Providing a careful derivation of the equations of motion is indeed quite necessary, as we will see, since "natural" modeling choices produce nonlinear boundary conditions for each plate model. That is to say: it is notable that for the 2D plate, the modeling hypotheses produce (nonlinear) boundary conditions which are not those of a standard, linear, cantilevered plate. Moreover, some aesthetic simplifications which present themselves in 1D will be conspicuously absent in 2D. *To the best of our knowledge, each of the plate systems here is novel.*

4.2.1 Outline of the Chapter

Section 4.3 is the principal modeling section. There, we walk through our choices for the potential energies, as well as the interpretation and enforcement of "inextensibility" in the plate. Ultimately, we present three distinct models in Section 4.3, with clear discussion of the relevant modeling and order hypotheses. Each model is presented as a system of partial differential equations in the elastic deflection variables, as well as constraint variables. We conclude Section 4.3 with a description of how to obtain a class of higher order models, though without explicitly producing the equations of motion.

Finally, in Section 4.4 we discuss and compare the derived models from both the engineering and analysis-of-PDEs points of view.

4.2.2 Conventions and Notation

We utilize the convention that spatial points $\mathbf{x}$ are identified with their position vector $\langle x, y, z\rangle$. We will sometimes write $x_1 = x$, $x_2 = y$, $x_3 = z$ when it is notationally expedient. The equilibrium (undeformed) domain under consideration will be cylindrical, namely, $\{\mathbf{x} \in \Omega \times (-h/2, h/2)\}$. The domain Ω will be identified as the centerline, $z = x_3 = 0$. We make use of the partial derivative notation $\dfrac{\partial}{\partial x_i} = \partial_{x_i}$, as well as the standard 2D spatial gradient $\nabla = \langle \partial_x, \partial_y \rangle$, divergence $[\nabla \cdot]$, and Laplacian (in rectangular coordinates) $\Delta = \nabla \cdot \nabla = \sum_{i=1}^{2} \partial_{x_i}^2$.

4.3 Inextensible Cantilevered Plates

Let $\mathbf{x} = \langle x, y \rangle \in \mathbb{R}^2$. We will let $\langle u(\mathbf{x},t), v(\mathbf{x},t), w(\mathbf{x},t) \rangle \in \mathbb{R}^3$ denote the mid-plate displacement (from equilibrium) of a rectangular, cantilevered plate that occupies (at equilibrium) the region $\Omega \times (-h/2, h/2)$. The coordinate u is span-wise displacement, with v being chord-wise; w is the transverse deflection. (Thus, $\langle x + u(\mathbf{x},t), y + v(\mathbf{x},t), w(\mathbf{x},t) \rangle$ describes the position of the equilibrium point $\mathbf{x}$ at the instant t.) The physical quantity $\nu \in (0, 1/2)$ represents the *Poisson Ratio.*

Consider the open rectangle $\Omega \equiv \{(x, y) \in (0, L_x) \times (0, L_y)\}$, representing the undeformed mid-plane ($z = 0$) of the thin, homogeneous, isotropic plate. Let us take the four components of the boundary $\partial\Omega = \Gamma$ (in standard orientation) to be given by

$$\Gamma_E = \{x = L_x,\ y \in (0, L_y)\}, \qquad \Gamma_N = \{x \in (0, L_x),\ y = L_y\},$$

$$\Gamma_W = \{x = 0,\ y \in (0, L_y)\}, \qquad \Gamma_S = \{x \in (0, L_x),\ y = 0\}.$$

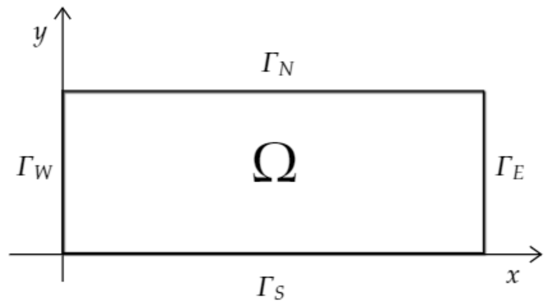

We have the associated outward unit normals: $\mathbf{n}_E = \mathbf{e}_1,\ \mathbf{n}_N = \mathbf{e}_2,\ \mathbf{n}_W = -\mathbf{e}_1,\ \mathbf{n}_S = -\mathbf{e}_2$ and corresponding tangentials (respectively): $\mathbf{e}_2, -\mathbf{e}_1, -\mathbf{e}_2, \mathbf{e}_1$.

Remark 4.3.1. For reference, we provide the classical clamped-free conditions associated with a *linear* cantilever in this configuration, that is, the plate is clamped on Γ_W and free elsewhere. On Γ_N, Γ_S the boundary conditions are:

$$\nu w_{xx} + w_{yy} = 0; \quad w_{yyy} + (2-\nu) w_{xxy} = 0.$$

On Γ_E the boundary conditions are:

$$w_{xx} + \nu w_{yy} = 0; \quad w_{xxx} + (2-\nu) w_{yyx} = 0.$$

And, of course, on Γ_W we have the clamped conditions:

$$w = 0; \quad w_x = 0.$$

The boundary conditions here are markedly simpler than the general case [16, 50] involving the well-known B_1 and B_2 operators, owing to the simplified rectangular geometry.

4.3.1 Full Elastic Potential Energy and Strain-Displacement Relations

In this section we discuss the plate potential energy. We have in mind to simplify it in accordance with the relevant plate inextensibility constraints, as done analogously for the beam. We begin with the bulk description of the potential energy, namely that the potential energy E_P has the form:

$$E_P = \frac{1}{2} \int_{-h/2}^{h/2} \int_{\Omega} \hat{\varepsilon}_{ij} \hat{\sigma}_{ij} d\Omega dz,$$

where $\hat{\varepsilon}$ and $\hat{\sigma}$ are the 3D strain and stress tensor (resp.) for 3D displacements. With the plate taken as homogeneous and isotropic, we invoke the standard Hookean stress-strain relation

$$\hat{\sigma}_{ij} = \frac{E}{1+\nu}\Big(\hat{\varepsilon}_{ij} + \frac{\nu}{1-2\nu}\hat{\varepsilon}_{kk}\delta_{ij}\Big), \; i,j = 1,2,3, \tag{4.3.1}$$

where $E > 0$ is the Young's modulus, $\nu \in (0, 1/2)$ is the Poisson ratio, and the Einstein summation convention is in force (above δ_{ij} is that of Kroenecker).

As is customary in thin plate theory, we assume the Kirchhoff–Love hypotheses.

Assumption 4.3.1. *Assume $\hat{\sigma}_{33} = 0$. We also assume that plate filaments that are originally orthogonal to the mid-surface remain so throughout deflection, and that said filaments have constant length; this implies $\hat{\varepsilon}_{13} = \hat{\varepsilon}_{23} = 0$.*

The above assumption reduces E_P to the following expression [18,50], which we will use throughout this treatment:

$$E_P = \frac{1}{2}\frac{E}{1-\nu^2}\int_\Omega \int_{-h/2}^{h/2} \left[\hat{\varepsilon}_{11}^2 + \hat{\varepsilon}_{22}^2 + 2\nu\hat{\varepsilon}_{11}\hat{\varepsilon}_{22} + \frac{1-\nu}{2}\hat{\varepsilon}_{12}^2\right] dz d\Omega. \tag{4.3.2}$$

We now attempt to simplify, utilizing only mid-plane strains ε, curvature κ, and the higher order tensor μ [62], yielding:

$$\hat{\varepsilon}_{11} = \varepsilon_{11} + z\kappa_{11} + z^2\mu_{11} \tag{4.3.3}$$

$$\hat{\varepsilon}_{22} = \varepsilon_{22} + z\kappa_{22} + z^2\mu_{22} \tag{4.3.4}$$

$$\hat{\varepsilon}_{12} = \varepsilon_{12} + z\kappa_{12} + z^2\mu_{12}. \tag{4.3.5}$$

In all of what follows we drop the terms scaled by z^2 above, consistent with [58,62].

Assumption 4.3.2. *In the expression for strains $\hat{\varepsilon}_{ij}$ for $i, j = 1, 2$, we assume that each $z^2\mu_{ij}$ for $i, j = 1, 2$, are negligible.*

It is necessary, at this point, to invoke strain-displacement relations [62]. Recalling that u, v and w denote the Lagrangian mid-plane displacements, we have

$$\varepsilon_{11} = u_x + \frac{1}{2}\left[u_x^2 + v_x^2 + w_x^2\right] \tag{4.3.6}$$

$$\varepsilon_{22} = v_y + \frac{1}{2}\left[u_y^2 + v_y^2 + w_y^2\right] \tag{4.3.7}$$

$$\varepsilon_{12} = u_y + v_x + u_x u_y + v_x v_y + w_x w_y, \tag{4.3.8}$$

which, as mentioned above, are the mid-plane extensible axial strains and the shear strain (resp.).

4.3.2 Inextensibility

The "true" inextensibility conditions would correspond to taking $\varepsilon_{ij} = 0$ [62, 75]; this translates to no extensional stresses along the mid-plane of the plate. In that case, we have three conditions, taken from (4.3.6)–(4.3.8) by equating each to zero:

$$(1+u_x)^2 + v_x^2 + w_x^2 = 1 \tag{4.3.9}$$

$$u_y^2 + (1+v_y)^2 + w_y^2 = 1 \tag{4.3.10}$$

$$u_y + v_x + u_x u_y + v_x v_y + w_x w_y = 0. \tag{4.3.11}$$

We refer to these as the *full* plate inextensibility conditions. The first condition is a span-wise inextensibility constraint, the second is chord-wise, with the lattermost corresponding to shear.

The first two inextensibility conditions can be re-written (discarding non-physical square roots) as:

$$u_x = -1 + \sqrt{1 - (v_x^2 + w_x^2)} \tag{4.3.12}$$

$$v_y = -1 + \sqrt{1 - (u_y^2 + w_y^2)}. \tag{4.3.13}$$

These can be truncated through Taylor expansions about equilibrium. Namely (up to quartic terms):

$$u_x = -1 + \sqrt{1-(v_x^2+w_x^2)} = \; -\frac{1}{2}v_x^2 - \frac{1}{2}w_x^2 - \frac{1}{4}v_x^2w_x^2 - \frac{1}{8}v_x^4 - \frac{1}{8}w_x^4 - ... \quad (4.3.14)$$

$$v_y = -1 + \sqrt{1-(u_y^2+w_y^2)} = \; -\frac{1}{2}u_y^2 - \frac{1}{2}w_y^2 - \frac{1}{4}u_y^2w_y^2 - \frac{1}{8}u_y^4 - \frac{1}{8}w_y^4 - ... \quad (4.3.15)$$

Remark 4.3.2. It is clear that any order analysis associated to truncating these identities—such as what is done for the beam in Chapter 1—will involve the quantities v_x, u_y, w_x, and w_y. Specifically, the above invites comparisons of u_x to both v_x, w_x and v_y to both u_y, w_y.

4.3.2.1 Effective Inextensibility Conditions

In working with the potential energy, we will invoke approximated versions of the inextensibility constraints (4.3.9)–(4.3.11), analogously with the 1D beam. However, in the case of the plate, there are more complex order comparisons which can be made, and a variety of assumptions can be taken.

In the simplest case, we can assert the following η^2-type scaling assumption:

Assumption 4.3.3. *Assume that $\partial_{x_i} w \sim \eta$ and assume that $[\partial_{x_i} u], [\partial_{x_i} v] \sim \eta^2$, for all $i = 1, 2$.*

That is to say, we assume the in-plane gradient is of higher order than the slopes associated to transverse deflection. With this assumption, we can reduce the full inextensibility constraints in (4.3.9)–(4.3.11) up to the order η^2 (thereby dropping terms of the form $[\partial_{x_i} u][\partial_{x_j} v]$, $[\partial_{x_i} u]^2$, $[\partial_{x_i} v]^2$). This produces a particular set of η^2-effective inextensibilty constraints:

$$u_x = -\frac{1}{2}w_x^2 \tag{4.3.16}$$

$$v_y = -\frac{1}{2}w_y^2 \tag{4.3.17}$$

$$u_y + v_x = -w_x w_y. \tag{4.3.18}$$

Remark 4.3.3. One can directly obtain, from the above equations, the identities:

$$4u_x v_y - 2u_y v_x = [u_y^2 + v_x^2] \quad \text{and} \quad w_{xx}w_{yy} = w_{xy}^2.$$

These are elaborated upon in [58, 75]. We note that neither of these "composite" constraints over-constrain the model, since they are derived from (combinations of) prior equations that each eventually correspond (one-to-one) with a Lagrange multiplier variable.

Remark 4.3.4. The latter equality in the previous remark does provide another interesting identity via the boundary conditions and integration by parts:

$$\int_\Omega w_{xy}^2 d\mathbf{x} = \int_\Omega w_{xx}w_{yy} d\mathbf{x} = \int_\Omega w_{xy}^2 d\mathbf{x} + w_x w_{yy}\Big|_{x=0}^{x=L_x} - w_x w_{xy}\Big|_{y=0}^{y=L_y}.$$

As we have yet to derive the higher order boundary conditions via a variational procedure, the only condition we can invoke is the essential condition that $w_x = 0$

on $\{x = 0\}$, which finally yields:

$$w_x(L_x)w_{yy}(L_x) = w_x w_{xy}\Big|_{y=0}^{y=L_y}.$$

Remark 4.3.5. Alternatively, in the choice of truncation above in Assumption 4.3.3, we could more closely follow the logic of our beam approximation in simplifying (4.3.9)–(4.3.11). Namely, we might assume only that $w_x \sim \eta$, from (4.3.9), and $w_y \sim \eta$ from (4.3.10). We could expand to see that $u_x \sim \eta^2$ with $v_x \sim \eta$, as well as $v_y \sim \eta^2$ with $u_y \sim \eta$. In this case, we can choose to retain terms in the Taylor expansions (4.3.14)–(4.3.15) up to order η^4:

$$u_x = -\frac{1}{2}v_x^2 - \frac{1}{2}w_x^2 - \frac{1}{4}v_x^2 w_x^2 - \frac{1}{8}v_x^4 - \frac{1}{8}w_x^4 \tag{4.3.19}$$

$$v_y = -\frac{1}{2}u_y^2 - \frac{1}{2}w_y^2 - \frac{1}{4}u_y^2 w_y^2 - \frac{1}{8}u_y^4 - \frac{1}{8}w_y^4 \tag{4.3.20}$$

$$u_y + v_x = -u_x u_y - v_x v_y - w_x w_y. \tag{4.3.21}$$

Note that, if we go up to order η^4, the shear inextensibility condition will be retained in full—no truncation is called for. In the final class of models in Section 4.3.6, we will discuss the use of higher order approximations of the inextensibility constraints.

4.3.2.2 Curvature Expressions

To obtain expressions for κ_{ij} of the $(x, y) \in \Omega$ middle surface of the plate, we follow the Kirchhoff–Love hypotheses ($\hat{\varepsilon}_{13} = \hat{\varepsilon}_{23} = \hat{\varepsilon}_{33} = 0$) and tracking the work in [62], we obtain:

$$\kappa_{11} = (1 + u_x)\theta_x + v_x\psi_x + w_x\chi_x \tag{4.3.22}$$

$$\kappa_{22} = u_y\theta_y + (1 + v_y)\psi_y + w_y\chi_y \tag{4.3.23}$$

$$\kappa_{12} = (1 + u_x)\theta_y + (1 + v_y)\psi_x + u_y\theta_x + v_x\psi_y + w_x\chi_y + w_y\chi_x, \tag{4.3.24}$$

with θ, ψ, χ given by:

$$\theta = -(1 + v_y)w_x + v_xw_y; \qquad \psi = -(1 + u_x)w_y + u_yw_x; \qquad \chi = u_x + v_y + u_xv_y - u_yv_x. \tag{4.3.25}$$

Remark 4.3.6. As noted in [62], the above expressions are themselves geometric approximations, assuming that strains are small compared to 1. In [62], the relations $\hat{u} = u + z\theta$, $\hat{v} = v + z\psi$, and $\hat{w} = w + z\chi$ are plugged in to the strain relations for $\hat{\varepsilon}_{i3}$, then themselves simplified by geometric order considerations.

We can thus obtain:

$$\kappa_{11} = (1+u_x)[v_{xx}w_y + v_xw_{xy} - v_{xy}w_x - (1+v_y)w_{xx}] \tag{4.3.26}$$
$$+ v_x[u_{xy}w_x + u_yw_{xx} - u_{xx}w_y - (1+u_x)w_{xy}]$$
$$+ w_x[u_{xx} + v_{xy} + u_{xx}v_y + u_xv_{xy} - u_{xy}v_x - u_yv_{xx}]$$

$$\kappa_{22} = u_y[v_{xy}w_y + v_xw_{yy} - v_{yy}w_x - (1+v_y)w_{xy}] \tag{4.3.27}$$
$$+ (1+v_y)[u_{yy}w_x + u_yw_{xy} - u_{xy}w_y - (1+u_x)w_{yy}]$$
$$+ w_y[(1+v_y)u_{xy} + (1+u_x)v_{yy} - u_{yy}v_x - u_yv_{xy}]$$

$$\kappa_{12} = (1+u_x)[v_{xy}w_y + v_xw_{yy} - v_{yy}w_x - (1+v_y)w_{xy}] \tag{4.3.28}$$
$$+ (1+v_y)[u_{xy}w_x + u_yw_{xx} - u_{xx}w_y - (1+u_x)w_{xy}]$$
$$+ u_y[v_{xx}w_y + v_xw_{xy} - v_{xy}w_x - (1+v_y)w_{xx}]$$
$$+ v_x[u_{yy}w_x + u_yw_{xy} - u_{xy}w_y - (1+u_x)w_{yy}]$$
$$+ w_x[(1+v_y)u_{xy} + (1+u_x)v_{yy} - u_{yy}v_x - u_yv_{xy}]$$
$$+ w_y[u_{xx} + v_{xy} + u_{xx}v_y + u_xv_{xy} - u_{xy}v_x - u_yv_{xx}].$$

In what follows we will use these expressions along with the inextensibility conditions in order to produce the potential energy from which we will obtain the equations of motion. Let us first truncate these relations by dropping principal terms (second spatial derivatives) with coefficients of order higher than η^2 (according to the scaling in Assumption 4.3.3). After various cancellations this yields :

$$\kappa_{11} = w_y v_{xx} + w_x u_{xx} - (1 + u_x + v_y) w_{xx} \tag{4.3.29}$$

$$\kappa_{22} = u_{yy} w_x + w_y u_{yy} - (1 + u_x + v_y) w_{yy} \tag{4.3.30}$$

$$\kappa_{12} = 2[v_{xy} w_y + u_{xy} w_x - (1 + u_x + v_y) w_{xy}]. \tag{4.3.31}$$

Remark 4.3.7. Note that, in higher order models, we may wish to retain more terms in the above.

4.3.3 Plate Model I: Three η^2-Inextensibility Conditions

We begin with the potential energy expression from Section 4.3.1. We invoke the three full inextensibility conditions in (4.3.9)–(4.3.11) to eliminate $\varepsilon_{11}, \varepsilon_{22}, \varepsilon_{12}$ from the energetic expression. Also, as previously mentioned, we drop all $z^2 \mu_{ij}$ terms in the expressions for ε_{ij}. This yields:

$$E_P = \frac{1}{2} \left[\frac{1}{12} \frac{Eh^2}{(1 - \nu^2)} \right] \int_\Omega \left[\kappa_{11}^2 + \kappa_{22}^2 + 2\nu \kappa_{11} \kappa_{22} + \frac{1 - \nu}{2} \kappa_{12}^2 \right] d\Omega. \tag{4.3.32}$$

We then invoke the curvature expressions in (4.3.29)–(4.3.31) and input them in (4.3.32).

After truncating terms, we will obtain a potential energy (shown in the next section) for which we can enforce three *effective inextensibility relations* in (4.3.16)–(4.3.18). Then, utilizing Hamilton's principle we will obtain a straightforward PDE model with clear equations of motion. On the other hand, enforcing the three effective inextensibilty constraints results in three Lagrange multiplier variables that cannot be simultaneously eliminated in the full description of the system.

4.3.3.1 Simplified Energies

We employ the effective inextensibility constraints (4.3.16)–(4.3.18) in the curvature expressions given in (4.3.29). In particular, we can differentiate (4.3.16)–(4.3.18) variously, simplify, and rewrite κ_{ij} solely in w

$$\kappa_{11} = -w_{xx}\left[1 + \frac{1}{2}w_x^2 + \frac{1}{2}w_y^2\right]$$

$$\kappa_{22} = -w_{yy}\left[1 + \frac{1}{2}w_x^2 + \frac{1}{2}w_y^2\right]$$

$$\kappa_{12} = -2w_{xy}\left[1 + \frac{1}{2}w_x^2 + \frac{1}{2}w_y^2\right].$$

We then form the appropriate products of κ_{ij} as they appear in (4.3.32). In line with the η^2 analysis of the beam, we retain in E_P only terms with coefficients up to and including η^2. (And thus we drop expressions of the form $[\partial_{x_i} w]^2[\partial_{x_j} w]^2\partial_{x_k}^2 w$.) The result is the potential energy we will employ for the two principal models in this treatment:

$$E_P = \frac{D}{2}\int_0^{L_y}\int_0^{L_x}\left[1 + w_x^2 + w_y^2\right]\left[w_{xx}^2 + w_{yy}^2 + 2\nu w_{xx}w_{yy} + 2(1-\nu)w_{xy}^2\right]dxdy, \tag{4.3.33}$$

where we have now denoted $D = \frac{1}{12}\frac{Eh^2}{(1-\nu^2)}$. We utilize the standard expression for the plate's kinetic energy (again with normalized mass density):

$$E_K = \frac{1}{2}\int_0^{L_y}\int_0^{L_x}\left[u_t^2 + v_t^2 + w_t^2\right] dxdy.$$

4.3.3.2 Equations of Motion

We introduce Lagrange multipliers $\lambda_i(\mathbf{x}, t),\ i = 1, 2, 3$ acting to enforce the effective inextensibility constraints. Let λ_1 be associated to the axial (effective) inextensibility condition (4.3.16), λ_2 to the chord-wise condition (4.3.17), and λ_3 to the shear constraint (4.3.18). We invoke Hamilton's principle for the Lagrangian, written in the λ_i, E_P, and E_K, with virtual displacements $\delta u, \delta v$, and δw. The calculations are involved but analogous to those in Chapter 1 for the 1D dynamics. Essential boundary conditions are enforced for u, v, and w (and their virtual changes) on Γ_W.

In this presentation, since the variables $\lambda_i(\mathbf{x}, t)$ serve to enforce a constraint in the equations of motion, *we will retain the equations* (4.3.16)–(4.3.18) *as part of the system*:

$$u_x + \frac{1}{2}w_x^2 = 0; \qquad v_y + \frac{1}{2}w_y^2 = 0; \qquad u_y + v_x + w_x w_y = 0. \tag{4.3.34}$$

For the dynamics, we obtain:

$$u_{tt} + \partial_x(\lambda_1) + \partial_y(\lambda_3) = 0 \tag{4.3.35}$$

$$v_{tt} + \partial_y(\lambda_2) + \partial_x(\lambda_3) = 0 \tag{4.3.36}$$

$$\begin{aligned} & w_{tt} + D\Delta[(1+|\nabla w|^2)\Delta w] - D\nabla\cdot[|\Delta w|^2\nabla w] \\ & \qquad + \partial_x(\lambda_1 w_x) + \partial_y(\lambda_2 w_y) + \partial_x(\lambda_3 w_y) + \partial_y(\lambda_3 w_x) = 0. \end{aligned} \tag{4.3.37}$$

The above system would be supplemented with appropriate initial displacement $w_0 = w(x, y; 0)$ and velocity $w_1(x, y) = w_t(x, y; 0)$, from which the initial conditions for u and v can be inferred through the relationships (4.3.16)–(4.3.17).

Taken as a system, the constraint equations in (4.3.34) and (4.3.35)—(4.3.37) constitute six equations in six principal unknowns. As such, boundary conditions should be available and complement these equations for each unknown, u, v, w and λ_i for $i = 1, 2, 3$.

Remark 4.3.8. Letting $\mathbf{u} = \langle u, v\rangle$ and $\Lambda = \begin{bmatrix} \lambda_1 & \lambda_3 \\ \lambda_3 & \lambda_2 \end{bmatrix}$, we have a nice vectorial description of the system that makes for an apt comparison against other nonlinear plate equations (e.g., the full von Karman equations of motion [18, 47, 50]):

$$\mathbf{u}_{tt} + \mathrm{div}\Lambda = 0 \tag{4.3.38}$$

$$w_{tt} + D\Big[\Delta\Big[(1+|\nabla w|^2)\Delta w\Big] - \nabla\cdot\Big(|\Delta w|^2\nabla w\Big)\Big] + \mathrm{div}\Big(\Lambda\nabla w\Big) = 0, \tag{4.3.39}$$

where the action of Λ on the gradient is that of matrix multiplication in this presentation. Although the Λ terms here serve to capture inertial effects due to the enforcement of three constraints, the full von Karman equations have a comparable formal structure with respect to these terms. They differ, however in the presence of the other nonlinear terms.

Formally comparing these equations against other standard plate dynamics, we, of course, note that the linear part of the plate corresponds to that of a Kirchhoff–Love or Euler–Bernoulli (linear) plate. The quasilinear terms in w in (4.3.39) seem novel, but are clear generalizations of the nonlinear stiffness terms appearing in the beam equation presented in Chapter 1.

4.3.3.3 Boundary Conditions

Here, we provide the boundary conditions for w and for the λ_i. From these, the boundary conditions for u and v can be inferred. On the clamped edge Γ_W, we again have the essential boundary condition

$$w = 0; \quad w_x = 0 \quad \text{on} \;\; \Gamma_W.$$

The minimization of the Lagrangian and the arbitrariness of virtual displacements yield the *natural* boundary conditions from the potential energy. For the second order conditions in w, we obtain those of the standard linear free plate:

$$w_{xx} + \nu w_{yy} = 0 \quad \text{on} \;\; \Gamma_E$$

$$w_{yy} + \nu w_{xx} = 0 \quad \text{on} \;\; \Gamma_S$$

$$w_{yy} + \nu w_{xx} = 0 \quad \text{on} \;\; \Gamma_N.$$

The potential energy produces nonlinear forces (cubic-type)—and thus boundary conditions—along the free edges Γ_E, Γ_S and Γ_N respectively:

$$(1-\nu)\left[(1+\nu)w_x w_{yy}^2 - 2w_x w_{xy}^2 - 4w_y w_{yy} w_{xy}\right] - \left[1 + w_x^2 + w_y^2\right]\left[w_{xxx} + (2-\nu)w_{yyx}\right] = 0$$

$$(1-\nu)\left[(1+\nu)w_y w_{xx}^2 - 2w_y w_{xy}^2 - 4w_x w_{xx} w_{xy}\right] - \left[1 + w_x^2 + w_y^2\right]\left[w_{yyy} + (2-\nu)w_{xxy}\right] = 0$$

$$(1-\nu)\left[(1+\nu)w_y w_{xx}^2 - 2w_y w_{xy}^2 - 4w_x w_{xx} w_{xy}\right] - \left[1 + w_x^2 + w_y^2\right]\left[w_{yyy} + (2-\nu)w_{xxy}\right] = 0.$$

Remark 4.3.9. The above conditions are **clearly not** the linear boundary conditions associated to the free plate, as presented in Remark 4.3.1.

The Lagrange multipliers λ_i, as variables, also have boundary conditions. These are readily obtained from Hamilton's principle along the free edges:

$$\lambda_1(x,y) = 0 \;\text{ and }\; \lambda_3(x,y) = 0 \quad \text{on} \;\; \Gamma_E$$

$$\lambda_2(x,y) = 0 \;\text{ and }\; \lambda_3(x,y) = 0 \quad \text{on} \;\; \Gamma_S$$

$$\lambda_2(x,y) = 0 \;\text{ and }\; \lambda_3(x,y) = 0 \quad \text{on} \;\; \Gamma_N.$$

Finally, we can express the boundary conditions for the Lagrange multipliers on the clamped edge Γ_W using (4.3.35)–(4.3.36) and the equations above:

$$\lambda_1(0,y) = \int_0^{L_x} \left[u_{tt} + \partial_y\left(\lambda_3\right)\right] dx;$$
$$\lambda_2(0,y) = \int_y^{L_y} \left[v_{tt} + \partial_x\left(\lambda_3\right)\right] dy\bigg|_{x=0};$$
$$\lambda_3(0,y) = \int_0^{L_x} \left[v_{tt} + \partial_y\left(\lambda_2\right)\right] dx,$$

as well as

$$\lambda_1(x,y) = \int_x^{L_x} \left[u_{tt} + \partial_y\left(\lambda_3\right)\right] dx\bigg|_{y=0} \quad \text{on} \ \ \Gamma_S,$$
$$\lambda_1(x,y) = \int_x^{L_x} \left[u_{tt} + \partial_y\left(\lambda_3\right)\right] dx\bigg|_{y=L_y} \quad \text{on} \ \ \Gamma_N,$$
$$\lambda_2(x,y) = \int_y^{L_y} \left[v_{tt} + \partial_x\left(\lambda_3\right)\right] dy\bigg|_{x=L_x} \quad \text{on} \ \ \Gamma_E.$$

Remark 4.3.10. Note that, above, we have suppressed the dependence of the Lagrange variables on time.

4.3.3.4 Reduction of System (4.3.35)–(4.3.37)

To be consistent with the beam system analysis, one may attempt to eliminate the λ_i, as well as the in-plane variables u, v in the system. This would yield a dynamic equation in the principal elastic displacement w only (as may be done for beam dynamics, and also as is possible in the case of von Karman's equations via the *Airy Stress Function* [18, 50]). Yet, for the plate dynamics above, there seems to be no clear way to accomplish this. We opt, here, to eliminate λ_1 and λ_2, and to use (4.3.16) and (4.3.17) to write u, v in terms of w. *This critically exploits the simplified nature of the span and chord-wise effective inextensibility constraints at the η^2-order.* In addition, we can see that, since the third (shear) constraint (4.3.18) does not permit us to explicitly solve for a displacement quantity, we will retain both w and λ_3 in our reduced system.

To that end, we integrate (4.3.35) from x to L_x and utilize the boundary condition $\lambda_1(L_x, y) = 0$. This yields:

$$\lambda_1(x, y) = \int_x^{L_x} [u_{tt} + \partial_y(\lambda_3)]\, dx. \tag{4.3.40}$$

Similarly, we integrate (4.3.36) from y to L_y and use the condition $\lambda_2(x, L_y) = 0$. This gives:

$$\lambda_2(x, y) = \int_y^{L_y} [v_{tt} + \partial_x(\lambda_3)]\, dy. \tag{4.3.41}$$

Substituting (4.3.40) and (4.3.41) into (4.3.37) we obtain:

$$\begin{aligned} w_{tt} - D\Big[\Delta[(1+|\nabla w|^2)\Delta w] - \nabla\cdot(|\Delta w|^2\nabla w)\Big] + \partial_x\left(w_x\int_x^{L_x} u_{tt}\right) + \partial_y\left(w_y\int_y^{L_y} v_{tt}\right) \\ +\partial_x\left(w_x\int_x^{L_x}\partial_y(\lambda_3)\right) + \partial_y\left(w_y\int_y^{L_y}\partial_x(\lambda_3)\right) + \partial_x(\lambda_3 w_y) + \partial_y(\lambda_3 w_x) = 0. \end{aligned} \tag{4.3.42}$$

In-plane inertial expressions, u_{tt} and v_{tt}, can be obtained, as in the case of the beam, by solving in (4.3.16), (4.3.17), and (4.3.18) and formally differentiating in time. Note that, using the essential boundary conditions at $x = 0$ for each of u, v, w, we have:

$$u(x,y) = -\frac{1}{2}\int_0^x w_x(\xi_1,y)^2 d\xi_1 \tag{4.3.43}$$

$$v(x,y) - v(x,0) = -\frac{1}{2}\int_0^y w_y(x,\xi_2)^2 d\xi_2 \tag{4.3.44}$$

$$v(x,y) = -\int_0^x w_x(\xi_1,y)w_y(\xi_1,y)d\xi_1 - \int_0^x u_y(\xi_1,y)d\xi_1, \tag{4.3.45}$$

where we have suppressed the dependence on t above. From which we have an expression for $v(x,y)$, and thence an expression for $u(x,y)$, where both depend only on the transverse variable w:

$$v(x,y) = \int_0^x \int_0^{\xi_1} w_x(\zeta,y)w_{xy}(\zeta,y)d\zeta d\xi_1 - \int_0^x w_x(\xi_1,y)w_y(\xi_1,y)d\xi_1. \tag{4.3.46}$$

From these we obtain the inertial expressions

$$u_{tt} = -\int_0^x [w_{xt}^2 + w_x w_{xtt}]d\xi_1 \tag{4.3.47}$$

$$v_{tt} = -\int_0^y [w_{yt}^2 + w_y w_{ytt}]d\xi_2 + v_{tt}(y=0). \tag{4.3.48}$$

The above formulae in (4.3.42)–(4.3.48) showcase of the principal strengths of the η^2-order effective inextensibility constraints: namely, we obtain straight-forward equations of motion in two unknowns, with a clear connection to the η^2-order *beam dynamics* we have seen in Chapter 1. On the other hand, owing to the structure of the third effective inextensibility constraint, (4.3.18), it does not seem that systematic integrations and/or differentiations—coupled with the given boundary conditions—will allow a clean elimination of the λ_3 variable. Thus, any analytical treatment of this system would seem to require both the w and λ_3 variables directly. That is to say, we would require retaining the constraint equation associated to λ_3:

$$u_y + v_x = \ -w_x w_y, \tag{4.3.49}$$

with u and v as above, written explicitly in terms of w. To this, initial and boundary conditions are affixed to w, as described above, and to λ_3, the boundary conditions described above.

4.3.4 Model II: Partial Use of Effective Shear Constraint

In this model, we retain the treatment of the potential energy in Section 4.3.3.1. To wit: we retain all three full inextensibility constraints (4.3.9)–(4.3.11) in eliminating the in-plane strains ε_{ij} from the potential energy in (4.3.2). After this, we truncate all three inextensibility constraints to quadratic order (as in (4.3.16)–(4.3.18)). Finally, we truncate the expanded potential energy as before to arrive at the potential energy expression in (4.3.33). On the other hand, in developing the equations of motion, we elect (with foresight coming from those issues associated to λ_3 above) to *enforce only the first two η^2-effective inextensibility conditions*, (4.3.16) and (4.3.17) through Lagrange multipliers λ_1, λ_2. Thus, in this model, shear inextensibility is only implicitly enforced from the point of view of the choice of the potential energy. We utilize only two Lagrange multipliers in the derivation of the equations of motion.

In this presentation, the constraint variables $\lambda_1,\ \lambda_2$ serve to enforce the span and chord-wise quadratic effective inextensibility constraints. Accordingly, *we retain these as part of the system*:

$$u_x + \frac{1}{2}w_x^2 = 0; \qquad v_y + \frac{1}{2}w_y^2 = 0. \tag{4.3.50}$$

For the dynamics, Hamilton's principle yields identical nonlinear terms in w, owing the use of E_P as in Section 4.3.3.2. Moreover, we do not retain any reference to the shear constraint in the equations, as there is no λ_3 present. The unforced equations of motion are then:

$$u_{tt} + \partial_x(\lambda_1) = 0 \tag{4.3.51}$$

$$v_{tt} + \partial_y(\lambda_2) = 0 \tag{4.3.52}$$

$$w_{tt} + D\left[\Delta[(1+|\nabla w|^2)\Delta w] - \nabla\cdot(|\Delta w|^2\nabla w)\right] + \partial_x(\lambda_1 w_x) + \partial_y(\lambda_2 w_y) = 0. \tag{4.3.53}$$

As before, the equations would be supplemented with appropriate initial displacement $w_0 = w(x,y;0)$ and velocity $w_1(x,y) = w_t(x,y;0)$, from which the initial conditions for u and v can be inferred.

4.3.4.1 Boundary Conditions

The boundary conditions for w (which then yield conditions for u and v through (4.3.50)) are identical to Section 4.3.3.3. The boundary conditions of the

Lagrange multipliers λ_1 in this case are:

$$\lambda_1(x,y) = \int_0^{L_y} u_{tt} dy \quad \text{on } \Gamma_W, \qquad \lambda_1(x,y) = 0 \quad \text{on } \Gamma_E,$$

$$\lambda_1(x,y) = \int_x^{L_x} u_{tt} dx \bigg|_{y=0} \quad \text{on } \Gamma_S, \qquad \lambda_1(x,y) = \int_x^{L_x} u_{tt} dx \bigg|_{y=L_y} \quad \text{on } \Gamma_N.$$

And for λ_2:

$$\lambda_2(x,y) = \int_y^{L_y} v_{tt} dy \bigg|_{x=0} \quad \text{on } \Gamma_W, \qquad \lambda_2(x,y) = \int_y^{L_y} v_{tt} dy \bigg|_{x=L_x} \quad \text{on } \Gamma_E,$$

$$\lambda_2(x,y) = 0 \quad \text{on } \Gamma_S, \qquad \lambda_2(x,y) = 0 \quad \text{on } \Gamma_N.$$

4.3.4.2 Reduction of System (4.3.51)–(4.3.53)

One of the primary benefits for this system, discussed further in Section 4.4, is that the Lagrange multiplier variables can be fully eliminated (as with the inextensible beam). Indeed, one obtains from (4.3.51) and (4.3.52) that

$$\lambda_1(L_x,y) - \lambda_1(x,y) = -\int_x^{L_x} u_{tt} d\xi; \qquad \lambda_2(x,y) - \lambda_2(x,0) = -\int_0^{y} v_{tt} d\zeta.$$

At this point we can invoke the boundary conditions for λ_i, as seen above on the appropriate edge of the plate, to conclude

$$\lambda_1(x,y) = \int_x^{L_x} u_{tt} d\xi; \qquad \lambda_2(x,y) = -\int_0^{y} v_{tt} d\zeta. \tag{4.3.54}$$

These quantities may be substituted directly into the equations of motion for w, which results in the following *closed* system—with no reference to the Lagrange variables:

$$\begin{aligned} w_{tt} + D\Delta[(1+|\nabla w|^2)\Delta w] - D\nabla \cdot [|\Delta w|^2 \nabla w] & \\ +\partial_x\Big(w_x \int_x^{L_x} u_{tt} d\xi\Big) - \partial_y\Big(w_y \int_0^y v_{tt} d\zeta\Big) = 0 & \qquad (4.3.55) \\ u_x + \frac{1}{2}w_x^2 = 0; \quad v_y + \frac{1}{2}w_y^2 = 0. & \qquad (4.3.56) \end{aligned}$$

A complete description, then, would again provide the relevant initial and boundary conditions from the principal variable here, w.

4.3.5 Model III: Complete Omission of The Shear Constraint

In natural succession from the previous models, one may inquire:

What happens if we omit the third (shear) constraint in the derivation?

This is a reasonable subsequent step, as we have in the previous model only partially made use of the shear constraint. For the model in this section, we refrain entirely from making mention of a shear constraint. With only span and chord-wise inextensibility enforced, we obtain the equations of motion. In particular, this showcases how convoluted the equations of motion become and demonstrates the usefulness of the shear constraint.

4.3.5.1 Addressing The Potential Energy

The two constraints approach forbids elongation in the x and y axes but *permits* shear strain. This translates into $\varepsilon_{11} = \varepsilon_{22} = 0$, but we will *not* take $\varepsilon_{12} = 0$. Immediately it is clear we will have more terms in the equations of motion. As before, after invoking the full inextensibility conditions $\varepsilon_{11} = 0$ and $\varepsilon_{22} = 0$, we will compute the associated potential energy and then truncate to a particular order.

Applying only two inextensibility constraints to eliminate $\varepsilon_{11}, \varepsilon_{22}$ into the bulk strain expressions (4.3.3)–(4.3.5) yields:

$$\hat{\varepsilon}_{11} = -z\left[w_{xx}\left(1 + u_x + v_y\right) - w_x u_{xx} - w_y v_{xx}\right]$$

$$\hat{\varepsilon}_{22} = -z\left[w_{yy}\left(1 + u_x + v_y\right) - w_x u_{yy} - w_y v_{yy}\right]$$

$$\hat{\varepsilon}_{12} = u_y + v_x + u_x u_y + v_x v_y + w_x w_y - 2z\left[w_{xy}\left(1 + u_x + v_y\right) - w_x u_{xy} - w_y v_{xy}\right].$$

We then invoke the η^2-order hypothesis to obtain the curvature expressions (4.3.29)–(4.3.31). We must also truncate

$$\varepsilon_{12} = u_y + v_x + u_x u_y + v_x v_y + w_x w_y \approx u_y + v_x + w_x w_y,$$

under the same η^2-hypothesis. And, as before, we invoke the (two) η^2-effective inextensibility constraints

$$u_x = -\frac{1}{2}w_x^2, \quad v_y = -\frac{1}{2}w_y^2,$$

from which we can differentiate to solve for u_{xx} and v_{yy}.

Remark 4.3.11. Without creating nonlocal conditions—and invoking boundary conditions, as yet undetermined—we can no longer obtain expressions for v_x, u_y as before. We note that this is a key point of distinction when we have imposed no notion of shear inextensibility.

Upon simplifying the terms as described above, we obtain:

$$\hat{\varepsilon}_{11} = z\left[-w_{xx}\left(1 + \frac{1}{2}w_x^2 - \frac{1}{2}w_y^2\right) + w_y v_{xx}\right]$$

$$\hat{\varepsilon}_{22} = z\left[-w_{yy}\left(1 - \frac{1}{2}w_x^2 + \frac{1}{2}w_y^2\right) + w_x u_{yy}\right]$$

$$\hat{\varepsilon}_{12} = u_y + v_x + w_x w_y - 2zw_{xy}\left[1 + \frac{1}{2}w_x^2 + \frac{1}{2}w_y^2\right].$$

Then, integrating in z and simplifying, with coefficients:

$$\int_{-h/2}^{h/2}[\hat{\varepsilon}_{11}^2+\hat{\varepsilon}_{22}^2]dz = \frac{h^3}{12}\Big[w_y^2v_{xx}^2+w_x^2u_{yy}^2-2w_yv_{xx}w_{xx}-2w_xu_{yy}w_{yy}$$
$$-w_y(w_x^2-w_y^2)v_{xx}w_{xx}+w_x(w_x^2-w_y^2)u_{yy}w_{yy}$$
$$+w_{xx}^2\Big(1+(w_x^2-w_y^2)+\frac{1}{4}(w_x^2-w_y^2)^2\Big)$$
$$+w_{yy}^2\Big(1-(w_x^2-w_y^2)-\frac{1}{4}(w_x^2-w_y^2)^2\Big)\Big]$$

$$2\nu\int_{-h/2}^{h/2}[\hat{\varepsilon}_{11}\hat{\varepsilon}_{22}]dz = \frac{\nu h^3}{6}\Big[v_{xx}u_{yy}w_xw_y+w_{xx}w_{yy}w_xw_{xx}u_{yy}-w_yv_{xx}w_{yy}$$
$$-\frac{1}{4}w_{xx}w_{yy}\Big(w_x^2-w_y^2\Big)^2+\frac{1}{2}\Big(w_x^2-w_y^2\Big)(w_yv_{xx}w_{yy}-w_xw_{xx}u_{yy}\Big)\Big]$$

$$\frac{1-\nu}{2}\int_{-h/2}^{h/2}[\hat{\varepsilon}_{12}^2]dz = \frac{h(1-\nu)}{2}(u_y+v_x+w_xw_y)^2+\frac{h^3(1-\nu)}{6}\Big(1+\frac{1}{2}w_x^2+\frac{1}{2}w_y^2\Big)^2w_{xy}^2.$$

Recalling the full potential energy expression (4.3.2), we input the above expressions for the strains. Since we are operating at the η^2-level here for coefficients, we discard *any terms* with coefficients scaled by η^3 or higher. Note that, in the (new) situation where first derivative terms appear independent of second derivative terms, we choose to retain. This yields

$$E_P = \frac{1}{2}\frac{E}{1-\nu^2}\int_\Omega\Big\{\frac{h^3}{12}\Big[w_y^2v_{xx}^2+w_x^2u_{yy}^2-2w_yv_{xx}w_{xx}-2w_xu_{yy}w_{yy}+w_{xx}^2\Big(1+w_x^2-w_y^2\Big)$$
$$+w_{yy}^2\Big(1-w_x^2+w_y^2\Big)\Big]+\frac{\nu h^3}{6}\Big[v_{xx}u_{yy}w_xw_y+w_{xx}w_{yy}w_xw_{xx}u_{yy}-w_yv_{xx}w_{yy}\Big]$$
$$+\frac{h^3(1-\nu)}{6}\Big(1+w_x^2+w_y^2\Big)w_{xy}^2+\frac{h(1-\nu)}{2}(u_y+v_x+w_xw_y)^2\Big\}\,d\Omega.$$

Remark 4.3.12. The terms in final line above represent an interesting contribution, both in terms of their "h" scaling, i.e., thickness, as well as being detached from principal second derivative terms.

Remark 4.3.13. For reference, the terms we discarded above include:

$$\frac{h^3}{12}\Big[w_x(w_x^2-w_y^2)u_{yy}w_{yy}-w_y(w_x^2-w_y^2)v_{xx}w_{xx}+\frac{w_{xx}^2}{4}(w_x^2-w_y^2)^2-\frac{w_{yy}^2}{4}(w_x^2-w_y^2)^2\Big]$$
$$-\frac{\nu h^3}{24}w_{xx}w_{yy}(w_x^2-w_y^2)^2+\frac{\nu h^3}{12}(w_x^2-w_y^2)(w_yv_{xx}w_{yy}-w_xw_{xx}u_{yy})$$
$$+\frac{h^3(1-\nu)}{6}\Big(\frac{1}{2}w_x^2w_y^2+\frac{1}{4}w_x^4+\frac{1}{4}w_y^4\Big)w_{xy}^2.$$

Now, invoking the definition of the constant D, the potential energy can then be written:

$$\begin{aligned}E_P=\frac{6D}{h}\int_0^{L_y}\int_0^{L_x}\Bigg\{&\frac{h^2}{12}\Big[w_{xx}^2+w_{yy}^2+2\nu w_{xx}w_{yy}+2(1-\nu)w_{xy}^2\left(1+w_x^2+w_y^2\right)\\&+(w_x^2-w_y^2)(w_{xx}^2-w_{yy}^2)-2w_yw_{xx}v_{xx}-2w_xw_{yy}u_{yy}\\&-2\nu\left(w_yw_{yy}v_{xx}+w_xw_{xx}u_{yy}\right)\Big]+\frac{1-\nu}{2}\Big[u_y+v_x+w_xw_y\Big]^2\Bigg\}dxdy.\end{aligned}\tag{4.3.57}$$

4.3.5.2 Equations of Motion

As before, λ_1 is used to enforce the span-wise effective constraint (4.3.16) and λ_2 the chord-wise (4.3.17). Utilizing the arbitrariness of the relevant virtual changes, we can gather the equations of motion. We recover both effective constraints (4.3.16) and (4.3.17) via the associated Lagrange multipliers λ_1 and λ_2 in Hamilton's principle. Following the procedure of the previous sections, the equations of motion for the in-plane displacements:

$$u_{tt} + \partial_x(\lambda_1) - D\left[w_{xyy}w_{yy} + 2w_{xy}w_{yyy} + w_x\partial_y^4 w + \nu w_{xyy}w_{xx} + 2\nu w_{xy}w_{xxy} + \nu w_x w_{xxyy}\right]$$
$$-\frac{12D}{h^2}(1-\nu)\left[u_{yy} + w_x w_{yy}\right] = 0$$

$$v_{tt} + \partial_y(\lambda_2) - 2D\left[w_{yxx}w_{xx} + 2w_{yx}w_{xxx} + w_y\partial_x^4 w + \nu w_{yxx}w_{yy} + 2\nu w_{yx}w_{yyx} + \nu w_y w_{yyxx}\right]$$
$$-\frac{12D}{h^2}(1-\nu)\left[v_{xx} + w_{xx}w_y\right] = 0.$$

We rewrite these, and include the equation for w:

$$u_{tt} + \partial_x(\lambda_1) - \frac{12D}{h^2}(1-\nu)\left[u_{yy} + w_x w_{yy}\right] - 2D\partial_y^2\left[w_x(w_{yy} + \nu w_{xx})\right] = 0 \quad (4.3.58)$$
$$v_{tt} + \partial_y(\lambda_2) - \frac{12D}{h^2}(1-\nu)\left[v_{xx} + w_{xx}w_y\right] - 2D\partial_x^2\left[w_y(w_{xx} + \nu w_{yy})\right] = 0 \quad (4.3.59)$$

$$
\begin{aligned}
&w_{tt} + \partial_x(\lambda_1 w_x) + \partial_y(\lambda_2 w_y) - D\Big[\partial_x^4 w(1 + w_x^2 - w_y^2) + \partial_y^4 w(1 - w_x^2 + w_y^2) + 2w_{xxyy}(1 + w_x^2 + w_y^2)\\
&-\nu w_{xxyy}(w_x^2 + w_y^2) - w_x \partial_y^4 u - w_y \partial_x^4 v + 4w_x w_{xx} w_{xxx} + 4w_y w_{yy} w_{yyy} - w_x w_{yy} w_{xyy} - w_y w_{xx} w_{yxx}\\
&+(4-2\nu) w_x w_{xy} w_{xxy} + (4-2\nu) w_y w_{xy} w_{yyx} - 4w_x w_{xy} w_{yyy} - 4w_y w_{yx} w_{xxx} - 2w_{xy} v_{xxx} - 2w_{xy} u_{yyy}\\
&+4(1-\nu) w_x w_{xx} w_{xyy} + 4(1-\nu) w_y w_{yy} w_{xxy} + w_{xx}^3 + w_{yy}^3 + w_{xx} w_{yy}^2 + w_{yy} w_{xx}^2 - (1+3\nu) w_{xx} w_{xy}^2\\
&-(1+3\nu) w_{yy} w_{xy}^2\Big] + \frac{6D}{h^2}(1-\nu)\Big[w_{xx} w_y^2 + 2w_x w_y w_{xy} + 2u_y w_{xy} + v_{xx} w_y + 2v_x w_{xy} + w_x^2 w_{yy} + u_{yy} w_x\Big]\\
&= 0.
\end{aligned}
$$

4.3.5.3 Boundary Conditions

On the clamped edge Γ_W, we have:

$$w = 0; \quad w_x = 0; \quad u = 0; \quad v = 0.$$

For the second order conditions, we have:

On Γ_E:

$$w_{xx} + \nu w_{yy} = 0, \qquad w_{xx}(1 + w_x^2 - w_y^2) - w_y v_{xx} + \nu w_{yy} - \nu w_x u_{yy} = 0.$$

On Γ_S and Γ_N:

$$w_{yy} + \nu w_{xx} = 0, \qquad w_{yy}(1 - w_x^2 + w_y^2) - w_x u_{yy} + \nu w_{xx} - \nu w_y v_{xx} = 0.$$

For the third order conditions we have:

On Γ_E:

$$\frac{h^2}{6} w_y \left[w_{xxx} + \nu w_{yyx} \right] + (1-\nu) \left[v_x + w_x w_y + u_y \right] = 0$$

$$\frac{h^2}{6} \Big\{ - w_x w_{xx}^2 - w_x w_{yy}^2 - w_{yy} u_{yy} - (2-\nu) w_x w_{xy}^2 - w_{xxx}(1 + w_x^2 - w_y^2) + 2 w_y w_{xx} w_{yx}$$

$$+ w_{yx} v_{xx} + w_y v_{xxx} - \nu w_{yyx} - \nu w_x^2 w_{xyy} - 2(1-\nu) \Big[w_{xyy}(1 + w_x^2 + w_y^2) + 2 w_y w_{xy} w_{yy} \Big] \Big\}$$

$$+ (1-\nu) \Big[w_x w_y^2 + u_y w_y + v_x w_y \Big] = 0.$$

On Γ_S and Γ_N:

$$\frac{h^2}{6} w_x \left[w_{yyy} + \nu w_{xxy} \right] + (1-\nu) \left[u_y + w_x w_y + v_x \right] = 0$$

$$\frac{h^2}{6} \Big\{ - w_y w_{yy}^2 - w_y w_{xx}^2 - w_{xx} v_{xx} - (2-\nu) w_y w_{xy}^2 - w_{yyy}(1 - w_x^2 + w_y^2) + 2 w_x w_{yy} w_{yx}$$

$$+ w_{yx} u_{yy} + w_x u_{yyy} - \nu w_{xxy} - \nu w_y^2 w_{yyx} - 2(1-\nu) \Big[w_{xxy}(1 + w_x^2 + w_y^2) + 2 w_x w_{xy} w_{xx} \Big] \Big\}$$

$$+ (1-\nu) \Big[w_x^2 w_y + u_y w_x + v_x w_x \Big] = 0.$$

The boundary conditions of the Lagrange multipliers λ_i are as follow:

$$\lambda_1(x,y) = 0 \quad \text{on} \quad \Gamma_E; \quad \lambda_2(x,y) = 0 \quad \text{on} \quad \Gamma_S; \quad \lambda_2(x,y) = 0 \quad \text{on} \quad \Gamma_N;$$

$$\lambda_1(x,y) = \int_0^{L_y} \left\{ u_{tt} - \frac{12D}{h^2}(1-\nu)\left[u_{yy} + w_x w_{yy}\right] - 2D\partial_y^2\left[w_x(w_{yy} + \nu w_{xx})\right] \right\} dy \bigg|_{x=0} \quad \text{on} \quad \Gamma_W$$

$$\lambda_1(x,y) = \int_x^{L_x} \left\{ u_{tt} - \frac{12D}{h^2}(1-\nu)\left[u_{yy} + w_x w_{yy}\right] - 2D\partial_y^2\left[w_x(w_{yy} + \nu w_{xx})\right] \right\} dx \bigg|_{y=0} \quad \text{on} \quad \Gamma_S$$

$$\lambda_1(x,y) = \int_x^{L_x} \left\{ u_{tt} - \frac{12D}{h^2}(1-\nu)\left[u_{yy} + w_x w_{yy}\right] - 2D\partial_y^2\left[w_x(w_{yy} + \nu w_{xx})\right] \right\} dx \bigg|_{y=L_y} \quad \text{on} \quad \Gamma_N$$

$$\lambda_2(x,y) = \int_y^{L_y} \left\{ v_{tt} - \frac{12D}{h^2}(1-\nu)\left[v_{xx} + w_{xx} w_y\right] - 2D\partial_x^2\left[w_y(w_{xx} + \nu w_{yy})\right] \right\} dy \bigg|_{x=0} \quad \text{on} \quad \Gamma_W$$

$$\lambda_2(x,y) = \int_y^{L_y} \left\{ v_{tt} - \frac{12D}{h^2}(1-\nu)\left[v_{xx} + w_{xx} w_y\right] - 2D\partial_x^2\left[w_y(w_{xx} + \nu w_{yy})\right] \right\} dy \bigg|_{x=L_x} \quad \text{on} \quad \Gamma_E.$$

4.3.6 Higher Order Models

We conclude the central part of the treatment of inextensible plates by addressing the natural question of including higher order terms in various modelling steps. We see that in the approaches above that, unlike for the beam, there are critical junctures where the order (of truncation) affects the inextensibility considerations, as well as (though not independent of) the analysis of the potential energy. On the one hand, it is possible to address some of the shortcomings of the previous three models via the inclusion of higher order effects; on the other hand, as we have already seen, the simplest possible (and lowest order) truncations already yield models which are notably complex.

4.3.6.1 Higher Order Inextensibility

We recall the "full" inextensibility constraints:

$$(1 + u_x)^2 + v_x^2 + w_x^2 = 1 \tag{4.3.60}$$

$$u_y^2 + (1 + v_y)^2 + w_y^2 = 1 \tag{4.3.61}$$

$$u_y + v_x + u_x u_y + v_x v_y + w_x w_y = 0. \tag{4.3.62}$$

We can, of course, expand the first two to read:

$$2u_x + u_x^2 + v_x^2 + w_x^2 = \ 0; \quad 2v_y + v_y^2 + u_y^2 + w_y^2 = \ 0. \tag{4.3.63}$$

Remark 4.3.14. If we were to combine the span and chord constraints, we would have:

$$\nabla \cdot \langle u, v \rangle = \ -\frac{1}{2}\Big[|\nabla u|^2 + |\nabla v|^2 + |\nabla w|^2\Big] \tag{4.3.64}$$

$$u_y + v_x = \ -[u_x u_y + v_x v_y + w_x w_y]. \tag{4.3.65}$$

Now, we may proceed as we did before in Assumption 4.3.3 (and the discussion thereafter), and retain higher order terms (up to η^4) in (4.3.14)–(4.3.15). In this case, we would obtain:

$$u_x = -\frac{1}{2}[w_x^2 + v_x^2] - \frac{1}{8}w_x^4 \tag{4.3.66}$$

$$v_y = -\frac{1}{2}[w_y^2 + u_y^2] - \frac{1}{8}w_y^4 \tag{4.3.67}$$

$$u_y + v_x = -u_x u_y - v_x v_y - w_x w_y. \tag{4.3.68}$$

On the other hand, more closely following the logic in 1D, we would have from (4.3.60) that $w_x^2 \sim \eta^2$, and also then that $u_x \sim \eta^2$, so we would discard **only** u_x^2 , but not u_y^2. Similarly, from (4.3.61), we would discard v_y^2 only but not v_x^2. We can formalize this into a separate hypothesis.

Assumption 4.3.4. *Assume that $\partial_{x_i} w, \partial_y u, \partial_x v \sim \eta$, and assume that $[\partial_x u], [\partial_y v] \sim \eta^2$, for all $i = 1, 2$.*

Formulating the reduced η^4 constraints from the Taylor expansions in (4.3.14)—(4.3.15), we obtain:

$$u_x = -\frac{1}{2}v_x^2 - \frac{1}{2}w_x^2 - \frac{1}{4}v_x^2 w_x^2 - \frac{1}{8}v_x^4 - \frac{1}{8}w_x^4 \tag{4.3.69}$$

$$v_y = -\frac{1}{2}u_y^2 - \frac{1}{2}w_y^2 - \frac{1}{4}u_y^2 w_y^2 - \frac{1}{8}u_y^4 - \frac{1}{8}w_y^4 \tag{4.3.70}$$

$$u_y + v_x = -u_x u_y - v_x v_y - w_x w_y. \tag{4.3.71}$$

4.3.6.2 Higher Order Potential Energy

With either of the choices in the previous section, we might develop an η^4 potential energy. (This is principally a distinction between taking Assumption 4.3.3

and Assumption 4.3.4.) In doing so, we would revisit the analysis as before, beginning with the potential energy expression

$$E_P = \frac{1}{2}\frac{E}{1-\nu^2}\int_\Omega \int_{-h/2}^{h/2} \left[\hat{\varepsilon}_{11}^2 + \hat{\varepsilon}_{22}^2 + 2\nu\hat{\varepsilon}_{11}\hat{\varepsilon}_{22} + \frac{1-\nu}{2}\hat{\varepsilon}_{12}^2\right] dz d\Omega. \tag{4.3.72}$$

We would reconsider the full strains, discarding the terms which are quadratic in z (as in Assumption 4.3.2):

$$\hat{\varepsilon}_{11} = \varepsilon_{11} + z\kappa_{11}; \quad \hat{\varepsilon}_{22} = \varepsilon_{22} + z\kappa_{22}; \quad \hat{\varepsilon}_{12} = \varepsilon_{12} + z\kappa_{12}. \tag{4.3.73}$$

Recalling the strain-displacement relations

$$\varepsilon_{11} = u_x + \frac{1}{2}\left[u_x^2 + v_x^2 + w_x^2\right] \tag{4.3.74}$$

$$\varepsilon_{22} = v_y + \frac{1}{2}\left[u_y^2 + v_y^2 + w_y^2\right] \tag{4.3.75}$$

$$\varepsilon_{12} = u_y + v_x + u_x u_y + v_x v_y + w_x w_y, \tag{4.3.76}$$

we may then choose to enforce inextensibility by taking each $\varepsilon_{ij} = 0, i, j = 1, 2$, or by only taking $\varepsilon_{11} = \varepsilon_{22} = 0$. In either case, we must then implement curvature expressions which are themselves "accurate" up to the order of η^4. For the sake of space, we do not reproduce the curvature expressions from (4.3.26)–(4.3.28) here, but suffice to say that one may implement either Assumption 4.3.3 or Assumption

4.3.4 *up to order* η^4. We demonstrate with (4.3.26):

$$\kappa_{11} = (1+u_x)[v_{xx}w_y + v_x w_{xy} - v_{xy}w_x - (1+v_y)w_{xx}] \quad (4.3.77)$$
$$+ v_x[u_{xy}w_x + u_y w_{xx} - u_{xx}w_y - (1+u_x)w_{xy}]$$
$$+ w_x[u_{xx} + v_{xy} + u_{xx}v_y + u_x v_{xy} - u_{xy}v_x - u_y v_{xx}].$$

Recall that under Assumption 4.3.3, up to order η^2, we obtained:

$$\kappa_{11} = \ w_y v_{xx} + w_x u_{xx} - (1 + u_x + v_y)w_{xx}.$$

Now, including all terms up to order η^4 (from either Assumption 4.3.3 or Assumption 4.3.4), we should retain all terms in (4.3.77). Indeed, coefficients on second order terms are at or below η^4 order in their coefficients. Additionally, unlike the resulting analysis from the η^2 inextensibility assumption, we cannot explicitly solve for $u_{x_i x_j}$ and $v_{x_i x_j}$ to cleanly simplify the expressions in κ_{11}. Thus, pursuing an η^4-order model from either Assumption 4.3.3 or Assumption 4.3.4 will require retaining expressions for κ_{ij} in their entirety, resulting in a rather perilous expression for the potential energy E_P.

We do not pursue this line further here. We have included the discussion above to demonstrate a general method of building a model that consistently implements an order hypothesis across the inextensibility constraints. Moreover, we observe that it is possible to do so to ever-increasing order. On the other hand, as we can already see through Models 1–3 above, the degree of complexity in the PDE models, boundary conditions, and enforcement of the inextensibility constraints through Lagrange multipliers, is notable at the level of even η^2.

4.4 Discussion and Future Work

We now provide some discussion of the plate models presented above.

- The principal benefit of building η^2-plate models is they maintain u and v as decoupled variables, in that one can solve for them in terms of w. (This was the case of the beam analysis.) This, of course, is tremendously useful in developing a clear and tractable set of equations of motion for analysis.

- The first point of departure from the beam theory presented in Chapter 1 is the emergence of nonlinear boundary conditions (Section 4.3.3.3); this is a necessary byproduct of invoking Hamilton's principle with the chosen potential energy (very similar to what occurs in [40] in an extensible situation). For any future theory of existence and uniqueness of solutions for the inextensible plate mirroring that of the beam [22], nonlinear boundary conditions will be a central issue. This is especially true, as the nonlinear boundary conditions emerge in the notoriously troublesome higher-order plate conditions, and differ markedly from the linear theory. In any approach making using mode functions, one has to be cognizant of this point, in particular, from the point of view of convergence analysis and associated error near the free edges.

- Furthermore, even the *linear mode functions* associated to 2D cantilevered plates are notoriously challenging [8], far beyond the simple cantilever mode functions in 1D [39, 40]. Moreover, with the aforementioned appearance of nonlinear boundary conditions, linear mode functions will not satisfy relevant inextensible plate boundary conditions, even if one could explicitly express such linear mode functions through separation [11, 55]. It is common in the engineering community to assume mode shapes are multiples of the 1D beam mode shapes, although for plates with free edges this is not exact [8].

- The second major point of departure is the inability to neatly and cleanly resolve the equations through the elimination of the Lagrange multipliers in Plate Models I and III. The benefit of Model II is that it yields equations of motion that are written explicitly in the transverse deflection w; on the other hand, it has an inherent discrepancy between the enforcement of the shear inextensibility constraint in the potential energy (taken) and the Lagrange analysis (ignored as a constraint).

- The dissertation [58] demonstrated a numerical implementation of Model I described in this paper using a Rayleigh–Ritz global modal method. It was found that the model was less stiff than a nonlinear model analyzed by ANSYS, a commercial Finite Element Method solver. Model III was proposed in the dissertation, and the same method was used to implement that model numerically. Using the potential energy associated to Model III resulted in a plate which was far stiffer than the one modeled in ANSYS.

- In the discussion of cantilever large deflections, it is not physically appropriate to discard u_{tt} or v_{tt} in the modeling as one would do in the case of the scalar von Karman dynamics [16, 50]. Such a decision would, of course, simplify the model; however, as nonlinear inertial effects are paramount here, doing so would be a poor modeling choice. For a cantilevered beam it is easily observed that these "acceleration terms" are on the order of nonlinear stiffness terms for the first mode [73, 75]. In general, this will be true for the cantilevered plate, though this is not the case for beams or plates which are restrained on opposing boundaries (again, see the von Karman plate theory [18, 50]).

- As a first mathematical step, one should solve the stationary problem(s) associated to the potential energy E_P in (4.3.33). This should be done from the point of view of internal and boundary loading. Some preliminary numerics—discussed above—have considered edge loading, but no thorough numerical or analytical studies have been undertaken. Mathematically, a first step will be developing a theory of strong solutions for the stationary version of Model I (dropping time derivatives and Lagrange multiplier terms). The resulting model is spatially-quasilinear with nonlinear boundary conditions.

- It is apparent from the analysis in Model III and the discussion in Section 4.3.6 that higher order methods can and should be developed. However, owing to the apparent complexity of such models, their development should be largely tailored to the context of what is to be modeled—for instance, paying close attention to the plate's aspect ratio.

- There is a substantial literature on cantilevered beams which bend in two mutually orthogonal directions and also twist about the beam axis. This corresponds to assuming that there is inextensibility only for deformations along the beam axis and that v is only a function of x and t and $w = h(x,t) + y\alpha(x,t)$, where x is the spatial coordinate along the beam axis (span), y is the spatial coordinate along the chord axis and alpha is the twist about the x axis. For example, see [38]. Thus, this is a special case of a nonlinear plate theory (not yet developed here or elsewhere), if only rigid body translation and rotation are considered in the y direction.

- In all of our order assumptions herein, we began by declaring $\partial_{x_i} w \sim \eta$. From the physical point of view, one could make separate assumptions about w_x and w_y. An interesting consideration would permit different orders for the slopes of w in the x and y directions, and it would be relevant to further allow different orders in u and v.

Chapter 5: Well-Posedness of the Linear Cantilevered Plate

5.1 Summary of the Chapter

In this chapter we revisit the evolutionary PDE that describes the *linear* (Kirchhoff–Love) cantilevered plate defined on a rectangular domain, and examine its well-posedness. Our goal is to employ a Lumer–Phillips approach and, by constructing a semigroup argument, prove the well-posedness of the model in this configuration. For this argument we will see how the lack of elliptic regularity and the mixed and higher order boundary conditions poses challenges in the interpretation the free boundary conditions.

5.2 Introduction

The linear theory for thin elastic plates has been well established and broadly studied from a mathematical and engineering point of view. The model that describes the classical linear plate is that of Kirchhoff–Love which is considered to be the extension of the Euler–Bernoulli beam theory. To derive the equations one has to make the following modeling assumptions [65]:

1. The straight lines that are normal to the mid-surface remain straight after

deformation

2. The straight lines that are normal to the mid-surface remain normal to the mid-surface after deformation

3. The thickness of the plate does not change during a deformation.

This means that we can use the potential expression (4.3.2) introduced in Chapter 3 to describe the energy for this system. In addition, the linear nature of the model necessitates the linearization of the strain expression [50] used in the energies. That being said, we commence by utilizing the strain expressions given by [62]:

$$\hat{\varepsilon}_{11} = \varepsilon_{11} + z\kappa_{11} + z^2\mu_{11}$$

$$\hat{\varepsilon}_{22} = \varepsilon_{22} + z\kappa_{22} + z^2\mu_{22}$$

$$\hat{\varepsilon}_{12} = \varepsilon_{12} + z\kappa_{12} + z^2\mu_{12}$$

and proceed by dropping z^2 terms to be consistent with assumption (4.3.2). Then, by combining the above with (4.3.6)–(4.3.8) and (4.3.29)–(4.3.31), we can write the *linearized* strain expressions as [50]:

$$\hat{\varepsilon}_{11} = u_x - zw_{xx}; \qquad \hat{\varepsilon}_{22} = v_y - zw_{yy}; \qquad \hat{\varepsilon}_{12} = u_y + v_x - 2zw_{xy}.$$

Thus, the potential energy that is due to bending (depending only on w), is given by:

$$E_P = \frac{D}{2}\int_0^{L_y}\int_0^{L_x}\left[w_{xx}^2 + w_{yy}^2 + 2\nu w_{xx}w_{yy} + 2(1-\nu)w_{xy}^2\right]dxdy, \tag{5.2.1}$$

where $D = \dfrac{1}{12}\dfrac{Eh^2}{(1-\nu^2)}$ (as before, $E > 0$ denotes the Young's modulus).

We note here that for the Kirchhoff–Love model, the derivation of the equations of motion usually include only the terms that contribute to the bending, since the primary interest from a physical point of view is the vertical deflection of the plate (which what we have denoted by w) [50].

Remark 5.2.1. Comparing the linear quadratic energy (5.2.1) with (4.3.33) obtained in Chapter 3, we can see that the nonlinear model generalizes the expression of the linear model.

Utilizing the same spatial domain that was introduced in Chapter 3; namely a rectangle of sides $\Gamma_N, \Gamma_W, \Gamma_S$, and Γ_E, we can invoke Hamilton's principle for the Lagrangian to derive the equations of motion for the linear plate. Note that the essential boundary conditions corresponding to the clamped end are enforced for w (and their virtual changes) on Γ_W. Through the calculus of variations argument we also derive the natural boundary conditions which are the linear second (moments) and third (shears) order boundary conditions that correspond to the free edges.

Having said that, the equations of motion that describe the evolutionary PDE for a linear plate on a rectangular domain Ω are given by:

$$\begin{cases} w_{tt} + \Delta^2 w = f(x,y,t) & \text{in } \Omega \\ w = w_x = 0 & \text{on } \Gamma_W \\ \nu w_{xx} + w_{yy} = 0, \quad w_{yyy} + (2-\nu) w_{xxy} = 0 & \text{on } \Gamma_N \text{ and } \Gamma_S \\ w_{xx} + \nu w_{yy} = 0, \quad w_{xxx} + (2-\nu) w_{yyx} = 0 & \text{on } \Gamma_E \\ w(t=0) = w_0(x,y), \;\; w_t(t=0) = w_1(x,y). \end{cases} \tag{5.2.2}$$

Here, ν is the Poisson ration and $f(x,y,t)$ corresponds to a body force.

Remark 5.2.2. The free boundary conditions for an arbitrary domain can be given through the operators B_1 and B_2 [16] which are defined by:

$$[\Delta w + (1-\nu) B_1 w] = \left[\frac{\partial \Delta w}{\partial n} + (1-\nu) B_2 w \right] = 0,$$

with

$$B_1 w = 2 n_1 n_2 w_{xy} - n_1^2 w_{yy} - n_2^2 w_{xx}; \qquad B_2 w = \frac{\partial}{\partial \tau} \left[(n_1^2 - n_2^2) w_{xy} + n_1 n_2 (w_{yy} - w_{xx}) \right],$$

where $n = (n_1, n_2)$ is the outer normal to $\Gamma = \partial\Omega$, and $\tau = (-n_2, n_1)$ is the unit tangent vector along $\partial\Omega$. These boundary conditions represent moments and shears.

For our rectangular domain Ω, since we have the associated normals for $\Gamma_N, \Gamma_W, \Gamma_S$ (respectively): $e_2, e_1, -e_2, -e_1$, and tangentials (respectively): $-e_1, -e_2, e_1, e_2$, we can see that we obtain the free boundary conditions presented in (5.2.2).

Well-posedness results for the free-clamped configuration have been established (see for example [16]) in the case where the clamped and the free portion of the boundary are disjoint. In the case of the rectangular domain, the free and clamped free portion of the boundary are not disjoint and thus the need to develop a theory that will address this case.

5.2.1 Notation and Preliminaries

For a given spatial domain Ω, we will denote the $L^2(\Omega)$ as $||\cdot||$. Inner products in a Hilbert space are written $(\cdot,\cdot)_H$ (or simply $(\cdot,\cdot)$ when $H = L^2(\Omega)$ and the context is clear). The expression $\langle\cdot,\cdot\rangle_{X\times X'}$ will be used for duality pairings for a given Banach space X, as well as the general notation for a norm, $||\cdot||_X$.

The space $H^s(\Omega)$ will indicate the standard Sobolev space of order s, defined on domain Ω, and $H^s_0(\Omega)$ will be the closure of $C_0^\infty(\Omega)$ in the $H^s(\Omega)$-norm $\|\cdot\|_{H^s(\Omega)}$, also written as $\|\cdot\|_s$. If it is not explicitly mentioned otherwise, we will simply write H^s to mean $H^s(\Omega)$. We will also use the seminorm notation $|\cdot|_s$ which consists of the L^2 norms of the highest order derivatives from the corresponding H^s norm. For $\Gamma \subset \partial\Omega$, boundary restrictions $u\Big|_\Gamma$ are taken in the sense of the trace theorem for $u \in H^{1/2^+}(\Omega)$.

The constant C we take to mean a generic constant that may change from line to line. Additionally, for situations where $||q_1||_X \le C||q_2||_Y$ for some quantities q_1, q_2 in spaces X and Y, with C having no critical dependencies, *we will simply* *write* $||q_1||_X \lesssim ||q_2||_Y$.

For the associated bilinear form that we will define later on, we will need to make use of the so called *von Karman bracket* which is defined by the equality:

$$[u,v] = u_{xx}v_{yy} + u_{yy}v_{xx} - 2u_{xy}v_{xy}. \tag{5.2.3}$$

The principal state space for cantilevered plate displacement that we will utilize and takes into account the clamped conditions is given by:

$$H^2_* = \left\{ u \in H^2(\Omega) : u = u_x = 0 \quad \text{on } \Gamma_W \right\}.$$

In the upcoming proofs, we will make use of the space $V = H^2_* \times L^2$. In addition, we equip H^2_* with the inner product:

$$(u,v)_{H^2_*} := a(u,v) = \int_\Omega (\Delta u \Delta v - (1-\nu)[u,v])\, dx, \quad u,v \in H^2_*, \tag{5.2.4}$$

where $\nu \in (0,1)$ and $[\cdot,\cdot]$ is the von Karman bracket defined in (5.2.3).

This bilinear form $a(u,v)$ introduced above can be equivalently written as [16]:

$$a(u,v) = \int_\Omega \left(\nu \Delta u \Delta v + (1-\nu)\left(u_{xx}v_{xx} + 2u_{xy}v_{xy} + u_{yy}v_{yy}\right)\right) dx, \quad u,v \in H^2_*.$$

We will use these two expressions interchangeably throughout this chapter. The above product induces a norm $||u||_{H^2_*}$ which we will utilize for the remainder of this chapter.

Corollary 5.2.1. *The $||u||_{H^2_*}$ norm is equivalent to the usual Sobolev norm $||u||_2$.*

Proof. It is straightforward to see that $||u||_{H^2_*} \leq \alpha ||u||_2$, for some $\alpha > 0$.

On the other hand, to form the lower bound that is necessary for proving the equivalency, we need to employ Poincare's inequality. Specifically, we know that the function vanishes on the clamped portion of the boundary and that $\nabla u = 0$ ($u_x = 0$ from boundary conditions and $u_y = 0$ since u is zero on Γ_w). By applying Poincare twice (both for u and ∇u), we know that the inequalities $|u| \lesssim |u|_1 \lesssim |u|_2$ hold. Hence,

$$||u||^2_{H^2_*} = \int_\Omega \left(\nu \Delta^2 u + (1-\nu)\left(u^2_{xx} + 2u^2_{xy} + u^2_{yy}\right)\right) dx \geq C|u|^2_2 \geq \beta ||u||^2_2,$$

for $\beta > 0$. $\square$

5.3 The Semigroup Argument

In this section we aim to develop a rigorous argument that will tackle the semigroup well-posedness for the linear cantilevered plate defined on a rectangle.

5.3.1 Theorems and Definitions

To achieve this, we utilize the standard semigroup theory and employ the Lumer–Phillips theorem. Before we proceed with the details of the argument, let us recall the following definitions [45] and theorem [64]. For what follows, X defines a Hilbert space.

Definition 5. *(C_0 semigroup of contractions) A semigroup $T(t)$, $0 \leq t < \infty$, of bounded linear operators on X is called a C_0 semigroup of bounded linear operators if*

$$\lim_{t \downarrow 0} T(t)x = x, \quad \forall x \in X.$$

If, in addition, $||T(t)|| \leq 1$, for $t \geq 0$, then the semigroup is called a C_0 semigroup of contractions.

Definition 6. *(Generator of a Semigroup) A linear operator A whose domain $D(A)$ is defined by:*

$$D(A) = \left\{ x \in X : \lim_{t \downarrow 0} \frac{T(t)x - x}{t} \quad \textit{exists} \right\},$$

and for all $x \in D(A)$

$$Ax = \lim_{t \downarrow 0} \frac{T(t)x - x}{t},$$

is called the infinitesimal generator of a semigroup $T(t)$.

Definition 7. *(Dissipativity) A linear operator A in X is called dissipative if $(Au, u) \leq 0$ for all u in $D(A)$.*

Theorem 5.3.1. *(Lumer–Phillips) Let A be a linear operator in X. If A is dissipative and there is a $\lambda > 0$ such that the range $R(\lambda I - A)$ is X, then A is the infinitesimal generator of a C_0 semigroup of contractions in X.*

The range requirement of this theorem will be referred to as the *maximality* condition, i.e. the operator A is called maximal if the range condition is satisfied.

5.3.2 Application of Lumer–Phillips

5.3.2.1 Semigroup Setup

The first step towards showing the existence of a semigroup is to rewrite (5.2.2) in the operator format. Taking $\mathbf{w}(t) = (w(t), w_t(t))^T$, we have:

$$\begin{cases} \frac{d}{dt}\mathbf{w}(t) + \mathbb{A}\mathbf{w}(t) = (0, f)^T \\ \\ \mathbf{w}(0) = \mathbf{w}_0 \equiv (w_0, w_1)^T. \end{cases} \tag{5.3.1}$$

Here $\mathbb{A} : D(\mathbb{A}) \subset V \to V$, where $V = H^2_* \times L^2$, is the operator that is defined as follows:

$$\mathbb{A}u = \begin{pmatrix} 0 & -I \\ A & 0 \end{pmatrix} u, \qquad \text{with } u \in D(\mathbb{A}) \equiv D(A) \times H^2_*.$$

5.3.2.2 Characterization of the Domain

We shall define the operator A that appears above. It is clear that the *action* of this operator should coincide with that of the biharmonic operator, i.e. $Au = \Delta^2 u$ for $u \in D(A)$. In the case of a domain where the portions of the boundary that correspond to the clamped and free conditions are disjoint, standard elliptic regularity argument can be used to show that the domain of the operator A consists of all functions $u \in H^4(\Omega) \cap H^2_*$ that in addition satisfy the second and third order boundary conditions [16].

In our case, the theory of elliptic regularity is subtle, which precludes the proof from proceeding in the standard manner. Hence, we will define the domain of A in a way that will accommodate for the challenge of interpreting the second and third boundary conditions through the standard application of the trace theorem. To achieve this, and in line with the analysis in [?], our definition for the domain will include trace terms on each individual edge of the boundary.

That being said, let P be the set of corners of the rectangle Ω and let Γ_j, $j \in \{N, S, E, W\}$ denote the disjoint, relatively open, and connected edges of $\Gamma \backslash P$. In addition, we introduce the spaces $\tilde{H}^{1/2}(I)$ and $\tilde{H}^{3/2}(I)$, I being an interval in $\mathbb{R}$, that define the restriction of functions $u \in \tilde{H}^{1/2}(\mathbb{R})$ (or $u \in \tilde{H}^{3/2}(\mathbb{R})$ respectively) that have their support in $\bar{I}$.

Let $J \equiv \{N, S, E\}$. By writing $\langle \cdot, \cdot \rangle_{\frac{1}{2},j}$ we denote the duality pairing between $(\tilde{H}^{1/2}(\Gamma_j))'$ and $\tilde{H}^{1/2}(\Gamma_j)$, with $j \in J$ (or $\langle \cdot, \cdot \rangle_{\frac{3}{2},j}$ for the corresponding duality pairing for $\tilde{H}^{3/2}(\Gamma_j)$).

Utilizing the above we now proceed to define the domain of A as follows:

$$\mathcal{D}(A) = \{u \in H^2_* : \Delta^2 u \in L^2 \text{ and } T_1^j u = 0 \text{ on } (\tilde{H}^{3/2}(\Gamma_j))',\ T_2^j u = 0 \text{ on } (\tilde{H}^{1/2}(\Gamma_j))',\ \ \forall j \in J\}. \tag{5.3.2}$$

T_1^j and T_2^j correspond to the continuous operators that can act on elements in $\mathcal{U} = \{u \in H^2_* \text{ such that } \Delta^2 u \in L^2\}$. They are the extensions of the second and third order boundary conditions as given in (5.2.2) (in the sense of duality of these trace spaces).

With the above definition in hand, let us see how the Lumer–Phillips argument unfolds.

5.3.2.3 Dissipativity

Corollary 5.3.2. *The operator $\mathbb{A}$ is dissipative.*

Proof. Let $\mathbf{w} = (u, v) \in D(\mathbb{A})$. We need to show that $(\mathbb{A}\mathbf{w}, \mathbf{w}) \leq 0$. Using [[16], Proposition 1.3.2, p.27] we can show that for $u \in D(A)$ and $v \in H^2_*$ we have that:

$$\int_\Omega (\Delta^2 u) v dx = a(u, v),$$

where $a(u, v)$ is given by (5.2.4). We note here that integration by parts holds in the sense of (5.3.2) and it is justified on the domain [4, 36].

Thus, for the dissipativity argument we obtain:

$$(\mathbb{A}\mathbf{w}, \mathbf{w})_V = -(u, v)_{H^2_*} + (\Delta^2 u, v) = -a(u, v) + a(u, v) = 0,$$

which concludes the proof. □

5.3.2.4 Maximality

For this part we need to show that there exists $\lambda > 0$ such that $\mathbb{R}(\lambda I - \mathbb{A}) = V$, where $\mathbb{R}(\cdot)$ denotes the range of $\lambda I - \mathbb{A}$. To that end, let $\mathbf{h} = (h_1, h_2) \in V$. We need to show that there exists $\mathbf{w} = (u, v) \in D(\mathbb{A})$ such that $(\lambda I - \mathbb{A})\mathbf{w} = \mathbf{h}$.

This is equivalent to finding $u \in D(A)$ and $v \in H^2_*$ such that:

$$\begin{cases} \lambda u + v = h_1 \\ -\Delta^2 u + \lambda v = h_2. \end{cases} \tag{5.3.3}$$

Subtracting these two equations we obtain:

$$\Delta^2 u + \lambda^2 u = \lambda h_1 - h_2 \equiv f \in L^2(\Omega). \tag{5.3.4}$$

For this problem we will introduce the associated weak formulation, use Lax–Milgram to show that there exists a weak solution, and then attempt to show that the weak solution is in fact in the domain of A.

To that end, let $a_w : H^2_* \times H^2_* \to \mathbb{R}$ with $a_w(p, v) = a(p, v) + \lambda^2(p, v)$ and $f : H^2_* \to \mathbb{R}$. The weak formulation associated to (5.3.4) reads:

$$a_w(p, v) = (f, v), \qquad \forall v \in H^2_*. \tag{5.3.5}$$

Corollary 5.3.3. *The problem* (5.3.5) *has a unique solution* $u \in H^2_*$*.*

Proof. Utilizing Lax–Milgram, to establish the existence of a weak solution we need to show that $a_w(p, v)$ is a continuous and coercive form on H^2_*. In addition, we need to show that the RHS, $f(v)$, is a continuous functional on the same space. The latter can be shown in a standard manner and thus omitted from the proof.

Let $p, v \in H^2_*$. We commence by showing that a_w is continuous. Using Cauchy–

Schwarz inequality we have:

$$|a_w(p,v)| \lesssim ||\Delta p||\ ||\Delta v|| + ||p_{xx}||\ ||v_{yy}|| + ||p_{yy}||\ ||v_{xx}|| + ||p_{xy}||\ ||v_{xy}|| \lesssim ||p||_2\ ||v||_2$$

$$\lesssim ||p||_{H^2_*}\ ||v||_{H^2_*},$$

where we used the norm equivalency from Corollary 5.2.1 for the last step.

In addition, a_w is also coercive since:

$$a_w(p,p) = a(p,p) + \lambda^2||p||^2 \geq a(p,p) = ||p||^2_{H^2_*}.$$

Thus, application of Lax–Milgram yields the existence of a (weak) solution $u \in H^2_*$. □

The next step towards showing that $u \in D(A)$ is to show that $\Delta^2 u \in L^2$. In the previous argument we have shown that there exists $u \in H^2_*$ that satisfies (5.3.5) for every $v \in H^2_*$. This implies that the same equality will hold for all $\phi \in C_0^\infty$, i.e.:

$$a_w(u,\phi) = (f,\phi), \qquad \forall \phi \in C_0^\infty.$$

Undoing the integration by parts, utilizing the fact that boundary terms do not appear, and moving terms to the right hand side, we obtain:

$$\langle \Delta^2 u, \phi \rangle = (f - \lambda^2 u, \phi),$$

where $< \cdot, \cdot >$ stands for the duality pairing in distributions.

Now, it is true that the set of C_0^∞ functions is dense in L^2 and thus the above equality holds for $\phi \in L^2$. In addition $f - \lambda^2 u$ is also an L^2 function. This means that we can identify the action of $\Delta^2 u$ against ϕ in the duality pairing as integration of an L^2 function against ϕ. Thus, we can conclude that $\Delta^2 u \in L^2$.

We know from [35] that for $f \in L^2$ elliptic regularity is applicable away from the corners. That being said, we know that $u \in H^4(\Omega \setminus V)$, for any neighborhood V of the rectangle's corners. But since a uniform regularity for this system cannot be guaranteed, the interpretation of the free boundary conditions classically through the trace theorem [45] is not possible. Hence we have to define a *generalized* meaning for these conditions.

According to [4, 36], there exist continuous operators $\mathbf{T}^j = (T_1^j, T_2^j)$ such that the Green's formula holds, and upon application yields:

$$\sum_{j \in J} \langle T_1^j u, \gamma_0 v \rangle_{\frac{3}{2}, j} + \langle T_2^j u, \gamma_1 v \rangle_{\frac{1}{2}, j} = 0, \quad \forall v \in H_*^2. \tag{5.3.6}$$

The operator $\mathbf{T}^j$ here maps $\mathcal{U} = \{u \in H_*^2 \text{ such that } \Delta^2 u \in L^2\}$ into the space $\mathcal{H} = (\tilde{H}^{3/2}(\Gamma_j))' \times (\tilde{H}^{1/2}(\Gamma_j))'$ for all $j \in J$. In addition, $\gamma_0 v$ and $\gamma_1 v$ denote the zeroth and first order trace mappings respectively.

Now, choosing functions $v \in H_*^2 \cap H_0^1$, equation (5.3.6) yields:

$$\sum_{j \in J} \langle T_2^j u, \gamma_1 v \rangle_{\frac{1}{2}, j} = 0, \quad \forall v \in H_*^2 \cap H_0^1. \tag{5.3.7}$$

We need to show that $T_2^j u = 0$ on $(\tilde{H}^{1/2}(\Gamma_j))'$ for every $j \in J$. This translates to proving that

$$\langle T_2^j u, \phi \rangle_{\frac{1}{2},j} = 0, \quad \forall \phi \in \tilde{H}^{1/2}(\Gamma_j).$$

Let's see why this holds. From [20] and [[36], Theorem 1.4.2] we know that the surjectivity of the trace theorem holds along each individual edge. Thus, for a given $\phi \in \tilde{H}^{1/2}(\Gamma_j)$ we can find an element $v \in H_*^2 \cap H_0^1$ such that $\gamma_1 v = \phi$ on Γ_j and $\gamma_1 v = 0$ on Γ_i for all $i \neq j$. Using this fact in (5.3.7) and repeating the argument for each $j \in J$, we deduce that $T_2^j = 0$ on $(\tilde{H}^{1/2}(\Gamma_j))'$ for all $j \in J$.

With this in hand, we can revisit (5.3.6) which now reads:

$$\sum_{j \in J} \langle T_1^j u, \gamma_0 v \rangle_{\frac{3}{2},j} = 0, \quad \forall v \in H_*^2.$$

Repeating the same argument as above, we consider a $\phi \in \tilde{H}^{3/2}(\Gamma_j)$. Then there exists an element $v \in H_*^2$ such that $\gamma_0 v = \phi$ on Γ_j and $\gamma_0 v = 0$ on Γ_i for all $i \neq j$. Thus, $T_1^j = 0$ on $(\tilde{H}^{3/2}(\Gamma_j))'$ for all $j \in J$.

Remark 5.3.1. We note that the above steps are only valid on each individual edge of the rectangle. Even though it is desirable, one should not expect a global application of the trace theorem [36].

Thus, we have shown that $u \in D(A)$ and from (5.3.3) it follows that $v \in H_*^2$. This concludes the maximality argument.

Chapter 6: Semigroup Generation for A Linear 2D Flow-Cantilever System

6.1 Summary of the Chapter

In this chapter we present the model that corresponds to the coupling of a cantilevered beam with a potential flow that has mixed boundary conditions of the *Kutta–Joukowsky* type and we go through the characterization of the domain of the associated operator.

6.2 Introduction

This chapter focuses on the study of the oscillations of a thin elastic cantilevered beam interacting with an inviscid potential flow in which it is immersed. Flow-structure interactions of elastic beams and plates have been a point of interest in the literature (see for example [17] and references therein), as many models have been suggested to accommodate various configurations and physical parameters. In this treatment we are concerned with analyzing the effect (from an infinite dimensional point of view) of the so called *Kutta–Joukowsky conditions* (KJC) in a flow-cantilevered model.

Preliminary investigations indicate that free beam and plate boundary conditions may better accommodate the KJC—this is in line with certain engineering applications (e.g. flag type models [19,34]). The KJC is stated in [5,7] as taking "a zero pressure jump off the wing and at the trailing edge"; which for our model, in line with the analyses in [5,7], this corresponds to taking the *acceleration potential* of the flow to be zero outside the beam.

Previous analyses on this topic include a more straightforward (Neumann type) flow boundary condition that is taken in the plane of the plate, in line with a standard *panel* configuration. In addition, the work of [54] deals with the mathematical framework and the PDE analysis of a *clamped plate* with the KJC. Nevertheless, since our interest focuses on the cantilevered configuration (of beams and plates), the aim for this work is to establish a semigroup well-posedness results that accommodate the Kutta–Joukowsky flow conditions. In this chapter, we introduce the model of interest and we make some remarks that, in future work, will facilitate the use Lumer–Phillips theorem to show that the that the *dissipative* part of this model is m-dissipative on the state space.

6.2.1 The Model of Interest

Consider a linear potential flow defined on $\mathbb{R}^2_+ \equiv \{z > 0\}$ (with $\partial\mathbb{R}^2_+ \equiv \{z = 0\}$) of magnitude $0 \leq U$ in the positive x direction. (The flow field about which we linearize Euler's equation is $\mathbf{U} = \langle U, 0\rangle$ to produce our linear flow equation.) We take this to represent an over-body flow for an elastic beam residing on $x \in (0, L)$.

We consider $x = 0$ to be the *leading edge* of the beam, with $x = L$ the *trailing edge*. We assume the beam is clamped at the leading edge, and we extend *upstream* with an inactive solid for $x \in (-\infty, 0)$. The *wake* is given as a subset of $\{z = 0\}$, with $x \in (L, \infty)$, extending from the trailing edge.

Assuming the flow is inviscid, irrotational, and compressible, we let $\phi(x, z, t)$ represent the flow's velocity potential, defined on $\mathbb{R}^2_+$. The boundary condition on the surface of the elastic beam is given through a velocity matching condition (impereability), which takes into account the Eulerian to Lagrangian variable change [12, 24]. In the context of potential flow, this translates to a dynamic Neumann condition representing the coupling for the flow. Upstream we take a zero normal velocity component against the inactive portion $x \in (-\infty, 0)$. Downstream, away from the trailing edge, we invoke the KJC extending in the wake. (This is a dynamic, mixed-type boundary condition [54, 67].)

6.2.1.1 Beam Equation

Let $\Omega = \{(x, z) : x \in [0, L],\ z = 0\} \subset \mathbb{R}^2$ and consider the scalar function $w(x, t)$ to represent the transverse displacement of the plate in the z-direction at the point x at the moment t. We take the Euler–Bernoulli cantilevered beam:

$$\begin{cases} w_{tt} + D\partial_x^4 w = p(x,t) & \text{in } \Omega \times (0,T), \\ w = w_x = 0 & \text{on } \{x = 0\} \times (0,T), \\ w_{xx} = w_{xxx} = 0 & \text{on } \{x = L\} \times (0,T), \end{cases} \tag{6.2.1}$$

where D corresponds to the constant stiffness. The coupling with the flow takes place in the external pressure term $p(x,t)$ acting on the beam via the *acceleration potential* of the flow.

6.2.1.2 Flow Equation

For the flow we make use of linearized potential theory, and [10, 12, 23] the (perturbed) flow potential $\phi : \mathbb{R}^2_+ \to \mathbb{R}$ must satisfy the perturbed wave equation below:

$$\begin{cases} (\partial_t + U\partial_x)^2\phi = \Delta_{x,z}\phi - \mu\phi & \text{in } \mathbb{R}^2_+ \times (0,T), \\ \phi(0) = \phi_0; \quad \phi_t(0) = \phi_1, & \\ \partial_z\phi = d(x,t) & \text{on } \Omega \times (0,T), \end{cases} \tag{6.2.2}$$

where $\mu > 0$ is a constant. For the remainder of this chapter we will refer to the RHS of the flow equation as $\Delta_\mu\phi$, i.e. $\Delta_\mu\phi = \Delta_{x,z}\phi - \mu\phi$. Additionally, without loss of generality, the density of the perturbed airflow is assumed to be equal to 1. We will be utilizing the *acceleration potential* $\psi \equiv \phi_t + U\phi_x$ as a state variable in what follows.

6.2.1.3 Coupling

The strong coupling in the model takes place in the downwash term of the flow potential by taking

$$d(x,t) = \left[(\partial_t + U\partial_x)u(x)\right]$$

for $x \in \Omega$. On $\mathbb{R}\backslash\Omega$ we implement the so called *Kutta–Joukowski continuity condition* [5, 7, 19]:

$$\gamma[\phi_t + U\phi_x] = \gamma[\psi] = 0, \quad x \in \mathbb{R}\backslash\Omega. \tag{6.2.3}$$

The aerodynamical pressure on the surface of the beam is of the form

$$p(x,t) = \gamma[\psi] \tag{6.2.4}$$

in (6.2.1) above. This gives the fully coupled model:

$$\begin{cases} (\partial_t + U\partial_x)^2\phi = \Delta_\mu \phi & \text{in } \mathbb{R}^2_+ \times (0,T), \\ \partial_z \phi = \begin{cases} 0 & \text{on } (-\infty,0)\times(0,T) \\ (\partial_t + U\partial_x)w & \text{on } (0,L)\times(0,T) \end{cases}, & \\ (\partial_t + U\partial_x)\phi = 0 & \text{on } (L,\infty)\times(0,T) \\ \phi(0) = \phi_0; \quad \phi_t(0) = \phi_1, & \\ w_{tt} + D\partial_x^4 w = r_{(0,L)}\gamma[\phi_t + U\phi_x] & \text{in } \Omega \times (0,T), \\ w = w_x = 0 & \text{on } \{x=0\}\times(0,T), \\ w_{xx} = w_{xxx} = 0 & \text{on } \{x=L\}\times(0,T), \\ w(0) = w_0; \quad w_t(0) = w_1. & \end{cases} \tag{6.2.5}$$

6.2.2 Notation

For the remainder of the chapter norms $||\cdot||$ are taken to be $L_2(D)$ for the domain dictated by context. Inner products in $L_2(\mathbb{R}^2_+)$ are written $(\cdot,\cdot)$, while inner products in $L_2(\mathbb{R} \equiv \mathbb{R}^2_+)$ are written $\langle\cdot,\cdot\rangle$. Also, $H^s(D)$ will denote the Sobolev space of order s, defined on a domain D, and $H^s_0(D)$ denotes the closure of $C^\infty_0(D)$ in the $H^s(D)$ norm which we denote by $\|\cdot\|_{H^s(D)}$ or $\|\cdot\|_{s,D}$. We make use of the standard notation for the trace of functions defined on $\mathbb{R}^2_+$, i.e. for $\phi \in H^1(\mathbb{R}^2_+)$, $\gamma[\phi] = \phi\Big|_{z=0}$ is the trace of ϕ on $\mathbb{R}$. In addition, we define $H^2_*(0,L) \equiv \{w \in H^2(0,L) \ : \ w(x = 0) = w_x(x=0) = 0\}$.

6.3 The Construction of the Argument

Motivated by previous analysis of a similar setup that appears in [17, 54], we decompose the dynamics into a dissipative piece $\mathbf{A}$ (with $\sigma = 0$ below) and a perturbation piece (with $\sigma = 1$ below):

$$\begin{cases} (\partial_t + U\partial_x)^2\phi = \Delta_\mu \phi & \text{in } \mathbb{R}^2_+ \times (0,T), \\ \partial_z \phi = \begin{cases} 0 & \text{on } (-\infty, 0) \times (0,T) \\ w_t + \sigma U w_x & \text{on } (0,L) \times (0,T) \end{cases} & \\ (\partial_t + U\partial_x)\phi = 0 & \text{on } (L,\infty) \times (0,T) \\ w_{tt} + D\partial_x^4 w = r_{(0,L)}\gamma[\phi_t + U\phi_x] & \text{in } \Omega \times (0,T), \\ w(x=0) = w_x(x=0) = 0, \quad w_{xx}(x=L) = w_{xxx}(x=L) = 0 & \end{cases} \tag{6.3.1}$$

We consider the dynamic states (ϕ, ψ, w, w_t), where $\psi = \phi_t + U\phi_x$ is the so called *acceleration potential* of the flow. Utilizing ψ and w_t as multipliers, we arrive the following (formal) energies, obtained via Green's Theorem applied to (6.3.1):

$$E_b(t) = \frac{1}{2}\Big(||w_t||^2 + D||w_{xx}||^2\Big), \quad E_f(t) = \frac{1}{2}\Big(||\psi||^2 + ||\nabla_{x,z}\phi||^2 + \mu||\phi||^2\Big), \tag{6.3.2}$$

and $\mathcal{E}(t) = E_b(t) + E_f(t)$. These energies provide the formal energy balance for the system (implementing the KJC)

$$\mathcal{E}(t) + \sigma U \int_0^t \langle w_x, \gamma[\psi]\rangle_{(0,L)} dt = \mathcal{E}(0). \tag{6.3.3}$$

This energy relation provides motivations for viewing the dynamics as the sum of a generating piece and a 'perturbation'.

6.3.1 The Argument for the Dissipative Part

In this part we consider (6.3.1) with $\sigma = 0$. To begin with, let us first define the operator $\mathcal{A}$ with $\mathcal{A}u = \partial_x^4 u \; \forall u \in \mathcal{D}(\mathcal{A})$ and $\mathcal{D}(\mathcal{A}) = \{w \in H^4(0,L) : w(0) = w_x(0) = 0;\; w_{xx}(L) = w_{xxx}(L) = 0\}$. From this we have in a standard fashion [53] that $\mathcal{D}(\mathcal{A}^{1/2}) = H_*^2$. In addition, to set up the model in a dynamical systems framework, we introduce the principal state space:

$$Y = Y_f \times Y_b \equiv \Big(H^1(\mathbb{R}_+^2) \times L^2(\mathbb{R}_+^2)\Big) \times \Big(H_*^2(0,L) \times L^2(0,L)\Big),$$

where the choice of norm on $H^1(\mathbb{R}_+^2)$ encodes the $\mu > 0$ parameter, i.e.:

$$||(\phi,\psi)||_{Y_f}^2 \equiv ||\nabla_{x,z}\phi||_{0,\mathbb{R}_+^2}^2 + \mu||\phi||_{0,\mathbb{R}_+^2}^2 + ||\psi||_{0,\mathbb{R}_+^2}^2.$$

From the semigroup point of view, we consider the state $y = (\phi,\psi; w, w_t) \in Y$. Then we. define the dynamics operator $\mathbf{A} : \mathscr{D}(\mathbf{A}) \subset Y \to Y$ by

$$\mathbf{A}\begin{pmatrix} \phi \\ \psi \\ w \\ v \end{pmatrix} = \begin{pmatrix} -U\partial_x\phi + \psi \\ -U\partial_x\psi + \Delta_\mu\phi \\ v \\ -\mathcal{A}w + \gamma[\psi] \end{pmatrix} \tag{6.3.4}$$

with $\mathscr{D}(\mathbf{A})$ given by

$$\mathscr{D}(\mathbf{A}) \equiv \left\{ y = \begin{pmatrix} \phi \\ \psi \\ w \\ v \end{pmatrix} \in Y \;\middle|\; \begin{array}{l} -U\partial_x \phi + \psi \in H^1(\mathbb{R}^2_+), \\ -U\partial_x \psi + \Delta_\mu \phi \in L^2(\mathbb{R}^2_+), \\ \psi = 0 \text{ on } \mathbb{R}\backslash\Omega, \quad \partial_\nu \phi = -v, \text{ in } \Omega \\ v \in \mathscr{D}(\mathcal{A}^{1/2}) = H^2_*(0,L), \\ -\mathcal{A}w + \gamma[\psi] \in L^2(0,L) \end{array} \right\} \tag{6.3.5}$$

The operator $\mathbf{A}$ will be the foundation of our abstract setup, and ultimately the dynamics of the evolution in (6.3.1) can be represented through $\mathbf{A}$ and a perturbation $Py = (0, 0; U^2 u_{xx}, 0)$.

To proceed with the analysis of semigroup generation, we must characterize the domain to obtain appropriate regularity for ϕ through elliptic regularity of the mixed problem. As we are in the subsonic case, $U < 1$, the description in the domain corresponds a strongly elliptic problem. To that end, let us take $(f_1, f_2; g_1, g_2) \in Y$, and consider:

$$-U\phi_x + \psi = f_1 \in H^1(\mathbb{R}^2_+) \tag{6.3.6}$$

$$-U\psi_x + \Delta_\mu \phi = f_2 \in L^2(\mathbb{R}^2_+) \tag{6.3.7}$$

$$v = g_1 \in \mathscr{D}(\mathcal{A}^{1/2}) \tag{6.3.8}$$

$$-\mathcal{A}w + \gamma[\psi] = g_2 \in L^2(\Omega), \tag{6.3.9}$$

with boundary conditions:

$$\begin{cases} \partial_\nu \phi = -v \\ \\ \psi = 0 \text{ in } \ \mathbb{R} \backslash \overline{\Omega}. \end{cases} \tag{6.3.10}$$

Using the first relation for f_1 and the last condition, we obtain the identity

$$U\phi_x = -f_1 \in H^{1/2}(\mathbb{R} \setminus \overline{\Omega})$$

via the trace theorem.

Let us read off some implications of domain membership:

- First, from the conditions with f_1 and f_2, we have $\Delta_U \phi \equiv \Delta_\mu \phi - U^2 \partial_x^2 \phi \in L^2(\mathbb{R}^2_+)$.

- To invoke the KJC, take the trace of the f_1 condition (valid in $H^1(\mathbb{R}^2_+)$) to obtain

$$\phi_x = \frac{1}{U}\Big[\psi - f_1\Big] \in H^{1/2}(\mathbb{R}).$$

Restricting to $\mathbb{R}\backslash\overline{\Omega}$, and invoking that $\psi \equiv 0$ here, we obtain: $\phi_x \in H^{1/2}(\mathbb{R}\backslash\overline{\Omega})$.

At this stage we must invoke two elliptic problems to obtain additional information for the regularity of the state functions. To that end, let $\tilde{\phi} = \phi_x$. We differentiate equation (6.3.6) twice in space and (6.3.7) once in space, combine them, and differentiate in x the first boundary condition appearing in (6.3.10). This yields the elliptic problem:

$$\begin{cases} \Delta_U \tilde{\phi} = f_{2,x} + U f_{1,xx} \in H^{-1}(\mathbb{R}^2_+) \\ \partial_\nu \tilde{\phi} = -g_{1,x} \in H^1(\Omega) \\ \tilde{\phi} = -\frac{1}{U} f_1 \in H^{1/2}(\mathbb{R}\backslash\Omega) \end{cases} \tag{6.3.11}$$

Using Lax–Milgram we can show that the problem above has sufficient regularity of the data to obtain a variational solution $\tilde{\phi} = \phi_x \in H^1(\mathbb{R}^2_+)$. With this information in hand we can return to (6.3.6) to conclude that $\psi \in H^1(\mathbb{R}^2_+)$. Moreover, (6.3.7) yields that $\Delta_\mu \phi \in L^2(\mathbb{R}^2_+)$, and since $\phi \in H^1(\mathbb{R}^2_+)$, we have that $\Delta\phi \in L^2(\mathbb{R}^2_+)$.

We proceed to read off the domain criteria:

- Since $\psi \in H^1(\mathbb{R}^2_+)$, we have $\gamma[\psi] \in H^{1/2}(\mathbb{R}) \subset L^2(\mathbb{R})$. Restricting this to Ω we have $r_{(0,L)}\gamma[\psi] \in L^2(\Omega)$.

- Using the result above, $r_{(0,L)}\gamma[\psi] \in L^2(\Omega)$, we can deduce from (6.3.9) that $-\mathcal{A}w \in L^2(\Omega)$.

- Returning to the v equation with g_1, we have $g_1 \in H^2_*(\Omega)$ and $-U\partial_x w \in H^3(\Omega)$, and thus we conclude that $v \in H^2(\Omega) \cap H^1_*(\Omega)$.

A.1 Appendix-Bounding potential energy

In this appendix we note that the beam's nonlinear potential energy associated to the nonlinear stiffness term introduced in Chapter 1 has the so called epsilon boundedness property. This property (as will be described in the lemma) is a "good" property for the potential energy of beams and plates when considering long time behavior of dynamics. It is observed for von Karman and Berger plates, and for the extensible Krieger–type nonlinear beam. We demonstrate that it holds for the inextensible beam potential energy.

Lemma A.1.1. *The functional*

$$\Psi(u; A, \delta) = ||u||_2^2 + ||u_x u_{xx}||^2 - A||u||_{2-\delta}^2$$

is bounded from below on $H^2_*(\Omega)$ for any $A > 0$ and $\delta \in (0, 2]$.

Proof. Let $\Psi(u; A, \delta) = ||u||_2^2 + ||u_x u_{xx}||^2 - A||u||_{2-\delta}^2$ with $A > 0$ and $\delta \in (0, 2]$ and let us assume that Ψ is *not* bounded from bellow. Then, there exists a sequence $\{u_n\}$ in $H^2_*(\Omega)$ such that:

$$M_n \equiv \Psi(u_n; A, \delta) \to -\infty \text{ as } n \to \infty.$$

Without loss of generality, we assume that $M_n < 0$ for all n. Then, since by our assumption $M_n \to -\infty$, we can conclude that $||u_n||_{2-\delta} \to \infty$. Define now

$w_n = u_n/||u_n||_{2-\delta}$. Then, we have $||w_n||_{2-\delta} = 1$ and:

$$||u_n||_{2-\delta}^2\left(||w_n||_2^2 + \frac{||u_x^n u_{xx}^n||^2}{||u_n||_{2-\delta}^2} - A\right) = M_n.$$

Or equivalently,

$$||w_n||_2^2 + ||u_n||_{2-\delta}^2||w_x^n w_{xx}^n||^2 = A + \frac{M_n}{||u_n||_{2-\delta}^2} < A. \tag{A.1.1}$$

This implies that $\{w_n\}$ is a bounded sequence in H_*^2 and by Banach–Alaoglu theorem there exists a weakly convergent subsequence $\{w_{n_k}\}$ such that

$$w_{n_k} \rightharpoonup w \text{ in } H_*^2(\Omega), \quad \text{ for some } w \in H_*^2(\Omega). \tag{A.1.2}$$

By the compactness of Sobolev embeddings, we can deduce that

$$w_{n_k} \to w \text{ strongly in } H^{2-\epsilon}(\Omega), \quad \text{ for any } \epsilon > 0. \tag{A.1.3}$$

In addition, since we know that $||u_n||_{2-\delta} \to \infty$ we can also show from (A.1.1) that:

$$||w_x^{n_k} w_{xx}^{n_k}||^2 \leq \frac{A}{||u_n||_{2-\delta}^2} \to 0 \text{ as } n \to \infty. \tag{A.1.4}$$

Our goal is to show that $\{w_x^{n_k} w_{xx}^{n_k}\}$ converges to $w_x w_{xx}$ in $L^1(\Omega)$, which would imply by (A.1.4) and uniqueness of limits that $w_x w_{xx} = 0$. Thus, let us consider the following difference which after adding and subtracting appropriate terms yields:

$$||w_x^{n_k} w_{xx}^{n_k} - w_x w_{xx}||_{L^1(\Omega)} \leq ||w_{xx}^{n_k}(w_x^{n_k} - w_x)||_{L^1(\Omega)} + ||w_x(w_{xx}^{n_k} - w_{xx})||_{L^1(\Omega)}. \tag{A.1.5}$$

For the first term that appears in the RHS of (A.1.5) we have:

$$||w_{xx}^{n_k}(w_x^{n_k} - w_x)||_{L^1(\Omega)} \leq ||w_{xx}^{n_k}||_{L^2(\Omega)} ||w_x^{n_k} - w_x||_{L^2(\Omega)}.$$

Since $||w_{xx}^{n_k}||_{L^2(\Omega)}$ is bounded for all n_k and $w^{n_k} \to w$ strongly in $H^{2-\epsilon}(\Omega)$, the above term goes to zero.

Additionally, since $w_{xx}^{n_k} \rightharpoonup w_{xx}$ in $L^2(\Omega)$ and $w_x \in L^2(\Omega)$, the definition of weak convergence yields:

$$||w_x(w_{xx}^{n_k} - w_{xx})||_{L^1(\Omega)} \to 0$$

Thus, we can now conclude $w_x w_{xx} = 0$, or equivalently $\partial_x(w_x^2) = 0$ almost everywhere (a.e.) in Ω. This implies that $w_x^2 =$ constant in Ω. But since $w \in H_*^2$, the first derivative vanishes on a portion of the boundary, and thus we conclude that $w_x = 0$ a.e. in Ω. Repeating the same argument, we can deduce that $w = 0$ a.e. in Ω.

Hence, from (A.1.2) and (A.1.3) we have $w^{n_k} \to 0$ strongly in $H^{2-\delta}$ which contradicts the fact $||w^{n_k}||_{2-\delta} = 1$ for all n_k. $\square$

Bibliography

[1] Antman, S.S., 2005. Nonlinear Problems of Elasticity, volume 107 of Applied Mathematical Sciences, Springer. New York.

[2] Argentina, M. and Mahadevan, L., 2005. Fluid-flow-induced flutter of a flag. Proceedings of the National Academy of Sciences, 102(6), pp.1829-1834.

[3] Ashley, H. and Zartarian, G, 1956. Piston theory: A new aerodynamic tool for the aeroelastician. *Journal of the Aeronautical Sciences*, 23(12), pp. 1109–1118.

[4] Aubin, J.P., 2007. *Approximation of elliptic boundary-value problems*. Courier Corporation.

[5] Balakrishnan A.V., *Aeroelasticity—Continuum Theory*, Springer-Verlag, 2012.

[6] Ball, J.M., 1973. Initial-boundary value problems for an extensible beam. *Journal of Mathematical Analysis and Applications*, 42(1), pp.61–90.

[7] Balakrishnan, A.V., 2007. Nonlinear Aeroelasticity Theory: Continuum Models. *Contemporary Mathematics*, 426, pp.79-102.

[8] Bassily, S.F. and Dickinson, S.M., 1975. On the use of beam functions for problems of plates involving free edges. *Transactions of the ASME*, 1975, pp.858–864.

[9] Berger, H., 1955. A New Approach to the Analysis of Large Deflections of Plates. *Journal of Applied Mechanics*, 22, 1955, pp.465–472.

[10] Bisplinghoff, R.L. and Ashley, H., 2013. *Principles of aeroelasticity*. Courier Corporation.

[11] Blevins, R.D., 2015. *Formulas for dynamics, acoustics and vibration.* John Wiley & Sons.

[12] Bolotin, V.V., 1963. *Nonconservative problems of the theory of elastic stability.* Macmillan.

[13] Bonheure, D., Gazzola, F., Lasiecka, I. and Webster, J.T., 2020. Long-time dynamics of a hinged-free plate driven by a non-conservative force. *arXiv preprint arXiv:2007.01801.*

[14] Chen, S.P. and Triggiani, R., 1989. Proof of extensions of two conjectures on structural damping for elastic systems. *Pacific J. of Mathematics*, 136(1), pp.15-55.

[15] Chueshov, I., Dowell, E.H., Lasiecka, I. and Webster, J.T., 2016. Nonlinear Elastic Plate in a Flow of Gas: Recent Results and Conjectures. *Applied Mathematics & Optimization*, 73(3), pp.475-500.

[16] Chueshov, I. and Lasiecka, I., 2010. *Von Karman Evolution Equations: Well-posedness and Long Time Dynamics.* Springer Science & Business Media.

[17] Chueshov, I., Lasiecka, I. and Webster, J.T., 2013. Evolution semigroups in supersonic flow-plate interactions. Journal of Differential Equations, 254(4), pp.1741-1773.

[18] Ciarlet, P.G., 1997. *Mathematical Elasticity: Volume II: Theory of Plates.* Elsevier.

[19] Crighton, D.G., 1985. The Kutta condition in unsteady flow. *Annual Review of Fluid Mechanics*, 17(1), pp.411-445.

[20] De Coster, C., Nicaise, S. and Sweers, G., 2019. Comparing variational methods for the hinged Kirchhoff plate with corners. *Mathematische Nachrichten*, 292(12), pp.2574-2601.

[21] Deliyianni, M., Gudibanda, V., Howell, J. and Webster, J.T., 2020. Large deflections of inextensible cantilevers: modeling, theory, and simulation. *Mathematical Modelling of Natural Phenomena*, 15, p.44.

[22] Deliyianni, M. and Webster, J.T., 2021. Theory of Solutions for An Inextensible Cantilever. *Applied Mathematics & Optimization*, pp.1-55.

[23] Dowell, E., 2014. *A Modern Course in Aeroelasticity*, Springer.

[24] Dowell, E.H., 1974. *Aeroelasticity of plates and shells* (Vol. 1). Springer Science & Business Media.

[25] Dowell, E.H., Clark, R. and Cox, D., 2004. *A modern course in aeroelasticity* (Vol. 3). Dordrecht: Kluwer academic publishers.

[26] Dowell, E. and McHugh, K., 2016. Equations of motion for an inextensible beam undergoing large deflections.*J. of Applied Mechanics*, 83(5), p.051007.

[27] Dragomir, S.S., 2003. *Some Gronwall type inequalities and applications*. Nova Science.

[28] Dunnmon, J.A., Stanton, S.C., Mann, B.P. and Dowell, E.H., 2011. Power extraction from aeroelastic limit cycle oscillations. *J. of Fluids and Structures*, 27(8), pp.1182-1198.

[29] Duvant, G. and Lions, J.L., 2012. *Inequalities in mechanics and physics* (Vol. 219). Springer Science & Business Media.

[30] Eden, A. and Milani, A.J., 1993. Exponential attractors for extensible beam equations. *Nonlinearity*, 6(3), p.457.

[31] Erturk, A. and Inman, D.J., 2011.*Piezoelectric energy harvesting*. John Wiley & Sons.

[32] Evans, L.C., 2010.*Partial differential equations* (Vol. 19). American Mathematical Soc.

[33] Fabiano, R.H. and Hansen, S.W., 2001. Modeling and analysis of a three-layer damped sandwich beam. In *Conference Publications* (Vol. 2001, No. Special, p. 143). American Institute of Mathematical Sciences.

[34] Frederiks, W., Hilberink, H.C.J. and Sparenberg, J.A., 1986. On the Kutta condition for the flow along a semi-infinite elastic plate. *Journal of engineering mathematics*, 20(1), pp.27-50.

[35] Grisvard, P., 2011. *Elliptic problems in nonsmooth domains*. Society for Industrial and Applied Mathematics.

[36] Grisvard, P., 1992. *Singularities in boundary value problems* (Vol. 22). Springer Verlag.

[37] Han, S.M., Benaroya, H. and Wei, T., 1999. Dynamics of transversely vibrating beams using four engineering theories. Journal of Sound and vibration, 225(5), pp.935-988.

[38] Hodges, D.H. and Dowell, E.H., 1974. Nonlinear equations of motion for the elastic bending and torsion of twisted nonuniform rotor blades. *NASA Technical Note TN D-7818*.

[39] Howell, J., Huneycutt, K., Webster, J.T. and Wilder, S., 2019. (In)stability of a cantilevered piston-theoretic Beam, *Mathematics in Engineering*.

[40] Howell, J.S., Toundykov, D. and Webster, J.T., 2018. A Cantilevered Extensible Beam in Axial Flow: Semigroup Well-posedness and Postflutter Regimes.*SIAM J. on Mathematical Analysis*, 50(2), pp.2048-2085.

[41] Huang, L., 1995. Flutter of cantilevered plates in axial flow. *J. of Fluids and Structures*, 9(2), pp.127-147.

[42] Huang, L. and Zhang, C., 2013. Modal analysis of cantilever plate flutter. *Journal of Fluids and Structures*, 38, pp.273–289.

[43] Ignatova, M., Kukavica, I., Lasiecka, I. and Tuffaha, A., 2014. On well-posedness and small data global existence for an interface damped free boundary fluid-structure model. *Nonlinearity*, 27(3), p.467.

[44] Kaltenbacher, B., Kukavica, I., Lasiecka, I., Triggiani, R., Tuffaha, A. and Webster, J.T., 2018. *Mathematical Theory of Evolutionary Fluid-Flow Structure Interactions*. Springer International Publishing.

[45] Kesavan, S., 1989. *Topics in functional analysis and applications*. New Age International.

[46] Kim, D., Cossé, J., Cerdeira, C.H. and Gharib, M., 2013. Flapping dynamics of an inverted flag. Journal of Fluid Mechanics, 736.

[47] Koch, H. and Lasiecka, I., 2002. Hadamard well-posedness of weak solutions in nonlinear dynamic elasticity-full von Karman systems. In *Evolution equations, semigroups and functional analysis* (pp. 197-216). Birkhäuser, Basel.

[48] Kouémou-Patcheu, S., 1997. Global existence and exponential decay estimates for a damped quasilinear equation. *Communications in Partial Differential Equations*, 22(11-12), pp.2007–2024.

[49] Lagnese, J.E. and Leugering, G., 1991. Uniform stabilization of a nonlinear beam by nonlinear boundary feedback.*J. of Differential Equations*, 91(2), pp.355-388.

[50] Lagnese, J., 1989. *Boundary Stabilization of Thin Plates*, *SIAM.*

[51] Lagnese, J. and Lions, J.L., 1988. *Modelling analysis and control of thin plates.* Recherches en Mathematiques Appliques.

[52] Lasiecka, I., Pokojovy, M. and Wan, X., 2019. Long-time behavior of quasilinear thermoelastic Kirchhoff–Love plates with second sound.*Nonlinear Analysis*, 186, pp.219-258.

[53] Lasiecka, I. and Triggiani, R., 2000.*Control theory for partial differential equations: Volume 1, Abstract parabolic systems: Continuous and approximation theories* (Vol. 1). Cambridge University Press.

[54] Lasiecka, I. and Webster, J.T., 2014. Nonlinear plates interacting with a subsonic, inviscid flow via Kutta-Joukowski interface conditions. *Nonlinear Analysis: Real World Applications*, 17, pp.171-191.

[55] Leissa, Arthur W., 1969. *Vibration of plates.* Vol. 160. Scientific and Technical Information Division, NASA.

[56] Levin, D. and Dowell, E., 2019. Improving Piezoelectric Energy Harvesting from an Aeroelastic System, submitted.

[57] Malatkar, P., 2003. Nonlinear vibrations of cantilever beams and plates (Doctoral dissertation, Virginia Tech University).

[58] McHugh, K.A., 2020. Large Deflection Inextensible Beams and Plates and their Responses to Nonconservative Forces: Theory and Computations (Doctoral dissertation, Duke University).

[59] McHugh, K.A., 2019. *Personal correspondence.*

[60] McHugh, K.A. and Dowell, E.H., 2019. Nonlinear Response of an Inextensible, Cantilevered Beam Subjected to a Nonconservative Follower Force.*J. of Computational and Nonlinear Dynamics*, 14(3), p.031004.

[61] McHugh, K.A., Beran, P., Freydin, M. and Dowell, E.H., 2019. Flutter and Limit Cycle Oscillations of a Cantilevered Plate in Supersonic/Hypersonic Flow. *Proceedings of IFASD.*

[62] Novozhilov, V.V., 1999. *Foundations of the nonlinear theory of elasticity*. Courier Corporation.

[63] Paidoussis, M.P., 1998. *Fluid-structure interactions: slender structures and axial flow* (Vol. 1). Academic press.

[64] Pazy, A., 2012. *Semigroups of linear operators and applications to partial differential equations* (Vol. 44). Springer Science & Business Media.

[65] Reddy, J.N. ed., 1999. *Theory and analysis of elastic plates and shells*. CRC press.

[66] Russell, D.L., 1991. A comparison of certain elastic dissipation mechanisms via decoupling and projection techniques. *Quarterly of Applied Mathematics*, 49(2), pp.373-396.

[67] SavarÃĪ, G., 1997. Regularity and perturbation results for mixed second order elliptic problems. *Communications in Partial Differential Equations*, 22(5-6), pp.869-899.

[68] Sayag, M.R. and Dowell, E.H., 2019. Nonlinear Structural, Inertial and Damping Effects in an Oscillating Cantilever Beam. *In Nonlinear Dynamics, Volume 1* (pp. 387-400). Springer, Cham.

[69] Semler, C., Li, G.X. and Paidoussis, M.P., 1994. The non-linear equations of motion of pipes conveying fluid.*J. of Sound and Vibration*, 169(5), pp.577-599.

[70] Serry, M. and Tuffaha, A., 2017. Static Stability Analysis of a Thin Plate with a Fixed Trailing Edge in Axial Subsonic Flow: Possio Integral Equation Approach. arXiv preprint arXiv:1708.06956.

[71] Stanton, S.C., Erturk, A., Mann, B.P., Dowell, E.H. and Inman, D.J., 2012. Nonlinear non-conservative behavior and modeling of piezoelectric energy harvesters including proof mass effects.*J. of Intelligent Material Systems and Structures*, 23(2), pp.183-199.

[72] Stoker, J.J., 1947.*Nonlinear elasticity*. Gordon and Breach.

[73] Tang, D., Gibbs, S.C. and Dowell, E.H., 2015. Nonlinear aeroelastic analysis with inextensible plate theory including correlation with experiment.*AIAA J.*, 53(5), pp.1299-1308.

[74] Tang, D.M., Yamamoto, H. and Dowell, E.H., 2003. Flutter and limit cycle oscillations of two-dimensional panels in three-dimensional axial flow. *Journal of Fluids and Structures*, 17(2), pp.225–242.

[75] Tang, D., Zhao, M. and Dowell, E.H., 2014. Inextensible beam and plate theory: computational analysis and comparison with experiment.*J. of Applied Mechanics*, 81(6), p.061009.

[76] Vedeneev, V.V., 2012. Panel flutter at low supersonic speeds. Journal of fluids and structures, 29, pp.79-96.

[77] White, H.E. and White, D.H., 2014. *Physics and music: the science of musical sound*. Courier Corporation.

[78] Woinowsky-Krieger, S., 1950. The effect of an axial force on the vibration of hinged bars.*J. Applied Mechanics*, 17(1), pp.35–36.